Processing and Characterization of Epoxy Composites Reinforced with Short Palmyra Fibers

Dissertation submitted in partial fulfillment
of the requirements of the degree of
Master of Technology (Research)

in

Mechanical Engineering

by

Somen Biswal

(Roll Number: 614ME1005)

based on research carried out

under the supervision of

Prof. Alok Satapathy

2016

Department Of Mechanical Engineering
National Institute of Technology Rourkela

Mechanical Engineering
National Institute of Technology Rourkela

Date:

Certificate of Examination

Roll Number: *614ME1005*

Name: *Somen Biswal*

Title of Dissertation: *Processing and Characterization of Epoxy Composites Reinforced with Short Palmyra Fibers*

We the below signed, after checking the dissertation mentioned above and the official record book (s) of the student, hereby state our approval of the dissertation submitted in partial fulfillment of the requirements of the degree of Master of Technology by Research in Mechanical Engineering at National Institute of Technology Rourkela. We are satisfied with the volume, quality, correctness, and originality of the work.

Prof. Alok Satapathy
(Principal supervisor)

Dr. Suman Ghosh
(Member, MSC)

Prof. S.C. Mishra
(Member, MSC)

Prof. K.K. Khatua
(Member, MSC)

Prof. R.K. Sahoo
(Chairperson, MSC)

Prof. S.K. Panigrahi
(External Examiner)

Prof. S.S. Mahapatra
(Head of Department, ME)

Mechanical Engineering
National Institute of Technology Rourkela

Prof. Alok Satapathy
Associate Professor

Date:

Supervisor's Certificate

This is to certify that the work presented in this dissertation entitled *Processing and Characterization of Epoxy Composites Reinforced with Short Palmyra Fibers* by *Somen Biswal*, Roll Number 614ME1005, is a record of original research carried out by him under my supervision and guidance in partial fulfillment of the requirements of the degree of *Master of Technology (Research)* in *Mechanical Engineering*. Neither this dissertation nor any part of it has been submitted for any degree or diploma to any institute or university in India or abroad.

_____
Prof. Alok Satapathy
Associate Professor

DEDICATED TO MY

BABA AND MAA

Declaration of Originality

I, *Somen Biswal*, Roll Number *614ME1005* hereby declare that this dissertation entitled *Processing and Characterization of Epoxy Composites Reinforced with Short Palmyra Fibers* presents my original work carried out as a postgraduate student of NIT Rourkela and, to the best of my knowledge, contains no material previously published or written by another person, nor any material presented by me for the award of any other degree or diploma of NIT Rourkela or any other institution. Any contribution made to this research by others, with whom I have worked at NIT Rourkela or elsewhere, is explicitly acknowledged in the dissertation. Works of other authors cited in this dissertation have been duly acknowledged under the section "References". I have also submitted my original research records to the scrutiny committee for evaluation of my dissertation.

I am fully aware that in case of any non-compliance detected in future, the Senate of NIT Rourkela may withdraw the degree awarded to me on the basis of the present dissertation.

Date:

NIT Rourkela *Somen Biswal*

Acknowledgment

It gives me immense pleasure to express my deep sense of gratitude to my supervisor ***Prof. Alok Satapathy*** for his invaluable guidance, motivation, consistent inspiration and above all for his ever co-operating, yet compassionate attitude that enabled me in bringing up this thesis in the present form. I would also like to express my sincere gratitude to ***Prof. S.S. Mahapatra***, Professor and Head of department of Mechanical Engineering for his timely help during my research work.

I would specially like to thank ***Mrs. Susmita Satapathy*** and ***Prof. Manoj Kumar Pradhan,*** *HOD, Mechanical Engineering Department (GITA, Bhubaneswar)* for their constant motivation and fruitful comments without which I would not have been evolved as a good researcher and overall as a good human being.

My thanks and appreciations also goes to my co-researchers ***Mr. Abhilash Purohit, Mr. Bishnu Prasad Nanda*** and ***Miss. Mimosha Dash*** for helping me out with their abilities for developing the research work and for making past couple of years more delightful. I would also like to thank my friends especially ***Miss. Akankshya Mansingh***, ***Mr. Priyadarshi Biplab Kumar***, ***Mr. Saroj Kumar Padhy***, ***Mr. Dhruti Sundar Pradhan***, ***Mr. Debashish Panda***, ***Mr. Sibashish Sahu*** and ***Mr. Hrudananda Sahoo*** and who were always there by my side and constantly supported and motivated me.

I owe a lot to my sister ***Miss. Sonalee Biswal*** who encouraged and supported me a lot for this research. I am thankful to god for giving me such a loving, caring and supporting sister. Finally, I want to thank my parents who have been a source of strength and support for me. Their teaching and sayings continuously guided me to achieve the excellence in my work and pushed me to think critically and never settle for anything less than my best.

At last, I thank ***Almighty God*** for giving me an opportunity to work in such an environment with such good and knowledgeable people around.

Date: *Somen Biswal*

NIT Rourkela Roll Number: 614ME1005

Abstract

The research reported in this thesis broadly consists of four parts: the first part has provided the detailed description of the materials used and experiments conducted during the research. The second part presents the characteristics of the epoxy composites reinforced with short palmyra fibers (SPF) in regard to their physical and mechanical properties like density, void fraction, tensile, flexural strength and micro-structural features. The third part of this thesis reports on the sliding wear performance of these epoxy-SPF composites under different test conditions. An empirical correlation has been proposed for estimating the specific wear rate. The last part of the thesis reports on the thermal and acoustic behavior of the epoxy-SPF composite samples under this study. The effects of increasing the SPF content on the thermal conductivity of the samples are studied. Further, its impact on the sound absorbing characteristics has also been discussed in detail in this part. Usually a new composite material's performance is often determined by its response under various mechanical, physical, tribological and thermal conditions as it gets very much essential for selecting materials of appropriate composition for application in a particular area. Hence, in the current investigation, an abundance of property information has been provided for a set of epoxy-SPF composites by processing them through hand-lay-up technique and by carrying out various physical, mechanical, tribological, acoustic and thermal tests on them under controlled laboratory conditions. It is observed that by reinforcing short palmyra fibers into the neat epoxy resin, its effects, as desired are achieved in the form of enhanced mechanical, physical, tribological, thermal and acoustic properties. When the concentration of SPF in the neat epoxy is increased, the specific wear rate decreased gradually and at the same time a reduction in the effective thermal conductivity is also observed as palmyra fiber is insulative in nature. This is accompanied by increase in both tensile and flexural strength. Further, the sound absorption coefficient also increased by a huge margin as the SPF concentration in the neat epoxy increased. The effects of SPF content on the coefficient of thermal expansion

and glass transition temperature of the composites are also found to be significant. With a moderate strength, decreased wear rate, high coefficient of sound absorption and lowered thermal conductivity, these epoxy-SPF composites can be successfully used for applications such as building insulation material, food containers, interior of automobiles, interior wall of halls where sound absorption in required, thermos flasks, packaging industries, rollers of conveyor belts, brake pads, etc.

Keywords: ***polymer composite; palmyra fiber; dry sliding wear; Taguchi method; artificial neural network.***

*****

Contents

List of Figures

List of Tables

CHAPTER 1

Introduction

Chapter 1

Introduction

1.1 Background and Motivation

As the concern over a depleting environment is increasing day-by-day, the need of the hour is to develop such materials which are sustainable and at the same time energy efficient in nature so as to minimize and reduce further damage to an already damaged environment. As a result of this, environment friendly and non-toxic materials are gaining popularity among researchers and industries. Generally, materials developed from agro-wastes are considered as environment friendly and bio-degradable materials. These materials are now becoming the centre of attraction because of the numerous advantages offered by them. Apart from providing a clean environment for production, these materials are also inexpensive which further increases the interest of the scientific community to explore the possibilities of using these materials in various application areas. More and more research works are being conducted to study the characteristics and to explore the potential applications of these environment friendly materials. In this context as far as composite materials are concerned, natural fibers are fast emerging as the most promising reinforcing elements with their inexpensive and some excellent properties that otherwise cannot be obtained from synthetic fibers. Now-a-days natural fibers are gradually replacing synthetic fibers in various applications.

1.2 Natural/Bio Fibers

Fibers that are extracted from the minerals, plant/vegetables, animals and agricultural wastes convertible into non-woven fabrics are generally considered as natural fibers. Currently, a wide variety of industrially viable natural fibers such as kapok, sisal, coconut, jute, bamboo, bagasse, hemp, nut shell, rice husk, etc. are available. Extensive work is being done on these fibers to explore the possibilities of using them in various application areas. Some of the prominent areas where these fibers have found application include fiber reinforced composites for building construction, thermal insulation, acoustic insulation,

etc. The chemical constituents of these natural fibers generally comprise of lignin, wax, pectin, cellulose, hemi-cellulose and water soluble substances. Among these substances, the concentration of cellulose is the highest which a semi-crystalline polysacharide having D glucopyraniose assembled together by glucocidic bonds. These fibers are hydrophilic in nature which is because of the huge amount of hydroxyl groups present in them. As a result of this hydrophilic nature, natural fibers and their composites have poor water and moisture resistant properties which pose a major challenge to researchers. Generally, natural fibers are pre-treated with alkaline in order to increase the water and moisture resistant properties prior to composite making. Table 1.1 shows some of the important natural fibers along with its origin and species.

Table 1.1: Natural fibers, origin and species (John and Thomas, 2008)

Fiber name	**Origin**	**Species**
Jute	Stem	*Corchorus capsularis*
Abaca leaf	Leaf	*Musa textilis*
Piassava	Leaf	*Attalea funifera*
Bagasse	Grass	*Saccharum officinarum*
Pineapple	Leaf	*Ananus comosus*
Kapok	Fruit	*Ceiba pentranda*
Oil palm	Fruit	*Elaeis guineensis*
Henequen	Leaf	*Agave fourcroydes*
Bamboo	Grass	*Acidosasa edulis*
Kenaf	Stem	*Hibiscus cannabinus*
Hemp	Stem	*Cannabis sativa*
Coir	Fruit	*Cocos nucifera*
Curaua	Leaf	*Ananas erectifolius*
Banana	Leaf	*Musa indica*
Cotton	Seed	*Gossypium sp.*
Flax	Stem	*Linum usitatissimum*
Date palm	Leaf	*Phoenix dactylifera*

Table 1.2: Chemical constituents of different natural fibers (Mohanthy et al, 2001)

Fibers	**Lignin (%)**	**Pectin (%)**	**Cellulose (%)**	**Hemicellulose (%)**	**Ash (%)**
Kenaf	15-19	-	31-57	21.5-23	2-5
Hemp	3.7-13	0.9	57-77	14-22.4	0.8
Flax	2.2	2.3	71	18.6-20.6	-
Jute	12-26	0.2	45-71.5	13.6-21	0.5-2
Ramie	0.6-0.7	1.9	68.6-91	5-16.7	-
Henequen	13.1	-	77.6	4-8	-
Sisal	7-11	10	47-78	10-24	0.6-1
Abaca	7-9	-	56-63	15-17	3

The chemical constituents of some of the important natural fibers are shown in Table 1.2. From the table it can be clearly seen that the cellulose percentage is higher in all the fibers in comparison to other substances such as lignin, pectin, hemi-cellulose and ash content.

1.3 Composite Materials

A composite is generally defined as a heterogeneous combination of two or more chemically distinct materials with a distinct interface between them having some desirable properties which are different from its parent constituent materials. Composite consists of two phases i.e. a continuous phase and a discontinuous phase. The continuous phase of the composite is known as the matrix while the discontinuous phase is known as the reinforcement. The primary function of the matrix phase is to give shape to the composite and transfer the stresses from the discontinuous phase. Further, it protects the discontinuous phase from any environmental and mechanical damages thereby acting as a shield. The main function of the discontinuous phase or the reinforcement is to provide stiffness, strength and other desired properties. Typically, the density of matrix material is more as compared to the reinforcing material. The components of the composites have different chemical and physical properties which are combined synergistically in order to take advantages of some superior properties of the constituent materials.

In recent days, composites have substituted the traditional materials successfully in the field of high strength and light weight applications. This rapidly increasing popularity of composite materials can be attributed to several advantages offered by them such as high

creep strength, improved strength-to-weight ratio, higher toughness, high tensile strength at increased temperature, etc. The strength property of a composite largely depends on the design and correctness of its fabrication process.

1.3.1 Classification of Composites

Generally, composites are broadly classified into three types on the basis of the matrix materials used. They are:

a) Metal Matrix Composites (MMC)
b) Ceramic Matrix Composites (CMC)
c) Polymer Matrix Composites (PMC)

a) Metal Matrix Composites:

A metal matrix composite offers several advantages over traditional metals such as higher specific modulus, low coefficient of thermal expansion, higher specific strength, and improved properties at higher temperatures. As a result of these advantages, MMCs are widely used in aerospace industries for the manufacturing of combustion chamber nozzle tubing, housings, heat exchangers, etc.

b) Ceramic Matrix Composites:

Ceramic matrix composites have very high toughness and have high heat resistant properties. CMCs are generally accompanied with improvement in stiffness and strength properties.

c) Polymer Matrix Composites:

Currently, polymers are the most widely used matrix materials. Although the processing of polymer matrix composites does not require any sophisticated technology, the strength and stiffness properties of polymer matrix are lower as compared to ceramic matrix and metal matrix. Because of this, these matrices are reinforced with reinforcing materials which have superior strength and other mechanical properties as compared to the polymer matrix. The popularity of polymer composites is increasing very rapidly in thermal, structural and even in micro-electronic applications.

Generally, polymer composites can be divided into two main categories based on the type of reinforcing material used. They are:

- Fiber reinforced polymers (FRP)
- Particulate reinforced polymers (PRP)

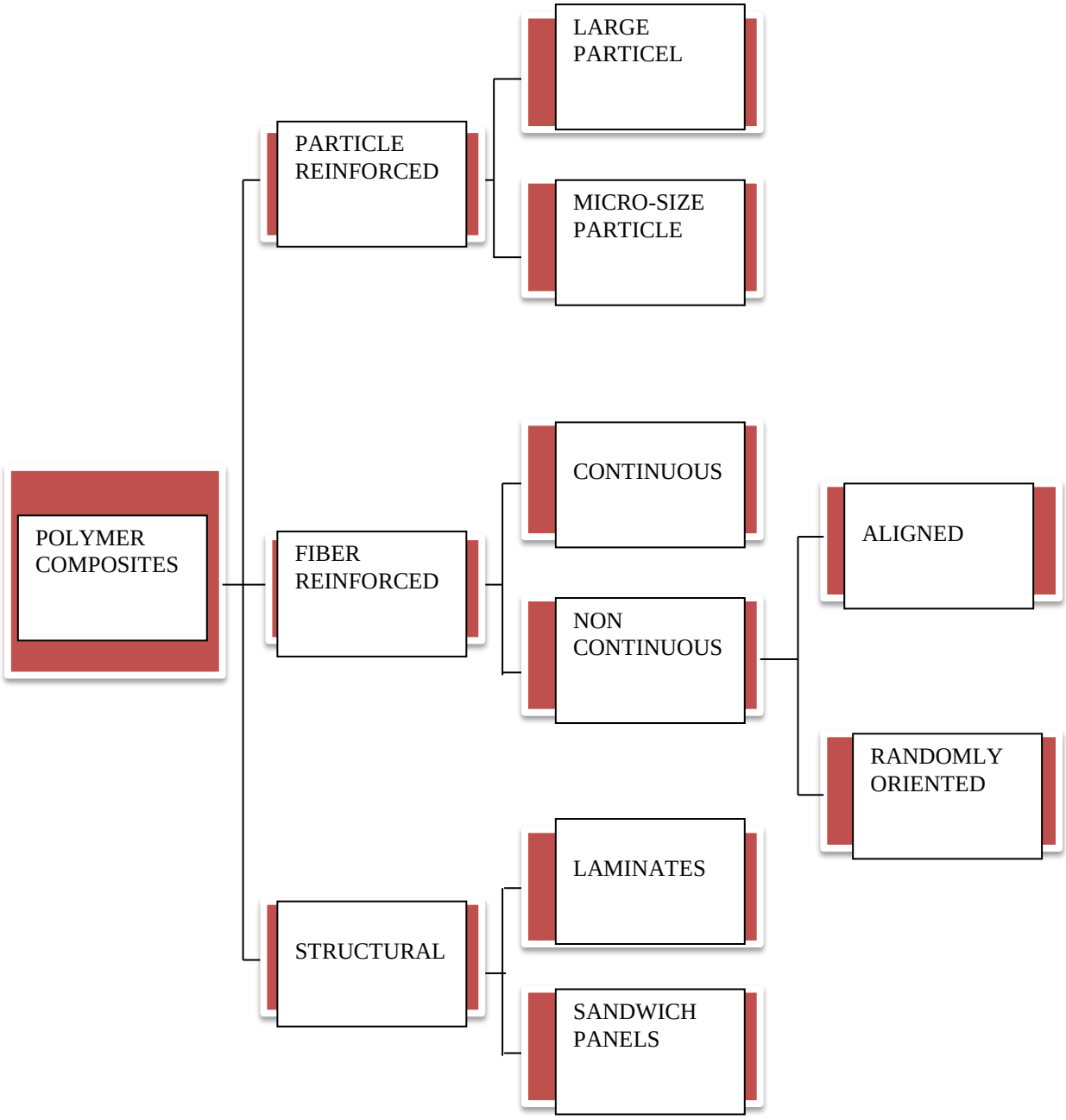

Figure 1.1: Broad classification of composite materials [1]

Fiber Reinforced Polymer:

Composites which consist of fibers as the reinforcing phase are classified under fiber reinforced polymer composites. The fiber is responsible for imparting strength to the composite while the matrix is responsible for holding together the fibers and transfer the stresses. The load is carried in the longitudinal direction of the fiber. At times, filler is added in order to ease the manufacturing process. Some of the commonly used fibers in industrial applications include glass fiber, carbon fiber, asbestos, natural fiber, etc. Likewise, phenolic resin, epoxy, vinyl ester, polypropylene, polyester, polyurethane, etc. are some of the commonly used matrix materials.

Particulate Reinforced Polymer:

Generally, the use of particulates in the reinforcing phase decreases the ductility of the material and at the same time increases its modulus. The cost of the composite is also considerably reduced by incorporation of particulates in the reinforcing phase. Particles used for reinforcing includes metal powders, small mineral particles, ceramics, etc. High strength, corrosion resistance, low density, wear resistance and high melting point are some of the viable properties of glasses and ceramics.

Apart from this two broad classification of polymer composite, there is another type which is known as hybrid composite. A hybrid composite is a combination of both fiber and particulate reinforced in a common matrix. This is done in order to get the combined advantages of both the fiber and the particulate.

1.4 Introduction to the Research Topic

The present research investigation aims to fabricate a new class of fiber reinforced composite material using short palmyra fiber (SPF) as the reinforcing element. The research work is an approach to explore the possibilities of using this new class of composite material in suitable application areas. The investigation deals with an extensive characterization of the newly developed composite on the basis of its physical, mechanical, micro-structural, wear, thermal and acoustic properties. The effects of addition of SPF on the thermal behavior and acoustic properties have been studied. The work also uses an optimizing tool in order to minimize the wear rate of the composite and the wear rate within and beyond the experimental domain has been successfully predicted by using Artificial Neural Network (ANN). A predictive equation for estimation of wear

rate has also been proposed in this work. Further, the micro-structural features of these composites have been studied using electron microscopy.

1.5 Thesis Outline

The remainder of this thesis is organized as follows:

Chapter 2:

Includes a literature survey which has been designed to provide a summary of the earlier investigations involving the areas of interest. It provides the research findings of previous investigators on polymer composites reinforced with natural fiber and particularly on the wear performance, thermal behavior and acoustic insulation properties.

Chapter 3:

This chapter includes the detailed description of the raw materials used and the methods followed in order to fabricate the composites. It also includes the details of experiments carried out in the entire investigation.

Chapter 4:

It presents the test results and discussion with respect to the physical, micro-structural and mechanical properties of the composite samples under investigation.

Chapter 5:

This chapter includes the study of dry sliding wear test results and determination of an optimal parameter setting for minimum wear rate. It also presents the wear rate prediction using Artificial Neural Network technique.

Chapter 6:

This chapter presents the test results related to thermal characteristics and acoustic absorption properties of the samples under investigation.

Chapter 7:

Provides the summary of the research investigation and outlines the specific conclusions drawn from the research findings. Further, it suggests some potential areas of application of this composite and suggests ideas and directions for future research.

*****

CHAPTER 2

Literature Review

Chapter 2

Literature Review

This chapter exhibits the summary of the papers overviewed during the research work in order to give brief information with respect to the issues to be considered in this work and consequently to outline the objectives of this investigation. This chapter covers different aspects of polymer composites and natural fiber reinforced polymer composites with special reference to their tribological, thermal and acoustic characterization. It includes the following available research findings:

- On fiber reinforced polymer matrix composites
- On natural fiber and natural fiber reinforced composites
- On mechanical properties of natural fiber reinforced composites
- On Palmyra Palm and polymer composites reinforced with Palmyra Palm fiber
- On wear characterization of polymer composites
- On thermal and acoustic properties of polymer composites

The chapter ends with the summary of the papers surveyed and the knowledge gap in the previous researches has been provided. Subsequently, the chapter outlines the objectives of the present investigation.

2.1 Fiber Reinforced Polymer Matrix Composites

Now-a-days, there has been a significant growth of fiber reinforced polymer (FRP) composites in composite industries. They are used widely in the field of aircraft manufacturing, automobiles, off-shore structures, space crafts, sporting goods, containers and piping and even in electronic appliances. They are easy to fabricate, offer very high mechanical strength and can be designed into any shape. Additionally, FRP composites are corrosion resistant, light in weight and have excellent fatigue and impact strength.

FRP composites are very popular in transportation industries owing to their tremendous strength–to-weight properties and high flexibility of design. A lot of research investigation

has been conducted by researchers on the mechanical properties, physical behavior and tribological characteristics of fiber reinforced polymer composites. A detailed review was made recently by Khalil et al. [1] on poly vinyl chloride (PVC) reinforced with natural fibers. The researchers studied the effect of plasticization, effect of reinforcement and the effect of modification by coupling agents on the properties of the composites. Abdulmajeeda et al. [2] studied the mechanical properties of composites reinforced with unidirectional glass fiber. The effect of reinforcing inter-penetrating polymer network (IPN)-polymer matrix with short E-glass fibers on the mechanical properties was investigated by Garoushi et al. [3]. It was observed that the mechanical properties improved with the use of short E-glass fibers as filler material as compared to conventional restorative composites. Similarly, the thermo-mechanical and tensile properties of polyamide-6 (PA6) composites reinforced with short carbon fibers were studied by Karsli et al. [4].

In order to achieve desired material properties, multi-fiber composites are being developed now-a-days in which two or more fibers are combined together and are used in a single matrix material. Although carbon fiber possesses very good mechanical properties, the low compressive-to-tensile strength ratio [5-7] makes the use of polymer composites reinforced with carbon fiber unfit for application in structural members subjected to flexural or compressive loading. While the tensile strength of glass fiber is low as compared to carbon fiber [8, 9], it has high strain-to-failure ratio because of its lower modulus. This makes the incorporation of a high elongation fiber into a low elongation fiber possible in order to increase the failure strains [10]. Dong and Davies [11] studied the flexural strength of S-2 glass and T700S carbon fiber reinforced epoxy composites. Encinas et al. [12] focused their study on improving the adhesion performance of wettable glass fiber reinforced in epoxy and polyester matrices. Sridhar et al. [13] investigated the optimal design of customized hip prosthesis using carbon fiber reinforced in poly-ether-ketone matrix lay-up. The development of fiber reinforced functionally graded composites (FGCs) was done by Kumar et al. [14] for application in aerospace sector using quartz fabric reinforcement. A detailed review on the application of fiber-reinforced polymer composites in underwater pipeline repair was presented by Shamsuddoha et al. [15]. The effectiveness of fiber reinforced composites in construction and retrofit of filled and hollow in-air, marine and underground cylinder [16] has already been proven. A comparative study between hybrid glass fiber and sisal/jute reinforced in epoxy matrix

was made by Ramesh et al. [17]. A lot of researchers have worked on the synergistic effects in which the material property observed in reality differs from those obtained by using rule-of-mixture prediction. A positive deviation of mechanical properties can be said as a positive hybrid effect and a negative deviation can be said as a negative hybrid effect [18].

FRPs are not just fiber dispersed in a matrix phase. It consists of fibers which are bonded to the matrix phase with distinct interfaces in between them. While the fiber serves as the basic load carrying element of the composite because of its high strength and modulus, the matrix transfers the load and thus serves as the load transferring element of the composite. In addition, the matrix also acts as a protective cover against environmental damages. Generally, the individual constituents of the composite retain their own properties while exhibiting many new desirable properties that cannot be exhibited by them individually. Among a wide variety of fiber available for reinforcement, some of the common fibers are carbon, aramid and glass fiber. Natural fibers such as sisal, bagasse, jute, hemp, etc. are some of the common reinforcing materials. Their combination thus can provide outstanding structural and functional properties. A judicious combination of matrix and reinforcement can yield a composite with tremendous strength and other desirable properties as compared to conventional metallic materials [19]. Fan et al. [20] and Kim et al. [21] noted that with the addition of filler materials to the fiber reinforced composites, the modulus increased and at the same time the cost of the material reduced. Such types of composites which consist of two or more reinforcing phases are known as hybrid composites. This was first suggested by Garcia et al. [22] in order to enhance the matrix dominated properties of FRPs. Few researchers have made attempts to investigate the mechanical, physical and tribological behavior of these composites [23, 24].

2.2 Natural Fibers and Natural Fiber Reinforced Composites

The reinforcing phase of a composite can basically be of two types i.e. fiber reinforcement or particulate reinforcement. A composite is said to be natural fiber reinforced composite if the fiber is obtained from natural resources like plants. A lot of research work is now being undertaken by researchers to explore these fibers for application in various fields. Natural fibers offer several advantages such as they are light in weight, they have high

strength properties, they are widely available, etc. Natural fibers are also environmental friendly and are biodegradable unlike synthetic fibers. Natural fibers are generally classified into three main categories, i.e. vegetable/plant fiber (sisal, jute, hemp, bagasse, flax, etc.), animal/protein fibers (chitin, wool, hair, silk, etc.) and mineral fibers (wollastonite, asbestos, etc.). Among these three, plant fibers are considered as ideal reinforcing materials. Natural fibers generally possess low density and high specific properties which are often at par with those of synthetic fibers. Another fact about natural fibers is that the structures of these fibers are non-uniform which makes the composite a unique structure. Some important properties of most commonly used natural fibers are given in Table 2.1 [25].

Table 2.1: Properties of natural fibers [25]

Fiber	**Tensile Strength (MPa)**	**Young's Modulus (GPa)**	**Elongation at Break (%)**	**Density (g/cm^3)**
Abaca	400.0	12.0	3.0-10.0	1.50
Alfa	350.0	22.0	5.80	0.890
Bagasse	290.0	17.0	-	1.250
Bamboo	140.0-230.0	11.0-17.0	-	0.6-1.10
Banana	500.0	12.0	5.90	1.350
Coir	175.0	4.0-6.0	30.0	1.20
Cotton	287.0-597.0	5.50-12.60	7.0-8.0	1.50-1.60
Curaua	500.0, 150.0	11.80	3.70-4.30	1.40
Flax	345.0, 035.0	27.60	2.70-3.20	1.50
Hemp	690.0	70.0	1.60	1.480
Henequen	500.0 ± 70	13.20 ± 3.1	4.80 ± 1.1	1.20
Jute	393.0-773.0	26.50	1.50-1.80	1.30
Kenaf	930.0	53.0	1.60	-
Pineapple	400.0-627.0	1.440	14.50	0.80-1.60
Sisal	511.0-635.0	9.40-22.0	2.00-2.50	1.50
E-Glass	3400.0	72.0	-	2.50

From Table 2.1, it can be seen that natural fibers have substantially low tensile strength than E-Glass fibers. The Young's moduli of glass fiber and hemp are almost same which

is about 70 GPa. However, it can be clearly concluded that the specific modulus of natural fibers are comparable and even better than glass fibers. This is the most essential property of natural fiber that makes it possible to be used in applications where high strength along with reduced weight is highly essential. Table 2.2 shows some of the advantages of natural fiber over E-Glass fiber [26].

Table 2.2: Comparison between natural fiber and E-Glass fiber [26]

	Natural fibers	**E-Glass fibers**
Density	Low	Twice that of natural fibers
Cost	Low	Low, but higher than natural fibers
Renewability	Renewable	Non- renewable
Recyclability	Recyclable	Non-recyclable
Energy consumption	Low	High
Distribution	Wide	Wide
CO_2 neutral	Yes	No
Abrasion to machines	No	Yes
Health risk when inhaled	No health risk	Yes
Disposal	Biodegradable	Not biodegradable

Sanadi et al. [27] studied the impact behavior of sunhemp fibers reinforced in polyester matrix. It is observed that the toughness of these composites is because of the interface fracture and fiber pull out. Similarly, many researchers have done a lot of work on natural fiber composites in order to substitute these fibers in place of synthetic fibers [28-31]. Nishino et al. [32] investigated the effects of orientation on the mechanical properties of kenaf fiber reinforced in polylactic acid resin. Studies have already been conducted on the potential of pineapple, jute, abaca, sisal and coir as reinforcing materials [33-41]. Joshi et al. [38] made a review on the life cycle assessment of natural fiber and glass fiber and found that the natural fibers are environmentally superior to glass fibers. A very elaborate review on natural fiber composites was presented by Saheb et al. [26] with special attention to type of matrix, treatment of fiber, type of fiber and fiber-matrix interface. Figure 2.1 [42] shows the schematic representation of some of the most commonly used matrix materials and natural fibers for preparing composites.

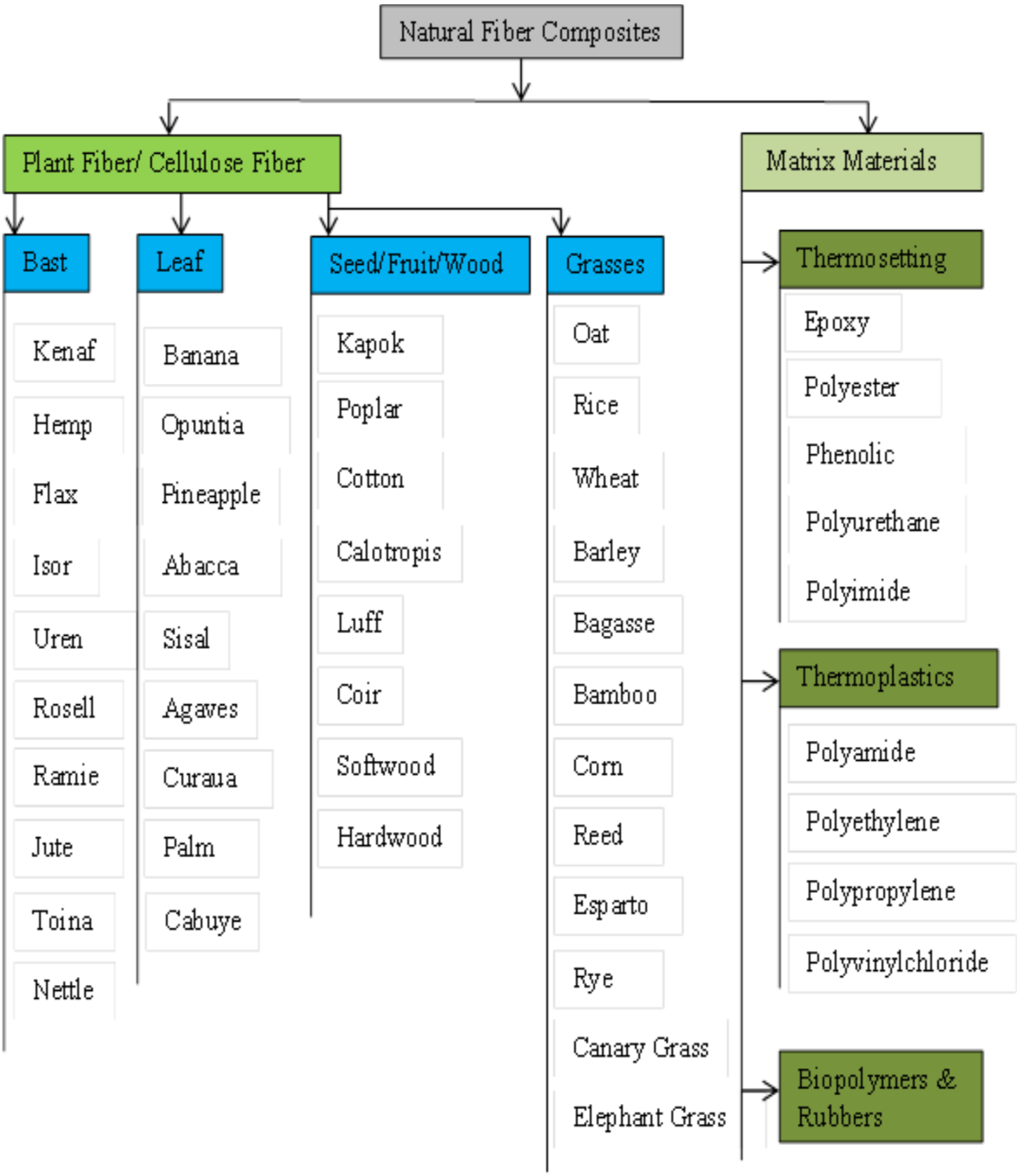

Figure 2.1: Commonly used natural fibers and matrix materials [42]

A lot of research works on fibers like rice husk, bamboo, sisal and jute have been reported in the recent past [43-50]. Khalil et al. [43] investigated chemically treated rice husk fiber for its mechanical properties. While Takagi [45] studied the degradation behavior of

Manila hemp fiber reinforced composites, Jiang et al. [46] studied the degradation behavior of flax and cotton fibers. Similarly, the effect of fiber orientation on the electrical properties of sisal fiber reinforced in a polyethylene matrix was studied by Chand et al. [47]. On the other hand, Joseph et al. [48] studied the tensile properties of such composites. It was observed that the tensile properties showed a gradual improvement with addition of the sisal fiber to the polymer.

2.3 Mechanical Properties of Natural Fiber Reinforced Composites

A lot of research work has been conducted by researchers in the past to study and to enhance the mechanical properties of natural fiber reinforced composites. It has been observed that fiber aspect ratio, volume fraction of fiber, fiber orientation, fiber-matrix adhesion, etc. influence the mechanical properties of natural fiber reinforced composites [51]. Kenaf, banana, jute, bamboo, cotton etc. are some of the natural fibers on which extensive research has been conducted in the past [52-54]. Gowda et al. [54] evaluated the mechanical characteristics of jute fibers reinforced in a polyester matrix. It was found that the jute fiber reinforced composites are superior to those of wood based composites. A lot of research reports are available related to banana fiber as the reinforcing material [55-57]. Pothan et al. [55] analyzed the mechanical properties of banana fiber reinforced in polyester matrix. They also studied the failure and ageing characteristics of these composites in a separate investigation [57]. Joseph et al. [58] and George at al. [59] studied the mechanical and thermal properties of sisal and pineapple fiber reinforced in polyethylene matrix. Amash et al. [60] investigated the influence of cellulose fiber on the stiffness and damping properties of polypropylene composites. Netravali et al. [61] compared the flexural as well as tensile properties of virgin resin with green composites having varied pineapple fiber content. An extensive study on the mechanical properties of henequen fiber was done by Cazaurang et al. [62]. Karmaker et al. [63] compared the mechanical properties of kenaf and jute fiber composites reinforced in a polypropylene matrix and found that jute fiber reinforced composites are much stronger than kenaf fiber reinforced polypropylene composites. The effects of loading on the mechanical properties of jute/glass fiber reinforced hybrid epoxy composite were investigated by Srivastav et al. [64]. The effects of physical factors such as fiber length and volume fraction on the mechanical properties of fibers like bagasse and kenaf was studied by Shinichi et al. [65].

Similarly, the tensile and flexural tests were conducted by Sapuan at al. [66] on epoxy reinforced with musaceae fiber.

Lot of investigations has also been carried out by researchers in the recent past on the mechanical properties of fiber reinforced composites fabricated by different techniques. A study was conducted by Chawla et al. [67] on the impact strength, tensile strength and Young's modulus of jute fibers in polyester resin made by leaky mould technique. Similarly, Hepworth et al. [68] studied the mechanical properties of hemp fiber reinforced in epoxy matrix which was fabricated by pinning-decortications and hand combing. The evaluation of mechanical properties of flax fiber composites manufactured by extrusion as well as batch kneading process was conducted by Harriette et al. [69]. Monteiro et al. [70] conducted experiments to study the molding pressure effect on the flexural strength of coir fiber/polyester composites.

Research works relating to the impact behavior of natural fiber reinforced composites are also available in the existing literature. Santulli [71] recorded poor impact performance of polyester composites reinforced with jute fiber when it is subjected to low velocity impact. Similarly, Charpy impact test method was used by Pavithran et al. [72] to determine the fracture energies of banana, sisal, coconut and pineapple fiber reinforced in a polyester matrix. Tobias [73] found that with increase in the fiber length in banana/epoxy composites, the impact strength decreased. But at the same time the impact strength showed improvement as the fiber content was increased. While Lakkad et al. [74] investigated and found that the strength and specific modulus of bamboo fiber are higher than glass reinforced plastics and mild steel, Chen et al. [75] compared the mechanical properties of bamboo fiber reinforced in a polypropylene matrix with commercial wood pulp.

2.4 Polymer Composites Reinforced With Palmyra Palm Fiber

Borassus flabellifer commonly known as Palmyra Palm tree is one of the most important tree in the region of Africa and South-East Asia because of the great benefits that are derived from the palmyra based products. The trees are very high and can grow up to 30 meter in height with leafs being fan-shaped. The leaf of these trees are in a sense natural

composites consisting of cellulose embedded in a lignin matrix. High tensile strength, rigidity and high flexural strength are imparted by the cellulose fiber in the longitudinal direction. Because of this, the bulk mechanical properties of the palmyra fiber are much higher. Palmyra Palm offers many advantages such as they are abundantly available in the tropical and sub-tropical region, they can be processed easily, are cheap and bio-degradable in nature. Currently, as high as 2600 species of palm trees with 200 genera are known to the scientific community.

In a recent experimental investigation, Chaurasiya et al. [76] extracted the pulp from the palmyra tree and studied the storage life of this pulp. Different ingredients were added to prepare the samples and from the experiments it was revealed that these pulps can be successfully stored for a maximum of 8 months. Velmurugan et al. [77] conducted investigation on the mechanical characteristics of a hybrid composite consisting of palmyra and glass fiber reinforced in rooflite resin. Venkateshwaran et al. [78] compared the mechanical properties and found that the tensile strength of palmyra/polyester composites is less as compared to banana fiber/epoxy composites which is about 43.54% higher than palmyra fiber reinforced in polyester matrix. Thiruchitrambalam et al. [79] investigated the static and dynamic mechanical properties of palmyra palm leaf fiber treated in alkali and jute fiber reinforced in a polyester matrix. The hybrid composites are fabricated with unidirectional arrangement of the fibers. It is observed that the addition of alkali treated palmyra fiber enhanced the impact strength of the composite more than addition of jute fiber to the composite. Similarly, Balakrishan et al. [80] studied the effects of alkali treatment, fiber volume and fiber length on the tensile strength of Asian palmyra fiber. Further, they developed a mathematical model to predict the tensile strength of the composite under the influence of varying factors. Daud et al. [81] studied the surface characteristics and mechanical properties of corn stalk and oil palm leaf fiber. An extensive work on the manufacturing processes and characterization of the palmyra palm fiber reinforced in polyester matrix was done by Srinivasababu et al. [82]. Higher tensile and flexural strength were recorded in chemically treated fiber as compared to those in case of untreated fiber.

Apart from the mechanical properties, efforts have also been made by researchers to study the pulping properties of palmyra palm. Sridach [83] studied the palmyra palm fruit bunch for its paper and pulping properties. Similarly, Ali et al. [84] investigated the palmyra palm fruits for its physio-chemical properties. Manikandan et al. [85] explored the

possibility of using saw-dust, coir pitch and palmyra fiber as reinforcement in polyester matrix. It was revealed that the impact strength, tensile strength and shear strength improved with addition of saw-dust and coir pitch to the sandwiched composite plates. Doko et al. [86] used palmyra palm and rice husk in cement matrix and studied its mechanical and physical characteristics. The study revealed that the cement reinforced with palmyra palm showed better mechanical performance than cement reinforced with rice husk. Researchers have also worked to explore the possibilities of using the palmyra palm in areas where high strength is required. Byrne [87] conducted experiments to use the timber of palmyra palm for constructing bridges. From the experiments carried out so far, it was concluded that palmyra palm timbers are suitable for construction of bridges especially in cyclone prone areas.

Attom at al. [88] investigated the effects of palmyra fiber and nylon fiber on the mechanical properties of clay soil. The results revealed that addition of fiber to the clay soil improved its stiffness, compressive strength and ductility with palmyra fiber showing a greater improvement in the mechanical properties than nylon fiber. Mahesh et al. [89] investigated the mechanical as well as thermal properties of chemically treated palmyra fiber reinforced in a polyester matrix. In addition to the palmyra fiber, chalk powder is also used in the matrix as a filler material. Nayak et al. [90] used the palmyra fruit fiber and studied its mechanical and water absorption properties. From the experiments it was found that with the increase in the fiber content, water absorbing characteristics of the composite also gradually increased.

Similarly, Dabade et al. [91] used polyester matrix to study the effect of fiber weight ratio and fiber length of palmyra fiber and sun hemp fiber on the tensile properties. It was observed that the tensile properties of palmyra fiber showed improvement up to a fiber length of 50mm and thereafter the tensile property degraded gradually stating an optimum fiber length for maximum tensile strength. Further, the tensile properties showed improvement up to a fiber weight ratio of 55% and then decreased with further increase in the fiber weight ratio. The influence of alkali treated palmyra fiber extracted from the leaf stalk of palmyra palm on the mechanical properties was studied by Shanmugam et al. [92]. While the benzoyl treated fiber showed 60% improvement in tensile strength, the permanganate treated fiber showed about 70% increase in flexural strength as compared to untreated fiber. Further, the thermogravimetric analysis revealed that treated fibers are thermally more stable than untreated fibers. Thirumurugan et al. [93] investigated the

flexural, tensile, impact and dynamic mechanical properties of continuous unidirectional palmyra leaf stalk fiber/glass reinforced in a polyester matrix. It was observed that the flexural, tensile and impact properties improved with hybridization as compared to non-hybridized composite. Prabu et al. [94] explored the possibility of using red mud as a filler material along with palmyra fiber in unsaturated polyester matrix. The addition of red mud as a filler material showed improvement in the tensile properties of the composites. Further, micro-structural analysis was carried out in order to find out the possible mechanism of failure. Similarly, Neher et al. [95] used acrylonitrile butadiene styrene (ABS) as the matrix material with palm fiber as the reinforcing material to study the physical and mechanical properties. It was observed that with addition of palm fiber to ABS matrix, the tensile and flexural properties decreased with 10% fiber content being an exceptional case. Gafur at al. [96] further studied the structural characteristics and surface morphology of palm fiber reinforced in ABS matrix. From the analysis it was observed that addition of palm fiber resulted in increase in the brittleness of the composite. While Sudhakara et al. [97] used palmyra fruit fiber reinforced polypropylene composite for investigating its mechanical, thermal and morphological characteristics, Ngargueudedjim et al. [98] focused only on the mechanical characteristics of palmyra fiber. Similarly, Goulart et al. [99] investigated the impact strength, flexibility and stiffness of palm fiber reinforced in polypropylene matrix and found that the mechanical properties of composites are enhanced with the addition of coupling agent as compared to pure polymer composites.

2.5 Wear Characterization of Polymer Composites

In general terms, wear can be defined as the mechanism of removal of materials from one or both the surfaces that are in contact with each other and have relative motion between them. Wear is not a mechanical property rather it occurs due to interaction of asperities of the surface in contact. Wear is generally classified into the following modes:

- Adhesive wear
- Abrasive wear
- Erosive wear
- Fatigue wear
- Corrosion wear

- Fretting wear
- Cavitation and oxidation wear

Mechanism of adhesive wear

Adhesive wear occurs when a stronger material is in adhesion to a weaker material and when there is a relative motion between both the surfaces in adhesion. This results in removal of material from the weaker surface. This adhesion can be explained by transfer of electron between the two surfaces in contact [100]. The free electrons present on the surface of the material are responsible for such bonding. This effect was described by the 'Jellium Model' [101].

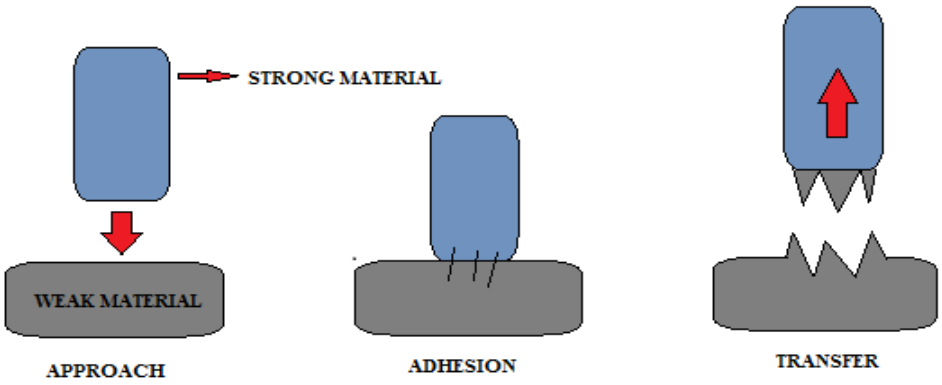

Figure 2.2: Schematic representation of adhesion wear mechanism

Mechanism of abrasive wear

Abrasive wear occurs because of sliding of a harder surface against a softer surface resulting in removal of material from the softer surface. Wear of shovels on heavy machineries and buckets in barrel are some of the examples of wear due to abrasion. Any material with bulk of it being soft may suffer from abrasive wear if hard particles are present. It is originally assumed that abrasive wear by grits or hard asperities closely resemble cutting by a series of machine tools or a file.

Mechanism of erosive wear

Erosive wear occurs due to the impact of a solid or a liquid particle on the surface of the material. This mechanism of wear is the most common type of wear encountered in

industries. Piping system, blades of gas turbine, etc. are some of the machinery where erosive wear is the most common phenomenon. This makes the detail study of erosive wear very much essential. The wear also depends on the properties of the eroding particles. At the same time, the impact speed of the particle is also an important factor that affects the wear rate [102].

Fatigue wear occurs due to repeated loading and unloading of the material. It can also occur in well lubricated contacts where adhesion wear is negligible. Soda et al. [103] described the wear mechanisms of FCC metals and the effect of atmospheric pressure and velocity of the particle on the wear. Similarly, material removal from the surface of the object due to chemical reaction is known as corrosive wear [104]. Fretting wear occurs due to repeated rubbing between two surfaces [105]. Fretting wear mostly occurs in bearing materials. This is a very serious phenomenon which can damage the material severely. Various researchers have elaborated the principles of wear in the recent past [106-108].

2.5.1 Sliding Wear of Polymer Composites

The rising concern over some of the critical issues such as friction and wear relating to industrial applications has led to the development of more and more advanced materials that can withstand these adverse conditions. Different types of filler and reinforcing materials are now being used in sliding applications which were earlier composed of only metallic materials. The friction and wear characteristics of polymeric materials can be improved by enhancing some of the key properties such as compressive strength, stiffness and hardness. In order to achieve these properties, special kind of filler/reinforcement can be used in the polymer composites.

The creep resistance and compressive strength of the polymeric materials can be improved by reinforcing it with short glass fiber (SGF), short aramid fiber (SAF) and short carbon fiber (SCF) [109-110]. Similarly, the stiffness and hardness can be improved by using ceramic as filler material in the composite. A lot of reports are available on the use of ceramic materials for enhancing the tribological properties of polymer composites [111-115]. Cirino et al. [116-117] studied the dry sliding wear behavior of neat epoxy, glass fiber/epoxy, carbon fiber/epoxy, neat polyetheretherketone (PEEK), aramid fiber/epoxy, carbon fiber/PEEK and aramid fiber/PEEK on a pin-on-flat test rig and evaluated the properties for applications against abrasive wear and sliding wear. Friedrich et al. [118]

studied the effects of temperature and roughness of the counter surface on the wear behavior of PEEK composites. They further made a review of polymer composites for application against wear and friction [119]. Tayeb et al. [120] studied the wear and frictional characteristics of E-glass fiber reinforced in epoxy matrix under different conditions using a pin-on-ring set up. Similarly, Rout et al. [121] studied the dry sliding wear behavior of epoxy composites reinforced with rice husk fiber and carried out the experiments following Taguchi's orthogonal array. They further used artificial neural network (ANN) technique to predict the wear behavior of this new class of composite within and beyond the experimental domain. Shivamurthy et al. [122] studied the sliding wear as well as the mechanical properties of glass fiber/graphite laminates reinforced in an epoxy matrix. Gyurova et al. [123-124] used ANN for analyzing the sliding wear and sliding friction of polyphenylene composites.

While Jia et al. [125] reported the self-lubricating properties of PTFE/serpentine Nano-composites against steel at varied conditions such as sliding velocity and normal load, Abdelbary et al. [126] investigated the effects of surface cracks on the wear behavior of polyamide 66 composites. Srivastava et al. [127] discussed the effects of addition of short glass fiber in epoxy matrix on the friction and wear properties of the composites. It was reported that the wear rate decreased steadily with addition of graphite to the glass fiber/epoxy composites. Further, it was observed that with increase in the sliding time, the wear rate increased.

Umeda et al. [128] characterized wear particles generated on a worn out surface of pin-on-disc set up using scanning electron microscopy images and established its relationship with the sliding conditions. They further used a well-trained artificial neural network to study this relationship between the wear particles and the sliding conditions. Xian et al. [129-130] investigated the influence of graphite flakes and short carbon fiber reinforcement on the sliding wear behavior of polyetherimide composites. Bajpai et al. [131] used sisal fiber, grewia optiva and nettle fiber as reinforcement in polypropylene matrix and investigated the frictional and sliding wear characteristics of these composites. The tests were carried out by using a pin-on-disc wear test rig under different conditions. Further, they investigated the morphological characteristics of these natural fiber reinforced in a polylactic acid (PLA) based matrix material [132]. The results revealed that polylactic acid based composites are superior to those of polypropylene based natural

fiber reinforced composites. Unal et al. [133] studied the sliding wear characteristics of graphite/polyamide6 and wax/polyamide6 composites under various conditions.

Recently, the sliding wear and friction characteristics of carbon, glass and aramid fiber reinforced in polyamide matrix was made by Zhao et al. [134] against steel and sand paper. The worn out surface of the composites were examined under scanning electron microscope in order to identify the wear mechanism. Similarly, Bajpai et al. [135] studied the tribological behavior of grewia optiva, nettle and sisal fiber reinforced PLA composites under varying operating parameters such as sliding distance, sliding velocity and normal load.

2.6 Acoustic and Thermal Characteristics of Natural Fibers and Polymer Composites

2.6.1 Acoustic Characteristics of Polymer Composites

Now-a-days there has been a rise in the demand for sound absorbing materials for the purpose of acoustic insulation. Acoustic insulating materials gaining importance in industrial application are very much essential in automobile sectors, building construction, etc. Because of this, a lot of research work is now being done in order to develop more advanced and low cost acoustic insulating materials. For a good sound absorbing material, it is essential that it possesses a high sound absorption coefficient. Generally, porous materials have good acoustic insulation properties.

In this regad, an investigation was carried out by Ersoy et al. [136] to study the sound absorbing capacity of tea leaf fiber which is an industrial waste. The tests were carried out within a range of 500 Hz to 3200 Hz and it was concluded that 1cm thick tea leaf fiber is capable of providing insulation which is equivalent to 6 layers of woven cloth thereby proving its capability as an ideal sound absorbing material. Berardi et al. [137] made an elaborate review of various natural fibers such as card board, kenaf, sheep wool, hemp, cork, wood, cane and coconut for its sound absorption coefficient. It was further observed that the acoustic absorption coefficients predicted from established models are in good agreement with the experimentally obtained values. Prabhakaran et al. [138] studied flax fiber reinforced polymer composites for its acoustic as well as vibrational damping characteristics and compared the results obtained with glass fiber. The comparison

revealed that maximum sound absorption coefficient was obtained at a frequency of 1000 Hz and the sound absorption coefficient of flax fiber reinforced composite materials is about 21.42 % higher than that of glass fiber reinforced polymer composites. Similarly, Koruk et al. [139] used the impedance tube testing method to study the sound absorbing behavior of bio luffa fiber and bio luffa fiber-epoxy composite materials which was followed by the determination of transmission loss levels. The sample with luffa fiber and linen was reported to have the highest absorption coefficient followed by luffa fiber-epoxy composites.

Likewise, the acoustic behavior of coir fiber was studied by Fouladi at al. [140] who reported the increase in the sound absorption coefficient with increase in the thickness of the samples at lower frequency range. A maximum absorption coefficient of 0.8 was obtained at a frequency of 1360 Hz. Further, they tried to improve the flammability, stiffness and anti-fungal properties of these coconut coir fibers. In the past, the sound absorption characteristics of wood based materials were made by Con Wassilieff [141]. In the year 1996, Ballagh [142] studied the acoustic properties of wool fiber and compared it with mineral fibers for application in suitable areas. He observed that in order to provide an appreciable sound insulation, a minimum 50 mm thickness of wool fiber should be used. Yang et al. [143] used rice straw and wood particles to prepare composites by using urea-formaldehyde as the binding material. It was observed that composite material with specific gravity of 0.4 and 0.6, have relatively higher sound absorption coefficient than composite material with specific gravity of 0.8. Dong et al. [144] used flax, ramie and jute fiber and compared its sound absorption coefficient with synthetic fibers viz. carbon and glass. It was observed that for a sample of 40 mm thickness, the sound absorption coefficient of jute was reported to be maximum at frequencies above 1000 Hz. Further, it was established that the sound absorption coefficient of carbon and glass fibers are much less than that of the natural fibers considered in the above investigation. Thilagavathi et al. [145] used the impedance tube method to investigate the noise isolation characteristics of jute, bamboo and banana fiber reinforced in a polypropylene matrix for application as interior panels of automobiles. They also studied the tensile strength, stiffness, thermal conductivity and air permeability properties of these samples. Among all the three samples, the bamboo/polypropylene composites recorded highest sound absorption coefficient at a frequency of 800 Hz. Similarly, Xiang et al. [146] used kapok fibers to study its sound insulation characteristics. From the experiments conducted, it was

established that kapok fiber can be considered as an effective and environmental friendly sound absorbing material. Jayamani et al. [147] studied the influence of fiber treatment on the thermal, mechanical and acoustic properties of betelnut fiber reinforced in a polyester matrix. It was recorded that with increase in the fiber content from 5wt% to 20 wt%, the sound absorption coefficient (α) increased from 0.03 to 0.27.

Apart from fibers, research works have also been conducted on the use of particulates as sound absorbing materials. Swift et al. [148] studied the sound absorption characteristics of recycled rubber granules. The investigation of the acoustic behavior of recycled rubber particles were further done by Hong et al. [149]. Zhou et al. [150] used polyurethane and polymer micro-particles to study its sound absorption characteristics. It was revealed that polymer micro-particles have remarkable sound absorbing properties because of their micro structural configuration. While Verdejo et al. [151] studied the acoustic behavior of carbon nano tube filled polyurethane flexible foam, Jiang et al. [152] investigated the sound absorbing characteristics of chlorinated polyethylene composites reinforced with seven hole hollow polyester fibers.

2.6.2 Thermal Characteristics of Polymer Composites

During the years 1960 to 1970, Knappe et al. [153], Ho et al. [154], Peng et al. [155] and Young et al. [156] reported considerable work related to heat transfer in polymer composites. The molecular orientations of polymers were successfully changed by Tavman [157] who studied the anisotropic heat conduction through these composites. More recently, Griesinger et al. [158] investigated and registered an increase in the thermal conductivity of neat polyethylene from 0.350 W/m-K to 50 W/m-K having an orientation ratio of 50. As it is often difficult to fabricate composites with desired molecular orientation, a more feasible option is to modify the thermal conductivity of the polymer by addition of conductive/insulating materials onto the polymer. In the recent past, a lot of investigations have been carried out in order to increase the thermal conductivity of polymers. Many experimental works have been conducted to enhance the effective thermal conductivity of particulate filled polymer composites [159-163].

While most of the available literature deal with the experimental determination of thermal conductivity of polymer composites, few investigations have also been devoted on the numerical analysis [164-165]. Veyret et al. [166] carried out a numerical analysis on the thermal conductivity of particulate/fiber reinforced composite. Similarly, Kumlutas et al.

[167] suggested a numerical model for finding the thermal conductivity of particulate filled polymer composites and compared it with the experimental values. While the thermal behavior of aluminum filled polypropylene composites was studied by Boudenne et al. [168], that of silver particulate filled epoxy composites was investigated by Bjornrklett et al. [169]. Extensive research works related to the study of thermal conductivity of graphite and carbon nanotubes as filler material in different polymer composites have also been done in the past [170-174].

Few research works have also been carried out by researchers on the thermal properties of polymer composites reinforced with natural and synthetic fibers. The thermal insulation characteristics of glass fiber reinforced in polymetalphosphate matrix was investigated by Kim et al. [175]. The investigation revealed the excellent water resistance properties of these composites and the thermal conductivity was reported to be within 1.12-3.34 W/mK. Study on the thermal conductivity of 3D woven fabrics composites were made by Schuster et al. [176]. Finite element method was employed in order to have a better understanding and to improve the thermal conductivity of the composites. A detailed review was made by Zhidong et al. [177] on the thermal characteristics of carbon nanotubes and polymer composites filled with carbon nano tubes. The study provides a detailed report on the effects of tube size, atomic structure and morphology on the conductivity of the composites. Yuksel et al. [178] studied the effective thermal conductivity and its dependency on the temperature in glass wool reinforced aluminium foil. An approach was made by Hang et al. [179] to improve the conductivity of fiber reinforced polymer composites.

Sharifah et al. [180] studied the thermal characteristics of alkali treated hemp blast and kenaf fiber using dynamic mechanical thermal analyzer. Similarly, Idicula et al. [181] investigated the specific heat and thermal conductivity of banana and sisal fiber reinforced polyester matrix. Doan et al. [182] used jute fiber reinforced in a polypropylene matrix and studied its thermal gravimetric characteristics. A lot of research works have been carried out by researchers on the mechanical and thermal characteristics of kenaf fiber reinforced polymer composites [183-185]. While, Khan et al. [186] investigated the thermal, mechanical and environmental degradation behavior of N, N-dymethylae jute fiber reinforced in polypropylene matrix, Braga et al. [187] investigated the thermal and mechanical properties of jute/glass fiber reinforced epoxy matrix. Silva et al. [188] registered a sharp decrease in the glass transition temperature of alkali treated sisal fiber

polyurethane composites with respect to neat polyurethane. Phiri et al. [189] used compression-injection moulding technique to prepare kenaf and sisal fiber reinforced polypropylene composites and studied their thermal and mechanical characteristics. Similarly, Milanese et al. [190] studied the mechanical and thermal behavior of sisal fiber reinforced phenolic resin. Marques et al. [191] used poly-butylene adipate co therepthalate and reinforced it with natural fibers and studied its mechanical and thermal properties.

2.7 Knowledge Gap in Earlier Investigations

From the exhaustive literature review, it is found that there is a huge knowledge gap as far as systematic and well-planned study of natural fiber reinforced polymer composites are concerned. The following points highlight some of these knowledge gaps:

- A lot of research investigations have been reported in the recent past on polymer composites reinforced with some most commonly used natural fibers such as bagasse, jute, hemp, sisal, bamboo, flax, etc. But research investigations related to palmyra fiber as a reinforcing material in polymer matrix are very few.
- Most of the available literature is connected with the use of thermoplastic matrix material. Almost no report is available on the use of epoxy (thermosetting matrix) as the matrix material in the palmyra fiber reinforced composite.
- Till now, no work has been reported relating to the molecular structure and crystallinity of epoxy composites reinforced with palmyra fiber.
- Available literature only focuses on the mechanical properties and no reports are available relating to the study of wear mechanism, thermal behavior and acoustic properties of these composites.
- A number of researches have been reported on polymers reinforced with either long unidirectional fiber or woven fiber mats, but investigations on composites with short natural fibers are limited.

In view of the above knowledge gap, the present work has been undertaken to investigate the physical, mechanical, micro-structural, wear, acoustic and thermal behavior of epoxy composites reinforced with short palmyra fibers (SPF) in different proportions.

2.8 Objectives of the Present Work

The specific objectives of the present research are outlined as follows:

- Processing and fabrication of a new class of epoxy composites reinforced with short palmyra fibers (SPF).
- Physical, mechanical and micro-structural characterization in regard to their density, void fraction, tensile strength, flexural strength and micro hardness.
- Study of the effects of fiber content on the wear behavior of the composite samples and development of an optimal parameter setting for minimum wear rate using Taguchi's orthogonal array.
- Implementation of Artificial Neural Network technique for prediction of the wear rate under different conditions within and beyond the experimental domain.
- Study of the effects of SPF content and composite thickness on the acoustic properties.
- Study of the effects of SPF content on the effective thermal conductivity, glass transition temperature and coefficient of thermal expansion of the samples.
- Exploring the possibilities of using these composites in suitable application areas.

Chapter Summary

This chapter has provided the following information:

- An exhaustive literature review related to polymer composites and various aspects of fiber reinforced polymer composites.
- The knowledge gap in earlier investigations.
- The objectives of the present investigation.

The next chapter provides the details of the materials used and the process of fabricating the composites along with the details of the experiments carried out subsequently.

*****

CHAPTER 3

Materials and Methods

Chapter 3

Materials and Methods

This chapter describes the details of materials and methods used in the current investigation for the fabrication and characterization of the composites under study. The chapter presents a brief description of experiments and parameters related to the physical, mechanical, micro-structural, tribological, acoustic and thermal behavior of the prepared epoxy-SPF composites.

3.1 Materials Used

A composite material essentially consists of two phases in which one is known as the matrix phase and the other is the reinforcing phase. The matrix material forms the base of the composite and is a continuous phase while the reinforcing material is a discontinuous phase which is embedded over the matrix material. The reinforcing phase is usually much harder and stronger as compared to the matrix material. The main purpose of the matrix material is to provide strength and rigidity to the composite and to transfer the stresses from the reinforcing phase. The matrix material also protects the reinforcing phase from mechanical and environmental damages. Generally, the properties of a composite are much superior to those of its parent constituents.

3.1.1 Matrix Material

Generally, the matrix material is divided into three broad categories i.e. metal matrix, ceramic matrix and polymer matrix. Among them, polymers are widely used because of their cost effectiveness, superior room temperature properties when compared to its counterparts and ease of fabricating complex structures and contours with a relatively decreased tooling cost. Polymers have excellent resistance towards corrosion, low coefficient of thermal expansion, wear resistance, etc.

The polymer matrices are again divided into two types i.e. thermoset and thermoplastic polymer. Thermosets are formed as a result of an irreversible chemical transformation of the resin into polymer matrix having amorphous cross-links [192]. Thermosets provide good thermal and electrical insulation because of its molecular structures. The low viscosity of thermosets facilitates proper fiber wetting, enhanced thermal stability and better resistance towards creep [193]. Polyester, epoxy, phenolic resin and vinyl ester are some of the most widely used thermoset polymers. On the other hand thermoplastic polymers because of the intermolecular forces are associated through chain and these forces permit the remolding of the thermoplastics. With increase in the cooling, the intermolecular interaction increases which restores the bulk properties. These types of polymer generally are produced in single step and then the products are manufactured in subsequent steps. Thermoplastics are also recyclable as they can be reshaped and can be formed into new material when reheated each time. Polyethylene, polystyrene, acrylic, teflon, nylon, polyvinyl chloride, polypropylene, etc. are some of the thermoplastic polymers available in the market.

Epoxy resins are the most commonly used thermosetting polymers among a wide variety of polymers available in the market for making many advance composites owing to their excellent mechanical and electrical properties, enhanced adhesion to a wide variety of fibers and better performance at increased temperatures. They also have good chemical resistance and have low shrinkage due to solidification. In the current investigation, epoxy (LY 556) has been selected as the matrix material because of the huge number of advantages offered by them as mentioned above. It chemically belongs to the 'epoxide' family and its common name is Bisphenol-A-Diglycidyl-Ether (commonly abbreviated to DGEBA or BADGE). Figure 3.1 shows the molecular chain structure of epoxy resin used in the present research. A solvent free curing system at room temperature is provided by the epoxy resin when it is mixed with tri-ethylene-tetra-amine (TETA) hardener which is essentially an primary aliphatic amine having commercial designation HY 951 (Figure 3.2). The epoxy resin LY-556 (Figure 3.3) and hardener HY-951 used in the present work are procured from Ciba Geigy India Ltd. Some of the important properties of epoxy are enlisted in Table 3.1.

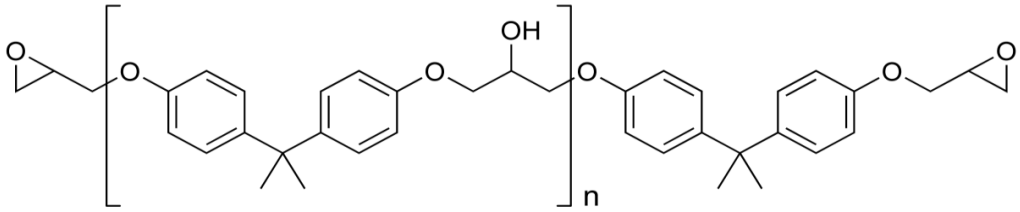

Figure 3.1: Unmodified epoxy resin ('**n**' denotes number of polymerized unit)

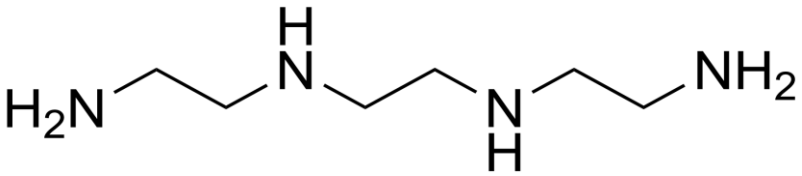

Figure 3.2: Tri-ethylene-tetramine (hardener used for epoxy matrix)

Table 3.1: Some essential properties of epoxy resin

Characteristic Property	**Inferences**
Density	1.10 gm/cc
Tensile strength	58.0 MPa
Compressive strength	90.0 MPa
Thermal conductivity	0.3630 W/m-K
Micro-hardness	0.0850 GPa
Coefficient of Thermal expansion	62.830 ppm /°C
Glass transition temperature	98.0°C
Electrical conductivity	0.105×10^{-16} S/cm

Figure 3.3: Epoxy resin and corresponding hardener

3.1.2 Reinforcement

The reinforcing phase of a composite can be in the form of particles, fibers, whiskers, mesh or lamellae. The present research work employs Palmyra Palm as the natural fiber reinforcement in the epoxy matrix to fabricate a set of fiber reinforced composites. Palmyra palm (Borassus flabellifer) belongs to the family of Arecaceae and is a genus of six species of fan palms [194]. These trees are found in the tropical region of Africa and Asia. The leaves of these trees are fan shaped and the tree can grow as high as 30 m (Figure 3.4). The leaves of the tree are used for thatching, fabricating mats, baskets, hats, umbrellas, broom sticks, painting brushes etc. The leaves are held by the stem called stalks (Figure 3.5) which is about 1m in length and it has a lot of fibers embedded in it. The stalks are normally used for making fences.

The structure of palmyra palm leaf stalk itself can be considered as a composite material which consists of long and aligned cellulose fibers immersed in a matrix of lignin. Most of the constituents of palmyra fiber consist of cellulose, hemicellulose, lignin, pectine and some extractives. In this work Short Palmyra Fibers (SPF) are used in the reinforcing phase for fabricating the composites (Figure 3.6). The palmyra fiber is extracted after cutting it from the palm tree. The stalks are cut into long strips and immersed in water for a period of 10 days which is followed by drying for 5 days in sunlight. The fibers are then cut into an approximate length of 3mm with scissor. This fiber has a very low density of about 1030 kg/m^3 and has an average tensile modulus of 2.75 GPa. Some of the important properties of palmyra fiber are listed in Table 3.2.

Figure 3.4: Palmyra Palm tree

Figure 3.5: Palmyra Palm leaf stalk

Figure 3.6: Short palmyra fiber

Table 3.2: Mechanical properties of palmyra fiber [194]

Properties	**Inference**
Tensile strain	13.71 %
Average tensile modulus	2.75 GPa
Specific tensile strength	0.3660 MPa
Specific tensile modulus	2.67 MPa
Density	1030 Kg/m^3
Moisture content	12.08 %

3.2 Composite Fabrication

In the present research work, the composites are fabricated using the simple hand-lay-up technique which is considered as the oldest and most inexpensive open molding method of composite fabrication. The pre-requirements of this process are very less and the fabrication steps are quiet simple. The following are the general steps used in this investigation for preparing epoxy-SPF composites of different compositions.

1) The low temperature curing epoxy resin (LY 556) and its corresponding hardener (HY 951) are mixed in the ratio of 10:1 by weight as recommended.
2) The short palmyra fiber (SPF) of 2-3 mm in length is then added to this solution of epoxy and hardener followed by thorough hand stirring.
3) Before the epoxy-SPF mixture is decanted into the mold, a silicon releasing spray (Figure 3.7) is done over the entire mold surface. This helps in easy removal of the cured composite samples. The thoroughly mixed dough is then slowly poured into the molds (Figure 3.8) so as to get the disc shaped specimens (50 mm diameter and 3 mm thickness), cylindrical shaped specimens (10 mm diameter and 70 mm length) and rectangular shaped specimens (150 mm length, 20 mm breadth and 3 mm thickness).
4) The cast of each sample is left to cure for about 24 hours before it is removed from the mold. The thermal conductivity and acoustic absorption coefficient are found by using the disc shaped samples. The cylindrical shaped specimens are used for carrying out the sliding wear test and the rectangular shaped specimens are used for evaluating the flexural, tensile and hardness of the samples.

Figure 3.9 shows the composite sample fabricated through hand-lay-up technique and Figure 3.10 shows the pictorial representation of the fabrication process. The compositions of the various composites fabricated are given in Table 3.3.

Figure 3.7: Silicon releasing spray

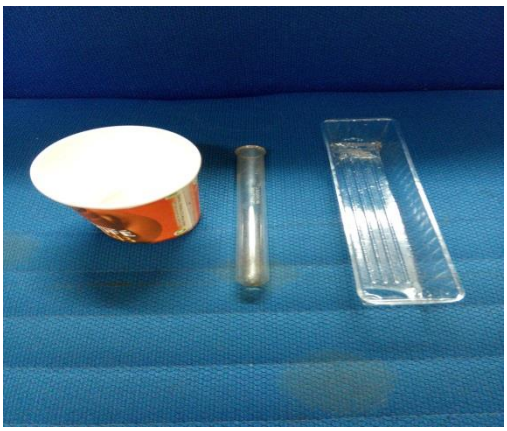

Figure 3.8: Molds used during fabrication

Figure 3.9: Epoxy-SPF composite sample

Figure 3.10: Fabrication process by using hand-lay-up technique

Table 3.3: Epoxy composites reinforced with short palmyra fiber

Designation	Composition
ESPF 1	Epoxy + 0 wt.% SPF
ESPF 2	Epoxy + 2.0 wt.% SPF
ESPF 3	Epoxy + 4.0 wt.% SPF
ESPF 4	Epoxy + 6.0 wt.% SPF
ESPF 5	Epoxy + 8.0 wt.% SPF
ESPF 6	Epoxy + 10.0 wt.% SPF
ESPF 7	Epoxy + 12.0 wt.% SPF
ESPF 8	Epoxy + 14.0 wt.% SPF

3.3 Physical Characterization

3.3.1 Density and Void Fraction

The composite density can be found out by using any one of the three methods: The Archimedes method, the density gradient method, or the sink-float method. In the present work, the Archimedes principle is used to determine the actual density (ρ_a) of the composites. The ASTM D 792 standard covers this method. According to the Archimedes principle, the apparent loss of weight in a body when it is immersed in a liquid medium is equal to the fluid displaced by it. The actual density of the composite can be calculated by using the equation 3.1.

$$\rho_a = \frac{\rho_w W_a}{W_a - W_w} \tag{3.1}$$

Here ρ_a denotes the actual density of the composite, ρ_w denotes the density of distilled water and W_a the weight of the sample in water. The theoretical density of the composite (ρ_t) in terms of weight fraction can easily be obtained as per the following equation given by Agrawal and Broutman [195].

$$\rho_t = \frac{1}{\left(W_p / \rho_p\right) + \left(W_m / \rho_m\right)} \tag{3.2}$$

Where, W represents the weight fraction and ρ represent the density respectively. The suffixes p and m stand for the reinforcement and matrix material respectively. The presence of voids will add to the total volume, but not to the weight of the composite. V_v is the void content which is then expressed as:

$$V_v = \frac{(\rho_t - \rho_a)}{\rho_t} \tag{3.3}$$

3.4 Mechanical Characterization

3.4.1 Tensile Strength

Generally, flat specimens are used to carry out the tensile test. The dimension of the specimen used to carry out the test is of 150 mm in length, 20 mm in width and 3 mm in thickness. A uniaxial load is applied at both ends of the specimen. The tests are carried out according to ASTM E 1309 standard. *Instron* 1195 (Figure 3.11a) universal testing machine has been used in the present investigation at a crosshead speed of 10 mm/min in order to conduct the experiment. Further, the results are used to calculate the strength of the composite. Figure 3.11b shows the loading arrangement of the specimen. The test has been conducted on 4 composite samples of each composition and the mean value of the 4 results obtained has been reported as the tensile strength of that specimen.

3.4.2 Flexural Strength

The flexural strength of any material is generally defined as the maximum bending it can withstand before it reaches the breaking point. The present test has been carried out by using *Instron* 1195 universal testing machine following the three point bending method. The dimension of each specimen used is of 60 mm length, 20 mm width and 3 mm thickness with span length of 40 mm. A constant crosshead speed of 10 mm/min is maintained throughout the test. The tests are repeated four times and the mean value of the 4 results obtained is used to calculate the flexural strength. The following equation is used to determine the flexural strength of the composite:

$$F.S. = \frac{3PL}{2bt^2} \tag{3.4}$$

Where, *L* is the span length of the sample (mm), *P* is maximum load (N), *b* is the width of the specimen (mm) and *t* is the thickness of the specimen (mm).

3.4.3 Micro-hardness

In the present research work, a Vaiseshika micro-hardness tester (Figure 3.12) is used to perform the micro-hardness test. A right pyramid form of diamond indenter with a square base having an angle of 136^0 between the opposite faces is forced with a force *F* into the material. The two diagonals *X* and *Y* of the indentation left on the surface of the material after removal of the load are measured and their arithmetic mean *L* is calculated. In the present work, a load of *F* = 0.5 N is applied and the Vickers hardness number is calculated by the following equation:

$$H_V = 0.1889\frac{F}{L^2} \tag{3.5}$$

$$\text{and} \qquad L = \frac{X+Y}{2} \tag{3.6}$$

where, *F* is the applied load (N), *L* is the diagonal of the square impression (mm), *X* is the horizontal length (mm) and *Y* is the vertical length (mm).

3.5 Wear Characterization

3.5.1 Sliding Wear Test

A MAGNUM pin-on-disc friction and wear monitoring test rig (Figure 3.13a) has been used in the current investigation in order to evaluate the response of the epoxy-SPF composites towards dry sliding wear as per the ASTM G 99 standards. The counter body is made up of hardened ground steel having 0.6 μm Ra surface roughness and 72 HRC hardness. The cylindrical shaped specimen is held stationary and the counter body is made to rotate. Lever mechanism is used to apply the normal load. A series of tests are conducted with varying parameters. Four sliding velocities of 63.0, 125.0, 190.0 and 250.0 cm.s−1 are chosen for the experiment and normal loads of 5, 10, 15 and 20 N are applied on each of the selected velocities. The loading arrangement for wear test is shown in Figure 3.13b.

(a) (b)

Figure 3.11: *Instron* 1195 universal testing machine and loading arrangement for tensile test

Figure 3.12: Vaiseshika micro-hardness tester

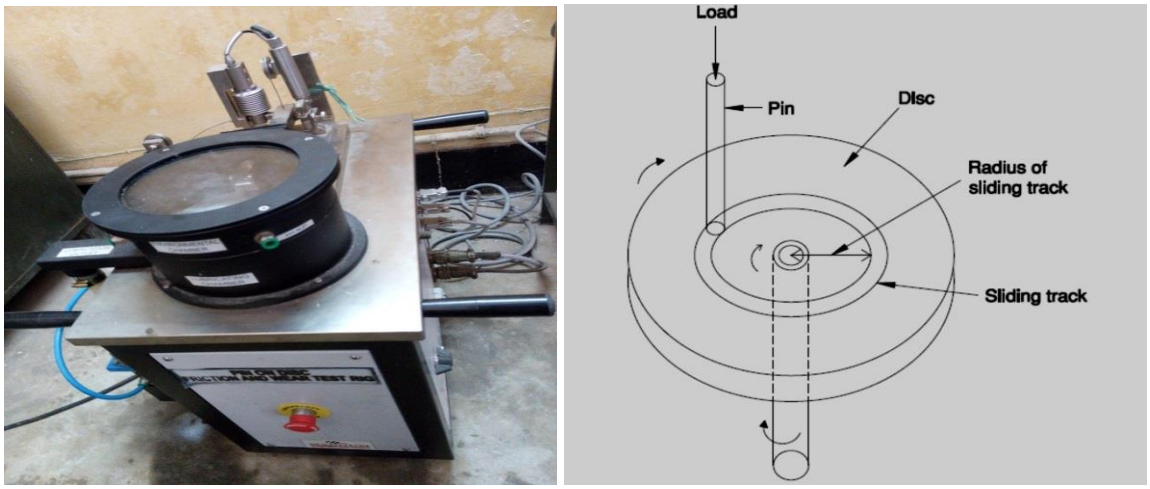

(a) (b)

Figure 3.13: Pin-on-disc wear test set up and its loading arrangement

A precision electronic balance with accuracy ±0.1 mg is used in order to find out the mass loss of material from the composite surface and the specific wear rate (mm^3/N-m) is found out by the following equation:

$$W_S = \frac{\Delta m}{\rho t V_s F_n} \tag{3.7}$$

Where the loss of mass of the composite is given by Δm, ρ represents the density of the composite (g/mm^3), t denotes the test duration (s), V_s the sliding velocity (cm.s−1), and the average normal load (N) is given by F_n.

3.5.2 Taguchi's Experimental Design for Sliding Wear Test

The influence of control factors on the output performance can be successfully analyzed using a very powerful tool known as design-of-experiment. The most critical stage of the design-of-experiment is the selection of the significant factors. Thus, the non-significant factors can be eliminated in the first step itself. In the current investigation of sliding wear rates of epoxy-SPF composites, four major factors have been considered such as fiber content, normal load, sliding distance and sliding velocity each at 4 levels according to Taguchi's L_{16} orthogonal array as shown in Table 3.4.

Table 3.4: Selected levels of control factors for dry sliding wear test

	Levels				
	1	**2**	**3**	**4**	**Units**
(A) Sliding velocity	63.0	125.0	190.0	250.0	Cm/sec
(B) Normal load	5.0	10.0	15.0	20.0	N
(C) Sliding distance	250.0	500.0	750.0	1000.0	m
(D) Fiber content	0.0	4.0	8.0	12.0	Wt. %

By using the Taguchi's L_{16} array the number of experiments reduced from 256 conventional runs to only 16 runs thereby saving a lot of experimental cost and time. The results obtained are again transformed to signal-to-noise (S/N) ratios. Generally, three types of S/N ratio are available depending on the type of characteristics such as:

"Smaller-the-better" characteristics: $$\frac{S}{N} = -10\log\frac{1}{n}\left(\sum y^2\right) \quad (3.8)$$

"Larger-the-better" characteristics: $$\frac{S}{N} = -10\log\frac{1}{n}\left(\sum\frac{1}{y^2}\right) \quad (3.9)$$

"Nominal-the-best" characteristics: $$\frac{S}{N} = 10\log\left(\sum\frac{\bar{Y}}{S^2}\right) \quad (3.10)$$

Where n represents the number of observations, y is the observed data, Y represents the mean and the variance is represented by S. As we need to minimise the specific wear rate, therefore "smaller is better" S/N ratio has been selected which is calculated as logarithmic transformation of loss function as shown below:

Smaller is the better characteristic: $$\frac{S}{N} = -10\log\frac{1}{n}\left(\sum y^2\right) \quad (3.8)$$

Table 3.5: Taguchi experimental design (L_{16} orthogonal array)

Test Runs	**(A) Sliding Velocity (cm/sec)**	**(B) Normal Load (N)**	**(C) Sliding Distance (m)**	**(D) SPF Content (wt. %)**
1	63	5	250	0
2	63	10	500	4
3	63	15	750	8
4	63	20	1000	12
5	125	5	500	8
6	125	10	250	12
7	125	15	1000	0
8	125	20	750	4
9	190	5	750	12
10	190	10	1000	8
11	190	15	250	4
12	190	20	500	0
13	250	5	1000	4
14	250	10	750	0
15	250	15	500	12
16	250	20	250	8

3.5.3 Wear Rate Prediction Using Artificial Neural Network

Artificial neural network (ANN) has emerged as one of the powerful intelligence concepts adopted on a wide range of engineering applications. ANN consists of massive parallel structures and has the capacity to learn from examples which helps it to provide an accurate analytical solution for different non-linear modelling problems. ANN has already been used in the field of medical science, classification and control of dynamic systems, image and speech recognition, etc.; but only recently it has been used in modelling the mechanical behavior of fiber reinforced composite materials [196-198].

It is difficult to find an accurate mathematical model to assess the performance of a newly developed material or an existing material under untested conditions using the few databases of the test results. In such situation, the biologically motivated computing paradigm on ANN has emerged as a superior modelling tool. Biological system functionality is based on inter-connection of a large number of neurons. In human beings, a neuron is simply a processing unit that receives and combines signals received from other neurons.

A simple ANN structure consists of three layers. The input parameters are applied to the input layer while the results are obtained at the output layer. In between these input and output layers, lies the hidden layer which consists of hidden neurons. Addition of more than one hidden layers to structures having large input size enables the network to extract higher-order statistics. The information signal travels through the system in a forward course on a layer by layer basis.

The following four stages summarize the process of creating ANN for material research:

1. Collection of database: analysis and pre-processing of the data.
2. Neural network training: this stage consists of choice for network structure, functions for training, training algorithms and network parameters.
3. Trained network testing: for evaluation of network performance.
4. Use of the trained ANNs for simulation and prediction.

A back propagation algorithm has been used for training and validating the input data obtained from various experimental trials in the present work.

3.6 Scanning Electron Microscopy, Thermal and Acoustic Characterization

3.6.1 Scanning Electron Microscopy

The micro-structural characteristics of the epoxy-SPF composite samples under study are examined by JEOL JSM-6480 LV Scanning Electron Microscope (Figure 3.14). The samples are properly cleaned, dried and mounted on the stubs using silver paste. A thin film of platinum is vacuum-evaporated onto the specimens before the images are taken in order to improve the penetration of light and for better surface micrographs.

3.6.2 Thermal Characterization

Effective thermal conductivity: Experimental Determination

Equipment used:

Unitherm Model 2022 thermal conductivity tester (Figure 3.15).

Operating principle:

Thermal conductivity is a material property which describes the flow of heat within a body per unit area for unit temperature difference. It is a measure of resistance of a material towards transmission of heat. The equation for one dimensional heat flow is given by:

$$Q = kA\left(\frac{T_1 - T_2}{x}\right) \tag{3.11}$$

Where, the heat flux is given by Q in Watt (W), A represents the cross-sectional area (m^2), k represents the thermal conductivity (W/mK), the sample thickness is given by x (m) and T_1-T_2 is the difference in temperature between two surfaces (^{0}C or K). The thermal resistance is given by the following equation:

$$R = \frac{T_1 - T_2}{Q} \tag{3.12}$$

Where, R represents the thermal resistance between the two surfaces.

The experiments are conducted according to ASTM E 1530 standards. In Unitherm 2022, the temperature difference between upper and lower plate and the value of heat flux Q is

measured by transducers. Thus, the thermal conductivity between the two surfaces can be successfully calculated by providing samples of known cross-sectional area and varying thickness as input parameters.

Glass transition temperature and coefficient of thermal expansion: Experimental Determination

Equipment used:

Thermal Mechanical Analyzer

Glass transition temperature (T_g) can be defined as the temperature at which the mechanical properties of amorphous polymer changes from brittle state to a rubbery state. Thermal conductivity is the critical property that changes swiftly from a relatively lower value to a higher value at the glass transition temperature. Such kind of change is not acceptable as stresses are induced in the material when it is subjected to high temperatures during production, assembly or during their service-life. Similarly, coefficient of thermal expansion (CTE) is the rate of change of the expansion of a material with temperature. In the present work, a *Perkin Elmer DSC-7 Thermal Mechanical Analyzer* (TMA) is used in expansion mode to measure the T_g and CTE of the composite samples (Figure 3.16).

At first, nitrogen gas is used to clean the TMA sample stage. The length of the samples is set between 6-8 mm while the width and the thickness is maintained at about 2-3 mm. The specimen is heated from 30 to 150 °C at a heating rate of 5°C/min during the TMA measurement. Two heating scans are used for each measurement. The first heating scan is used to remove any possible internal stress and moisture in the sample which is likely to be generated during the curing and sample preparation process. The second heating scan is used to determine the T_g and CTE of the material.

3.6.3 Acoustic Characterization

Absorbing materials plays a vital role in designing soundproof automobile interior, buildings, studio halls, etc. The extent to which a material can absorb the intensity of sound falling on it is represented by the sound absorption coefficient (α) of the material. The more the sound absorption coefficient, the more will be its soundproofing capacity. In the present study, an impedance tube tester is used to calculate the sound absorption coefficient of the given composite materials as per the ASTM E 1050 standards. Figure 3.17 shows the schematic representation of apparatus used for measuring the sound absorption coefficient.

Figure 3.14: Scanning electron microscope (JEOL JSM-6480 LV)

Figure 3.15: Thermal conductivity tester *Unitherm* 2022

Figure 3.16: Perkin Elmer DSC-7 Thermal Mechanical Analyzer

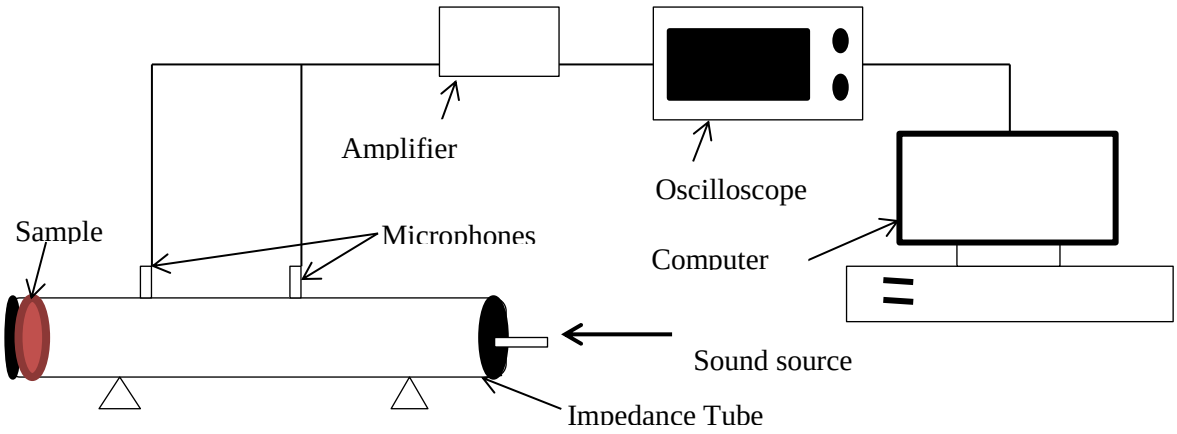

Figure 3.17: Schematic representation of apparatus used for measuring sound absorption coefficient

In the current investigation, Bruel&Kjaer Frequency Analyzer Type 2107 has been employed which is designed especially for use with the Standing Wave Apparatus Type 4002, so that the sound power absorption coefficients may be measured directly without calculation. The impedance tube testing method is implemented by the generation of plane wave in a tube by a sound source and then the sound pressures are measured in a microphone position in close proximity of the sample. The set-up consists of an impedance tube in which the samples are placed at one end and sound source (loudspeaker) is connected at the other end of the tube. Sample size of 3 mm and 100 mm diameter are used for the above test. The loudspeaker generates random sound waves which propagates through the tube and strikes the sample under consideration. As the sound waves strike the sample, some waves are absorbed and the rest are reflected back. In the present test, a frequency range of 125 – 4000 Hz is selected for calculating the sound absorption coefficient. The computer connected to the set-up then tests the sound absorptive material, processes the results, and reports the results in a graph of the absorption coefficient for various frequencies. Thus, the absorption coefficient of each sample is obtained.

3.7 Fourier Transform Infrared Spectroscopy

Fourier Transform Infrared (FTIR) spectroscopy is a workhorse tool to determine the molecular structure of a material. It is based on the principle that no two molecular structures will provide the same infrared spectrum and thus, it is also called the fingerprint

of molecules. When a sample is placed in the spectrometer and IR radiation is passed through it, some radiation gets trapped while others are transmitted. This resulting spectrum represents the molecular transmission and absorption, creating a fingerprint which helps to determine the molecular structure. FTIR spectroscopy is very helpful in determining the unknown material and its amount present in the material.

In the present research work, Perkin Elmer FTIR spectrometer (Figure 3.18) is used for analyzing the molecular structures present in the raw short palmyra fiber (SPF) and the epoxy-SPF composites under consideration. A hydraulic press is used to prepare the pellet shaped samples prior to performing the test.

Figure 3.18: Perkin Elmer FTIR spectrometer

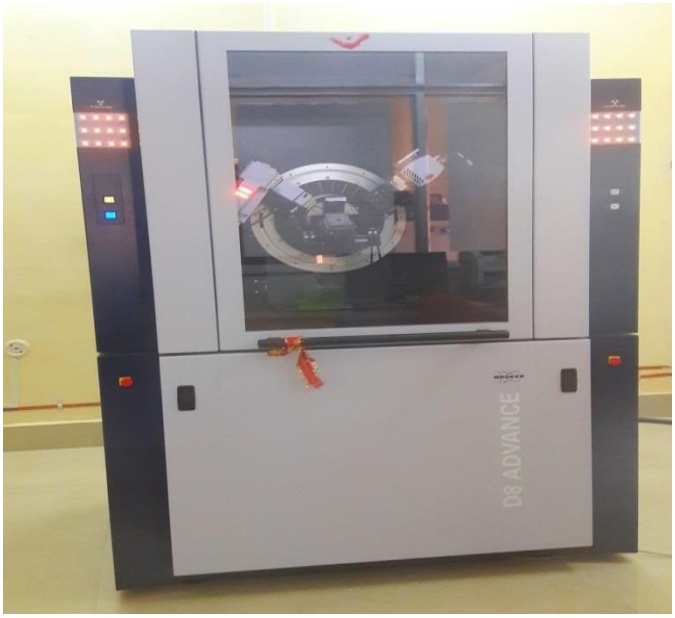

Figure 3.19: BRUKER D8 ADVANCE X-Ray diffractometer

3.8 X-Ray Diffraction

X-Ray diffraction is a very essential technique to study and determine the crystallinity, crystallite size and atomic arrangement of a sample in depth. It is based on the principle that when a focused beam of monochromatic X-Ray is incident on the sample, it gets irradiated. When the atoms present in the sample interact with each other, the diffracted X-Ray is produced and the Bragg's equation is satisfied. The phase and chemical composition of the samples are characterized by this resulting spectrum.

In the present research work, BRUKER D8 ADVANCE X-Ray diffractometer (Figure 3.19) is used for carrying out the test. The samples are scanned in 2θ ranging from 5^0 to 40^0 (1^0/min).

Chapter Summary

This chapter has provided:

- The description of materials (matrix and fiber) used in this research.
- The details of fabrication of the composites.
- The details of physical, mechanical, wear, thermal and acoustic characterization tests.

The next chapter presents the test results related to the physical, mechanical and micro-structural properties along with the FTIR spectroscopy and XRD analysis of the polymer composites under study.

*****

CHAPTER 4

Results and Discussion: I Physical, Mechanical and Micro-structural Characteristics of the Composites

Chapter 4

Results and Discussion: I
Physical, Mechanical and Micro-structural Characteristics of the Composites

This chapter presents the test results in regard to the physical and mechanical properties of the epoxy composites reinforced with short palmyra fibers (SPF). The effects of the fiber reinforcement on the mechanical and physical characteristics of the epoxy-SPF composites under study have been discussed in this chapter.

4.1 Physical Characteristics

4.1.1 Density and Void Fraction

Table 4.1 shows the measured and the theoretical density of the epoxy-SPF composites along with the void fraction. It is found that the measured density of the composites obtained from Equation 3.1 is somewhat less than that of the theoretical density of these composites obtained from Equation 3.2. This difference can be attributed to the presence of voids and pores in the composites which are formed during the fabrication process. It is also found that with the increase in the fiber content, the density of the composite decreases steadily. While the density of the composite is found to be 1.1 gm/cc at 0 wt% of fiber content, it registers a decrease in the density from 1.1 gm/cc to 1.089 gm/cc when the fiber content is increased to 14 wt%. However, the void fraction increases as the fiber content is increased in the epoxy composites.

The density of a composite is one of the most detrimental factors to determine its properties which largely depend on the relative proportion of the matrix material and reinforcement. The difference between the values of theoretical density and measured

density is a result of void present in the composites. The presence of voids in a composite adversely affects its mechanical properties and at the same time the performance of these composites in workplace is hampered.

Table 4.1: Theoretical and measured densities of epoxy-SPF composites

SPF Content (wt%)	**Theoretical Density (gm/cc)**	**Measured Density (gm/cc)**	**Volume Fraction of Voids (%)**
0	1.1	1.095	0.454
2	1.098	1.090	0.728
4	1.097	1.085	1.093
6	1.095	1.082	1.187
8	1.094	1.078	1.462
10	1.092	1.072	1.831
12	1.091	1.069	2.016
14	1.089	1.053	3.305

A higher void content increases the susceptibility to water penetration, increased weathering and decrease in the fatigue resistance [195]. Thus, it is essential to have knowledge of void content in order to estimate the actual quality of the composites. The less is the void content, the better will be the properties of the composites. However, presence of void is unavoidable particularly in composites made through hand-lay-up technique.

4.2 Mechanical Characteristics

For a new class of composites, the strength and other mechanical property evaluation is very much essential in order to characterize the composites. In the present work, a set of data has been provided that are obtained from various tests conducted under controlled laboratory conditions in order to evaluate the characteristics of these composites.

4.2.1 Tensile Strength

The tensile strengths of the composite specimens are evaluated and the test results for various epoxy-SPF composites are presented in Figure 4.1. It is found that with increase in the SPF content, tensile strength of the composite increases. With a reinforcement of 2

wt% of SPF, the tensile strength of the composite is found to be improved from 65MPa to 78MPa, which indicates an improvement of about 20%. With further addition of the SPF, the tensile strength increases steadily and registers an increment of about 143 % at 14 wt% of SPF content. This can be attributed to the reason that with increase in fiber content, the axial load carrying capacity of the composite improves.

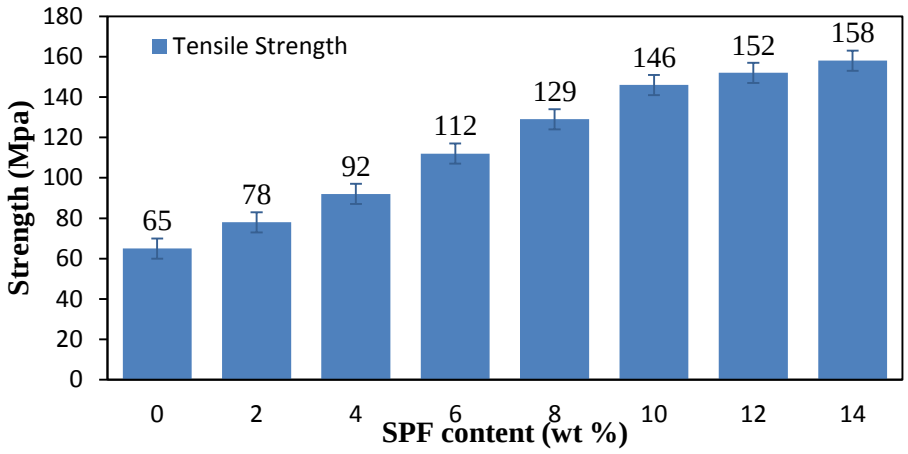

Figure 4.1: Graphical representation of tensile strength

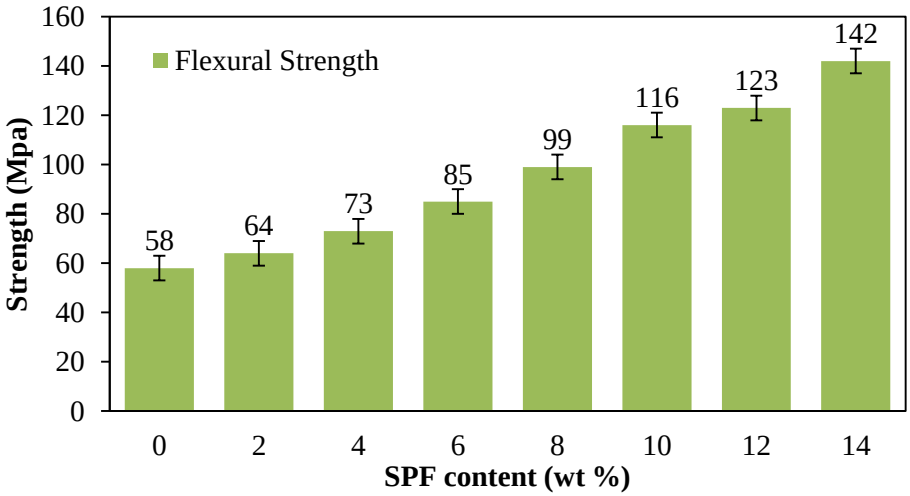

Figure 4.2: Graphical representation of flexural strength

4.2.2 Flexural Strength

Since composite materials are used in structural applications, they are prone to failure by bending in many situations. So, it is essential to have composites with good resistance to bending. In the present work, the flexural strength values of the epoxy-SPF composites are evaluated and the variations are presented in Figure 4.2. A gradual improvement in flexural strength is recorded in case of epoxy composite reinforced with short palmyra

fibers and this improvement is found to be proportional to the fiber content. It is found that while the flexural strength of neat hardened epoxy is about 58MPa, with the addition of just 2wt% of SPF, it increases to about 64MPa. Similarly, with incorporation of 14wt% of SPF, the flexural strength of the composite improves by about 144% and attains a value of 142MPa. The Table 4.2 shows the flexural strength and the tensile strength of the epoxy-SPF composites.

Table 4.2: Mechanical properties of epoxy-SPF composites

Sample	**Tensile strength (MPa)**	**Flexural strength (MPa)**
Epoxy + 0wt % SPF	65	58
Epoxy + 2wt % SPF	78	64
Epoxy + 4wt % SPF	92	73
Epoxy + 6wt % SPF	112	85
Epoxy + 8wt% SPF	129	99
Epoxy + 10wt% SPF	146	116
Epoxy + 12wt% SPF	152	123
Epoxy + 14wt% SPF	158	142

4.2.3 Micro-hardness

The wear resistance of any material is dependent on the hardness of that material. In the present research work, the micro-hardness values of the epoxy-SPF composites with different SPF content have been obtained and are presented in Figure 4.3. It is evident that with addition of SPF, micro-hardness of the composite is improved. With an addition of 2 wt% of SPF in the neat epoxy, the micro-hardness of the neat epoxy increases from 0.085 GPa to 0.091 GPa which is an increase of about 7%. With further addition of fiber to the neat epoxy, the micro-hardness increases and at 14 wt% it registers an increase of about 114%.

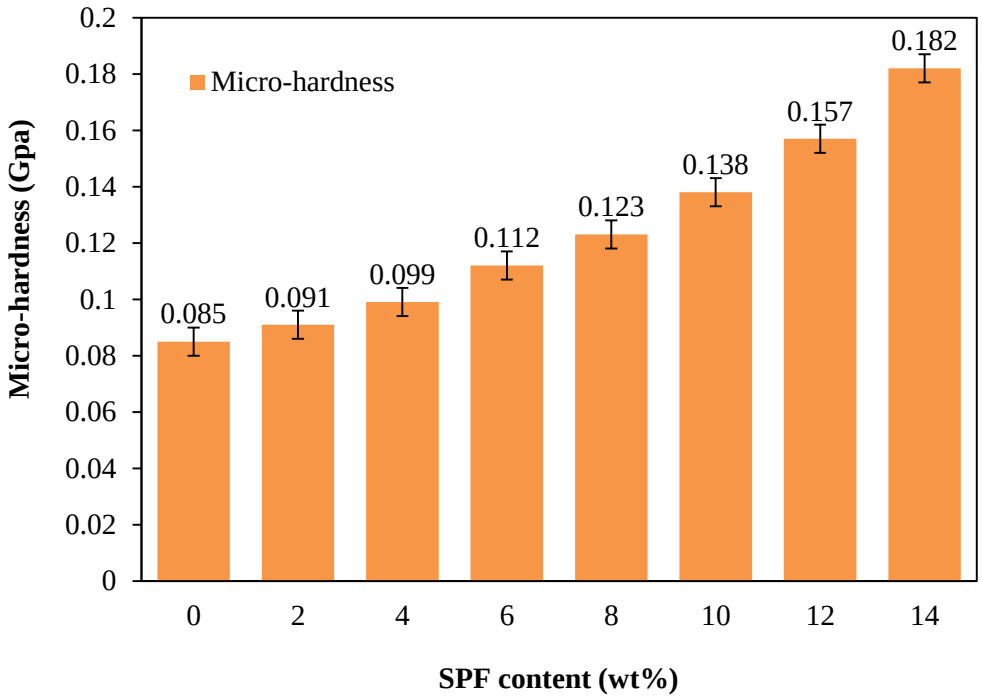

Figure 4.3: Micro-hardness of SPF-epoxy composites

4.3 Fourier Transform Infrared Spectroscopy

The FTIR spectroscopy was carried out using the Perkin Elmer spectrometer on the raw palmyra fiber and on the epoxy-SPF composites. The spectroscopy results for both raw fiber and epoxy-SPF composite are shown in Figure 4.4 and Figure 4.5 respectively. Figure 4.4 reveals nine major downward peaks. The band at 3374.02 cm^{-1} suggests the formation of amines and amides stretching (N-H bond). Peaks at 2887.95 cm^{-1} and 2828.02 cm^{-1} suggests the presence of alkane (C-H) and aldehydes (H-C=O: C-H) stretching respectively. Wavenumber 1645.81 cm^{-1} shows the presence of –C=C- stretching. Peak at 1514.82 cm^{-1} suggests the formation of nitro compounds. There is a major peak at 1053.08 cm^{-1} suggesting the presence of aliphatic amine stretching (C-N). Figure 4.5 shows the FTIR analysis of the epoxy-SPF composites. The analysis revealed many new peaks which are sharper than the Figure 4.4.

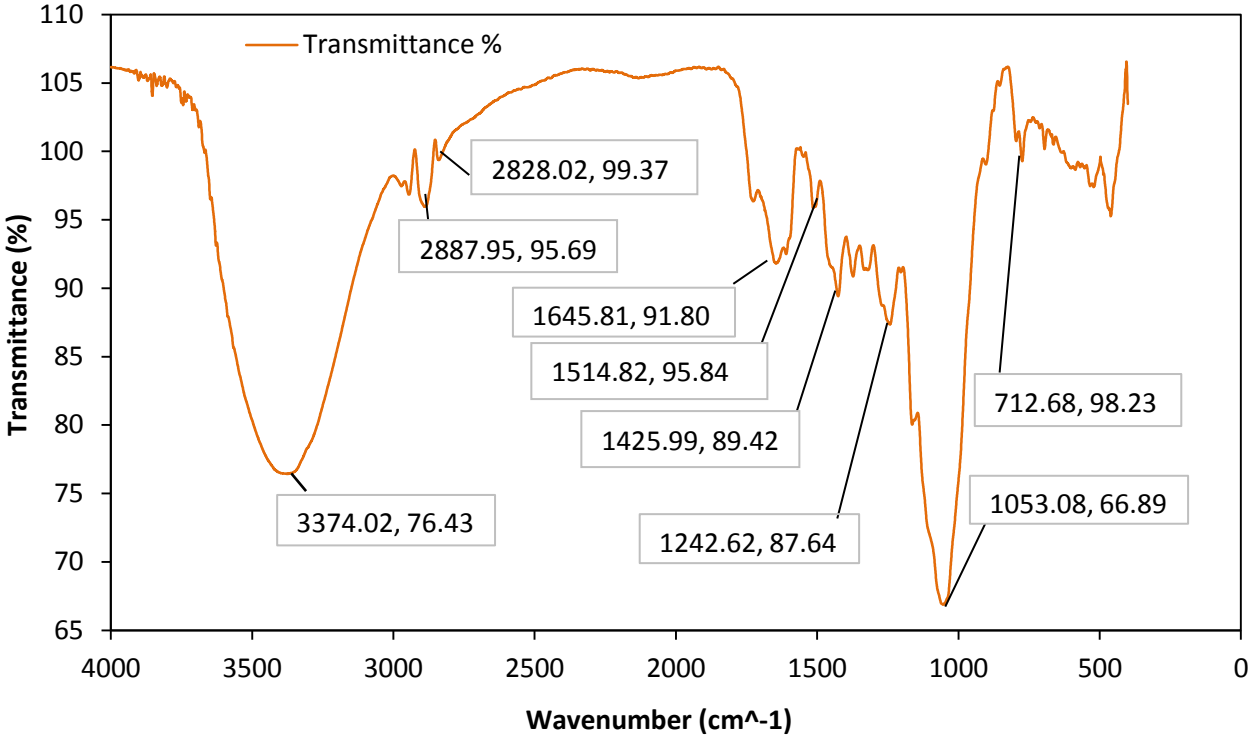

Figure 4.4: FTIR spectroscopy of raw SPF

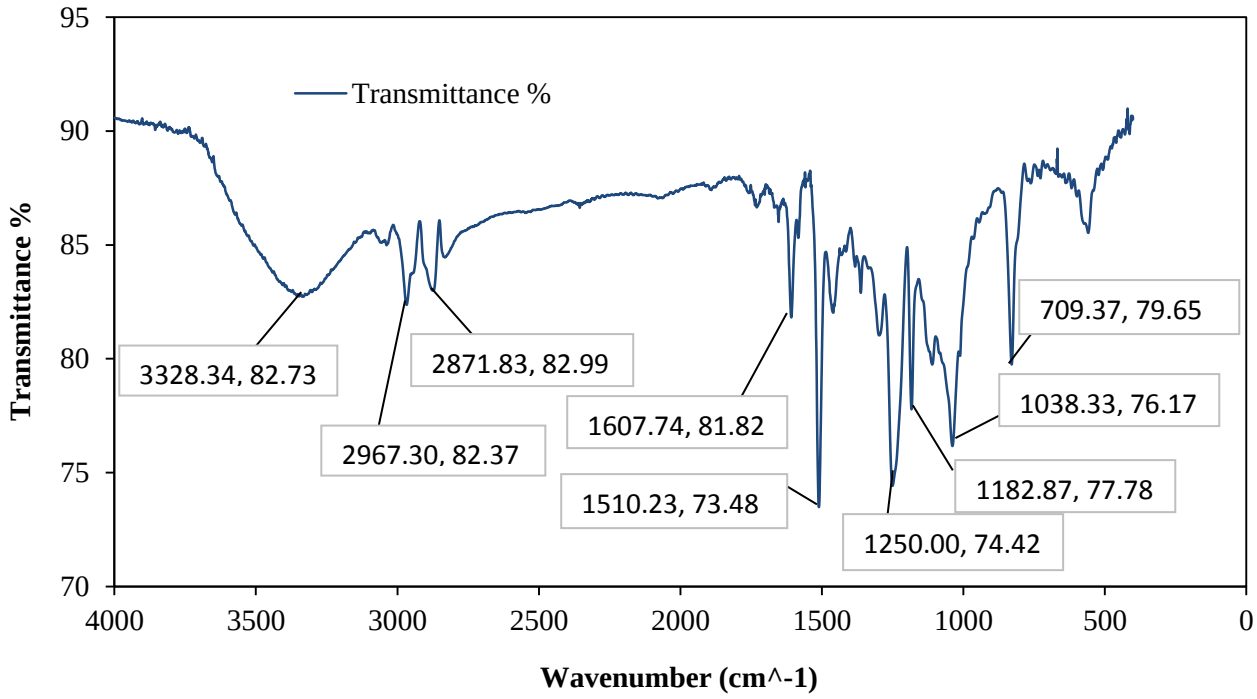

Figure 4.5: FTIR spectroscopy of epoxy-SPF composite

The wavenumber 3328.34 cm^{-1} and 2967.30 cm^{-1} suggests the presence of alkynes and alkanes stretching respectively in the epoxy-SPF composite with increased transmittance than Figure 4.4. Wavenumber 1607.74 cm^{-1} reveals the presence of 1^0 amines (N-H bend). A very sharp peak at wavenumber 1250.00 cm^{-1} is formed with increased absorbance suggesting the presence of aliphatic amines (C-N stretch).

4.4 X-Ray Diffraction

The crystallographic nature of the raw palmyra fiber under study was investigated through X-Ray diffraction technique using a BRUKER D8 ADVANCE X-Ray diffractometer. The test results are shown in Figure 4.6. From the figure the occurrence of a major peak was seen at 2θ with range of 21^0 to 24^0 corresponding to the 0 0 2 cellulose crystallographic plane. According to this technique, a crystallinity of 29% is observed.

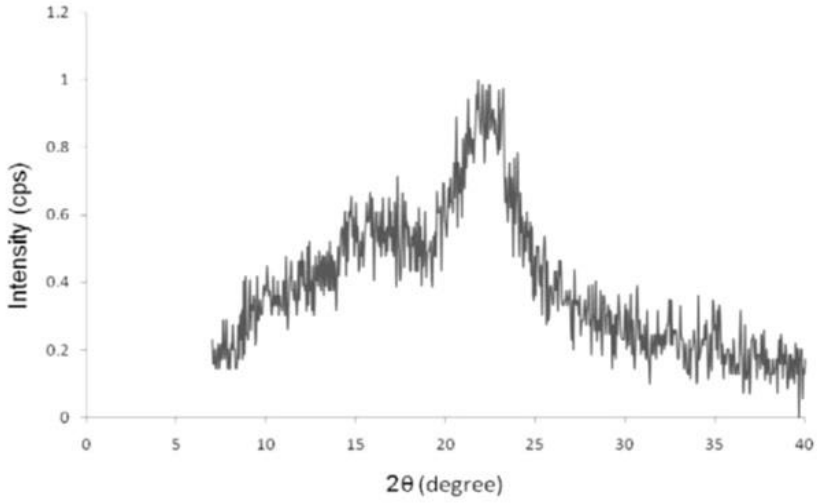

Figure 4.6: XRD image of raw palmyra fiber

4.5 Surface Morphology

Figure 4.7a presents a typical SEM micrograph of the surface of a single palmyra fiber and Figure 4.7b is a magnified image of the same fiber. These micrographs exhibit a peculiar arrangement of bony ridges of different relative size and thickness on the fiber body. Similarly, Figure 4.7c and 4.7d present the surface morphology of a typical epoxy-SPF composite which clearly show the embedment of short palmyra fibers within the epoxy resin.

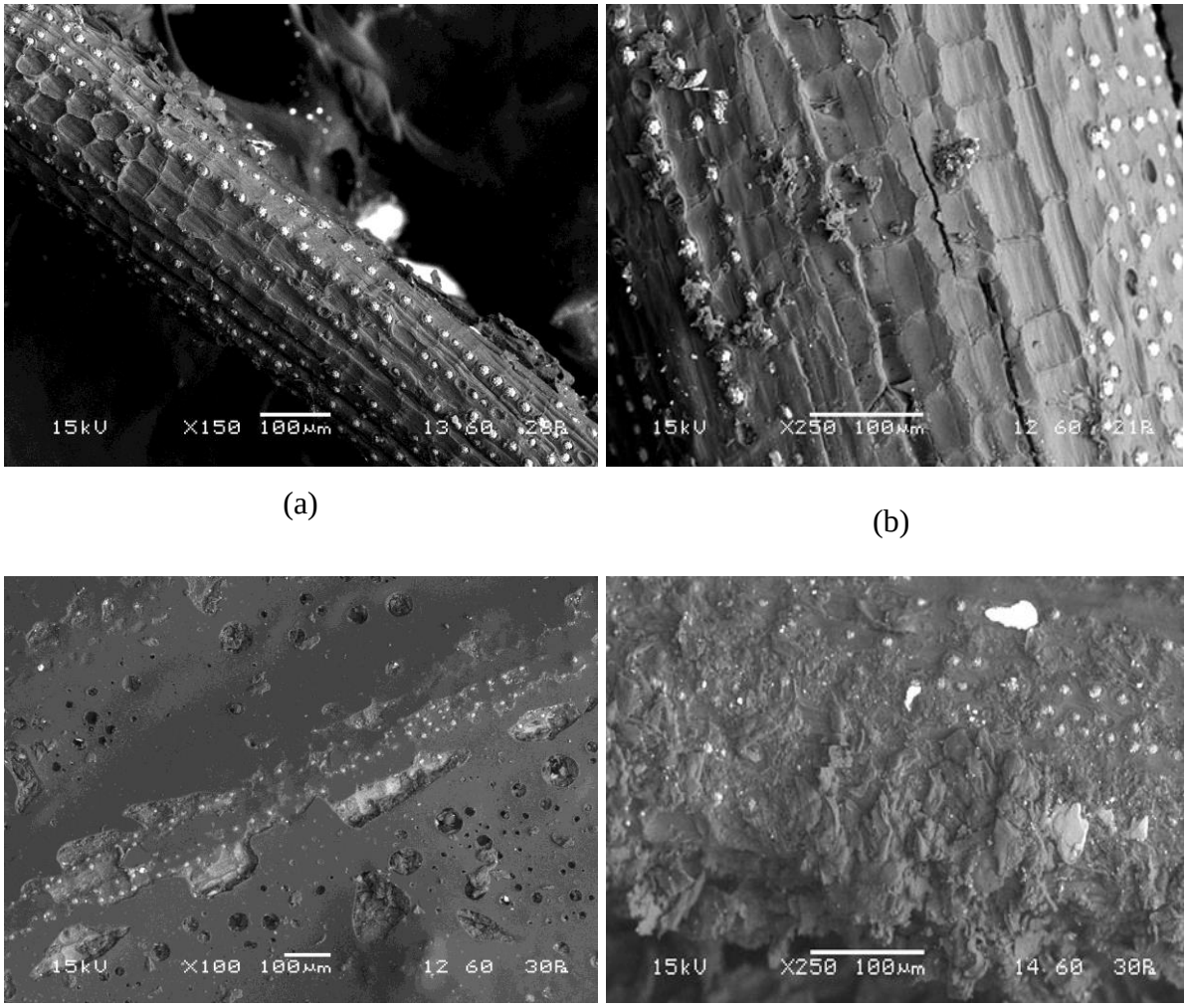

(a) (b)

(c) (d)

Figure 4.7: Surface morphology of epoxy-SPF composites

Chapter Summary

This chapter has provided:

- The physical and mechanical characterization of epoxy composites filled with short palmyra fiber.
- The effect of SPF content on the composite properties.

The next chapter presents the results and discussion for sliding wear performance of the epoxy based composites under different test conditions.

*****

CHAPTER 5

Results and Discussion: II
Dry Sliding Wear Performance

Chapter 5

Results and Discussion: II
Dry Sliding Wear Performance

This chapter presents the effects of reinforcement of short palmyra fibers (SPF) on the dry sliding wear behavior of epoxy composites under varying test conditions. Attempt has been made to develop an empirical correlation between the sliding wear rate and the control factors selected during the experiment. Artificial neural networks (ANN) prediction tool has been successfully used to determine the dry sliding wear rates within and beyond the range of experiment. A correlation has been proposed for minimum specific wear rate and it has been compared with the experimental results of sliding wear and the results determined from the ANN prediction. Taguchi method and signal-to-noise ratio have also been employed for parametric analysis using the test results obtained from the experiments. The dry sliding wear tests are carried out as per the ASTM G 99 standards.

5.1 Morphology of Worn Surface

The Figure 5.1 presents the typical SEM micrographs of the surfaces of worn epoxy-SPF composites. The surface features of epoxy SPF composite with a fiber content of 8 wt% are shown in Figure 5.1a. The worn surface morphology (sliding velocity of 63.0 cm/sec and normal load of 5.0 N) of the same composite is presented in Figure 5.1b in which local removal of the matrix layer as a result of the dry sliding wear is clearly visible. Removal of the upper matrix layer and protrusion of fibers beneath the epoxy resin are revealed. The direction of sliding is also clear in this micrograph. Figure 5.1c presents another typical worn surface of a composite with low fiber content (4 wt%). Formation of wear debris, surface cracks and signs of plastic deformation are evident. But such features are not adequately seen in Figure 5.1d which presents the worn surface morphology of an epoxy-SPF composite with fiber content as high as 12 wt%. Signs of plastic deformation are however clearly seen in the micrograph and the wear tracks indicated by arrows.

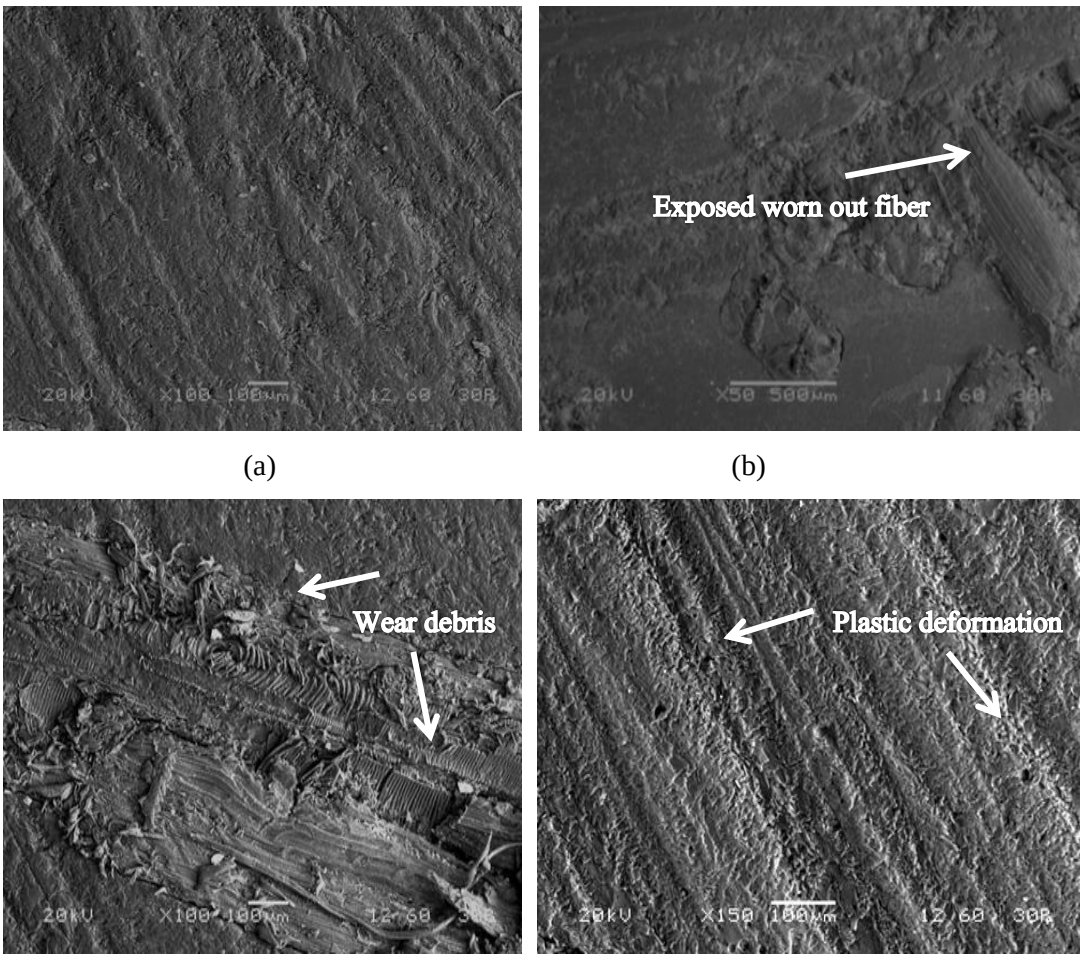

(a) (b)

(c) (d)

Figure 5.1: SEM micrographs of worn surfaces

5.2 Taguchi Experimental Analysis

In the present research work, four major factors (sliding distance, fiber content, sliding velocity and normal load) have been chosen according to Taguchi's L_{16} orthogonal array each at four levels as shown in Table 5.1. The results of the sliding wear experiments carried out according to the predetermined design on epoxy-SPF composites are presented in Table 5.2. This table provides the experimental value of specific wear rate for each individual test run and the average of three replications has been taken as the value of wear rate. Similarly, Table 5.3 provides the signal-to-noise ratio for specific wear rate for each individual test run.

Table 5.1: Factors selected for dry sliding wear test and their corresponding levels

Control factors	**Levels**				
	1	**2**	**3**	**4**	**Units**
(A) Sliding velocity	63.0	125.0	190.0	250.0	cm/sec
(B) Normal load	5.0	10.0	15.0	20.0	N
(C) Sliding distance	250.0	500.0	750.0	1000.0	m
(D) Fiber content	0.0	4.0	8.0	12.0	wt %

Table 5.2: Experimentally obtained values of specific wear rates

Test Runs	**(A) Sliding Velocity (cm/sec)**	**(B) Normal Load (N)**	**(C) Sliding Distance (m)**	**(D) SPF Content (wt %)**	**Specific Wear Rate ($10^{-4}mm^3$/N-m)**
1	63	5	250	0	6.3600
2	63	10	500	4	5.4690
3	63	15	750	8	3.6250
4	63	20	1000	12	0.9165
5	125	5	500	8	3.8560
6	125	10	250	12	2.3320
7	125	15	1000	0	7.8180
8	125	20	750	4	5.8230
9	190	5	750	12	1.4440
10	190	10	1000	8	2.8280
11	190	15	250	4	6.4300
12	190	20	500	0	8.8180
13	250	5	1000	4	7.4690
14	250	10	750	0	9.4840
15	250	15	500	12	2.6660
16	250	20	250	8	3.6560

From the experiments conducted on the epoxy-SPF composites, the overall mean S/N ratio is found to be -012.44290 dB. Figure 5.2 depicts the main effect plot which shows the effects of the four selected control factors on the specific wear rate of the epoxy- SPF composites.

Table 5.3: S/N ratios for different epoxy-SPF composites

Test Runs	**(A) Sliding Velocity (cm/sec)**	**(B) Normal Load (N)**	**(C) Sliding Distance (m)**	**(D) SPF Content (wt%)**	**S/N Ratio (dB)**
1	63	5	250	0	-16.0691
2	63	10	500	4	-14.7582
3	63	15	750	8	-11.1862
4	63	20	1000	12	0.7574
5	125	5	500	8	-11.7227
6	125	10	250	12	-7.3546
7	125	15	1000	0	-17.8619
8	125	20	750	4	-15.3029
9	190	5	750	12	-3.1913
10	190	10	1000	8	-9.0296
11	190	15	250	4	-16.1642
12	190	20	500	0	-18.9074
13	250	5	1000	4	-17.4652
14	250	10	750	0	-19.5398
15	250	15	500	12	-8.5172
16	250	20	250	8	-11.2601

From the Figure 5.2, it can be observed that the specific wear rate of the epoxy-SPF composites under study is minimum with a factor combination of A_1-B_4-C_4-D_4 i.e. at normal load (B) of 20.0 N, sliding velocity (A) of 63.0 cm/s, SPF content (D) of 12.0 wt.% and sliding distance (C) of 1000.0 m. Further, the S/N ratio responses of the epoxy-SPF composites under study are provided in Table 5.4. It can be clearly concluded from the table that among all the four factors selected for the experiment, the fiber content of the samples mostly affects the specific wear rate which is followed by the sliding velocity. The effects of normal load and sliding distance are not so significant on the specific wear rate of the epoxy-SPF composite as can observed from the Table 5.4.

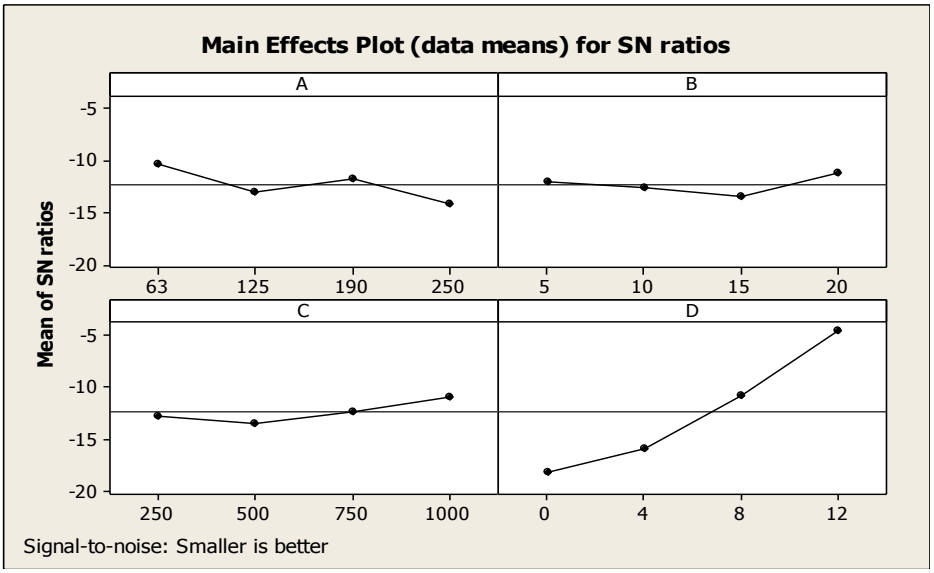

Figure 5.2: Effect of control factors on the specific wear of epoxy-SPF composites

Table 5.4: S/N ratio responses of the epoxy-SPF composites

Levels	**A**	**B**	**C**	**D**
1	-10.3140	-12.1120	-12.7120	-18.0950
2	-13.0610	-12.6710	-13.4760	-15.9240
3	-11.8230	-13.4320	-12.3050	-10.8000
4	-14.1960	-11.1780	-10.9000	-4.5760
Delta	3.8820	2.2540	2.5770	13.5180
Rank	**2**	**4**	**3**	**1**

5.3 Factor Settings for Minimum Specific Wear Rate

In the present research work in order to minimize the specific wear rate, an approach has been made to find the optimal control factor settings. A non-linear regressive predictive equation has been used to predict the specific wear rate that defines the relationship between the individual control factors and the specific wear rate. A statistical software *SYSTAT 7* has been used for the development of this equation. The following equation has been proposed for expressing the specific wear rate in terms of control factors:

$$W_S = K_0 + K_1 \times A + K_2 \times B + K_3 \times C + K_4 \times D \qquad (5.1)$$

Where, W_s denotes the specific wear rate in mm^3/N-m which is the performance output and K_i (i = 0,1,2,3 and 4) are the constants of the model. *A* represents the sliding velocity in cm/s, *B* represents the normal load (N), *C* denotes the sliding distance (m) and *D* represents the fiber content in wt%.

Table 5.5: Comparison of experimental and predicted values of sliding wear rate

Epoxy- SPF Composites		
Specific Wear Rate ($10^{-4}mm^3$/N-m) (Predicted)	**Specific Wear Rate ($10^{-4}mm^3$/N-m) (Experimental)**	**Error %**
7.353	6.36	15.6
5.189	5.469	5.1
3.525	3.625	2.7
0.861	0.9165	6.0
3.521	3.856	8.6
2.357	2.332	1.0
7.849	7.818	0.3
5.685	5.823	2.3
1.577	1.444	9.2
2.441	2.828	13.6
6.205	6.43	3.4
8.369	8.818	5.0
6.685	7.469	10.4
8.849	9.484	6.6
2.357	2.666	11.5
4.012	3.656	9.7

SYSTAT 7 software has been used to calculate the values of the constants and the final expression for specific wear rate of these composites in terms of sliding velocity and fiber content is given as follows:

$$W_S = 6.849 + 0.008 \times A - 0.541 \times D \quad (5.2)$$

The correlation coefficient (r^2) is found to be 0.988 for the epoxy-SPF composites which is quite high to confirm the correctness of the calculated constants and thus making it possible for further analysis. Table 5.5 shows the comparison between wear rates obtained from experiment and those calculated from the predictive equation. The corresponding error percentages are also reported in the Table 5.7.

5.4 Analysis and Prediction of Specific Wear Rate Using ANN

As elaborately discussed before, ANN is a prediction tool which involves database training for prediction of the input-output evolutions. In the present attempt, four input parameters (sliding distance, sliding velocity, SPF content and normal load) are taken in order to simulate the sliding wear rate and predict the specific wear rate under various test conditions for the epoxy-SPF composites under study. These input parameters are represented by four neurons in the input layer of the ANN structure. The output layer is represented by one neuron which denotes the performance output i.e. the specific wear rate.

Table 5.6: ANN structure input training parameters (epoxy-SPF)

Selected Input Parameters	**Values**
(I) Number of neurons in input layer	04
(H) Number of neurons in hidden layer	010
(O) Number of neurons output layer	01
No of epochs	1,00,00,000
Error tolerance	0.0030
(β) Learning ability	0.0020
(α) Momentum parameter	0.0020
(NF) Noise factor	0.0010

A set of ANN structures with different number of neurons in the hidden layer have been tested at constant cycles, error tolerance, momentum parameter, learning rate, noise factor, and slope parameters. Finally, the structure with least error is selected for the training purpose. The Table 5.6 shows the selected training parameters of the input-output data. An optimized three-layer neural network is shown in Figure 5.3. A software package MATLAB is used for ANN prediction which is based on the back propagation algorithm.

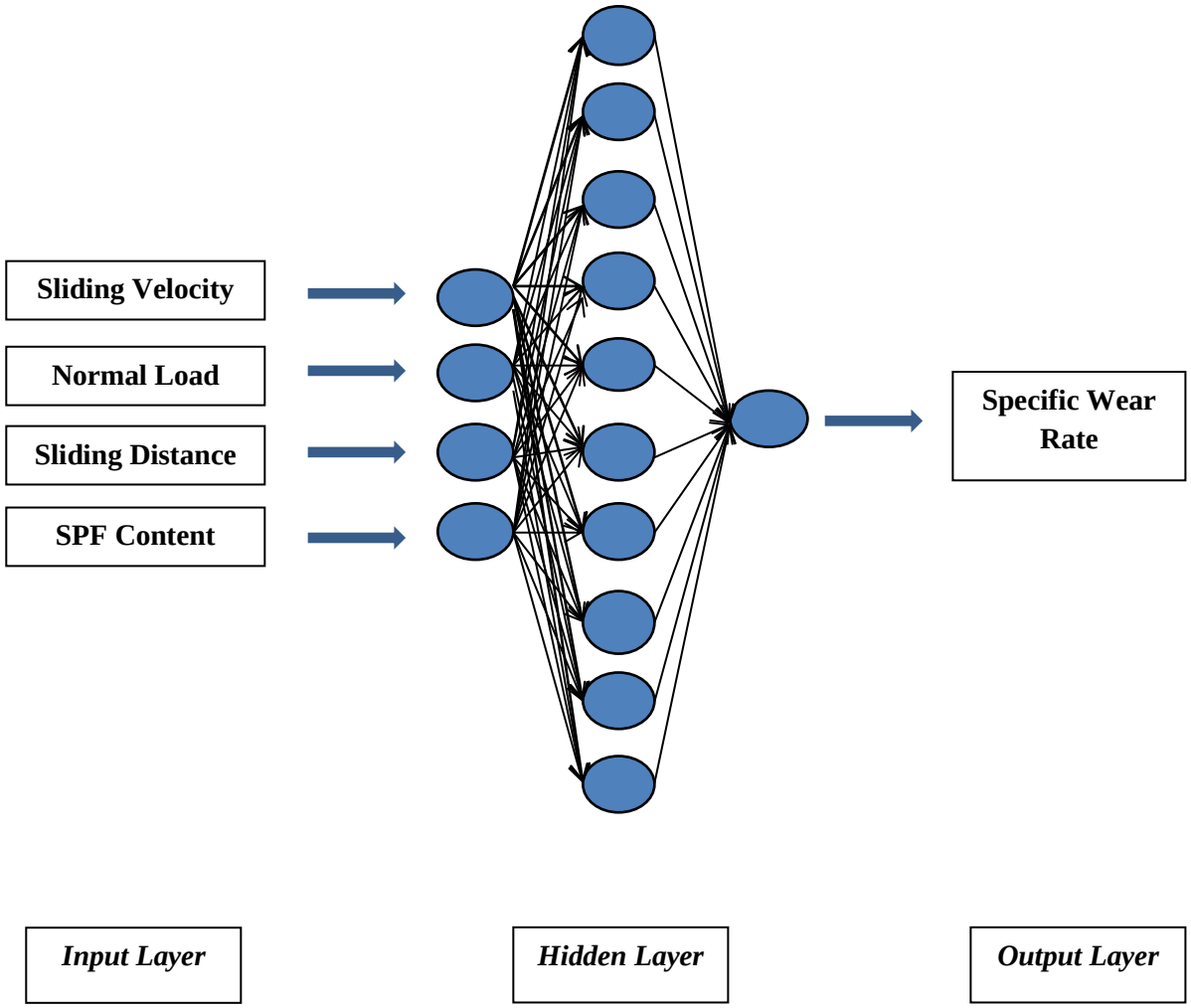

Figure 5.3: The three layer neural network structure

The ANN prediction results for specific wear rate for the epoxy-SPF composites are shown in Table 5.7 along with the error percentages for all the 16 test runs and have been compared with the experimental values. From the Table 5.7, it can be seen that the percentage errors for most of the test runs lie within the range of 0-5% which suggests that the ANN predicted results are in good agreement with the experimental results. However, the prediction quality can be improved further by increasing the database size and optimizing the neural network construction.

Table 5.7: Comparison of ANN predicted values with experimental results

Specific wear rate (10^{-4} mm^3/N-m)			
Test Runs	**Experimental Results**	**ANN Predicted Values**	**Error %**
1	06.360	06.359136	00.013
2	05.469	05.468302	00.012
3	03.625	03.601238	00.655
4	00.917	0.942864	02.820
5	03.856	04.021859	04.301
6	02.332	02.328292	00.159
7	07.818	07.773308	00.571
8	05.823	05.818631	00.075
9	01.444	01.443930	00.004
10	02.828	02.805736	00.787
11	06.430	06.425846	00.064
12	08.818	08.512651	03.462
13	07.469	07.382000	01.520
14	09.484	09.433750	00.529
15	02.666	02.654097	00.446
16	03.656	03.660072	00.111

A well trained ANN can be very productive for analyzing the specific wear rate characteristics for any given set of composite materials and thus making it possible to determine the effects of each input parameter on the output result (specific wear rate) quantitatively. The chosen parameter range can be beyond the experimental domain, thus permitting to use the generalization property of ANN in a wider set of parameter domain. In the present research work, two most dominant factors have been chosen i.e. the SPF content and the sliding velocity to explore this possibility in a range beyond the limit of the experimental work.

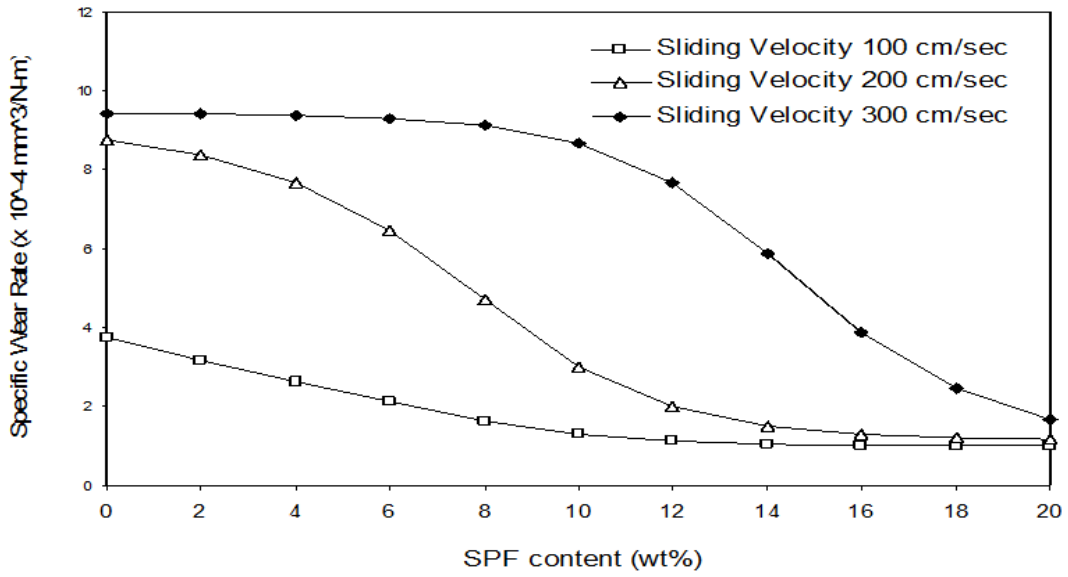

Figure 5.4: ANN prediction for specific wear rate with variation in SPF content for epoxy-SPF composites.

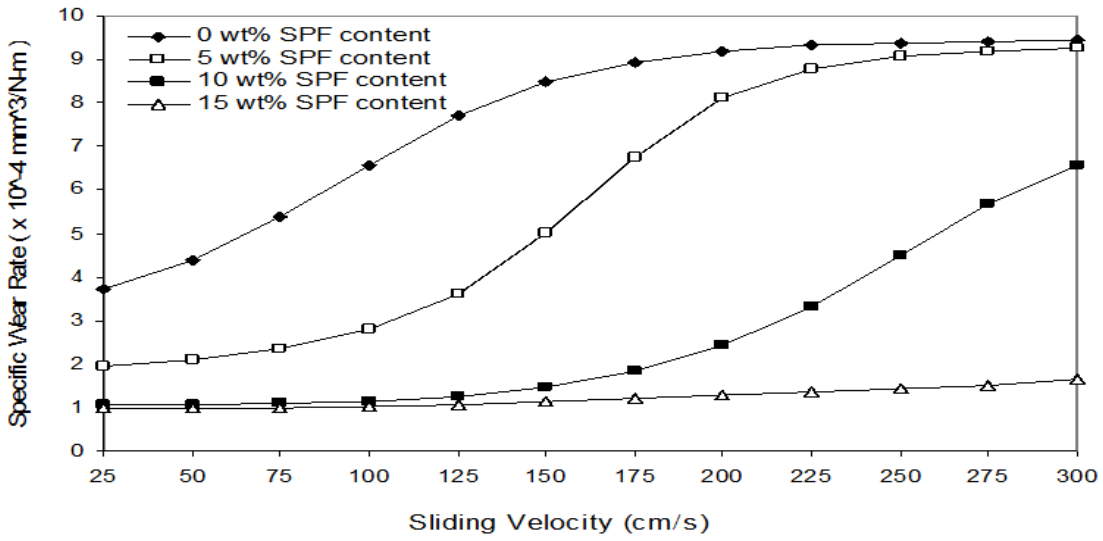

Figure 5.5: ANN prediction for specific wear rate with variation in sliding velocity for epoxy-SPF composites.

Figure 5.4 and Figure 5.5 show the ANN prediction results of specific wear rate with different SPF content and sliding velocity. It is can be seen from the graph that as the sliding velocity is increased, the specific wear rate also steadily increases. This can be attributed to the fact that as the sliding velocity increases, the interface temperature between the counter surface of the pin-on-disc set-up and the specimen increases. Since

both the fiber and the epoxy matrix have different thermal expansion coefficient, it creates an interfacial stress. When this interfacial stress exceeds the bonding strength of the fiber and epoxy, cracks starts forming and more wear takes place. But at the same time it is very interesting to note here that as the SPF content increases, the specific wear rate decreases gradually even at high sliding velocity. This decrease can be explained by the increase in the hardness of the composite as the SPF content increases thus, decreasing the wear rate.

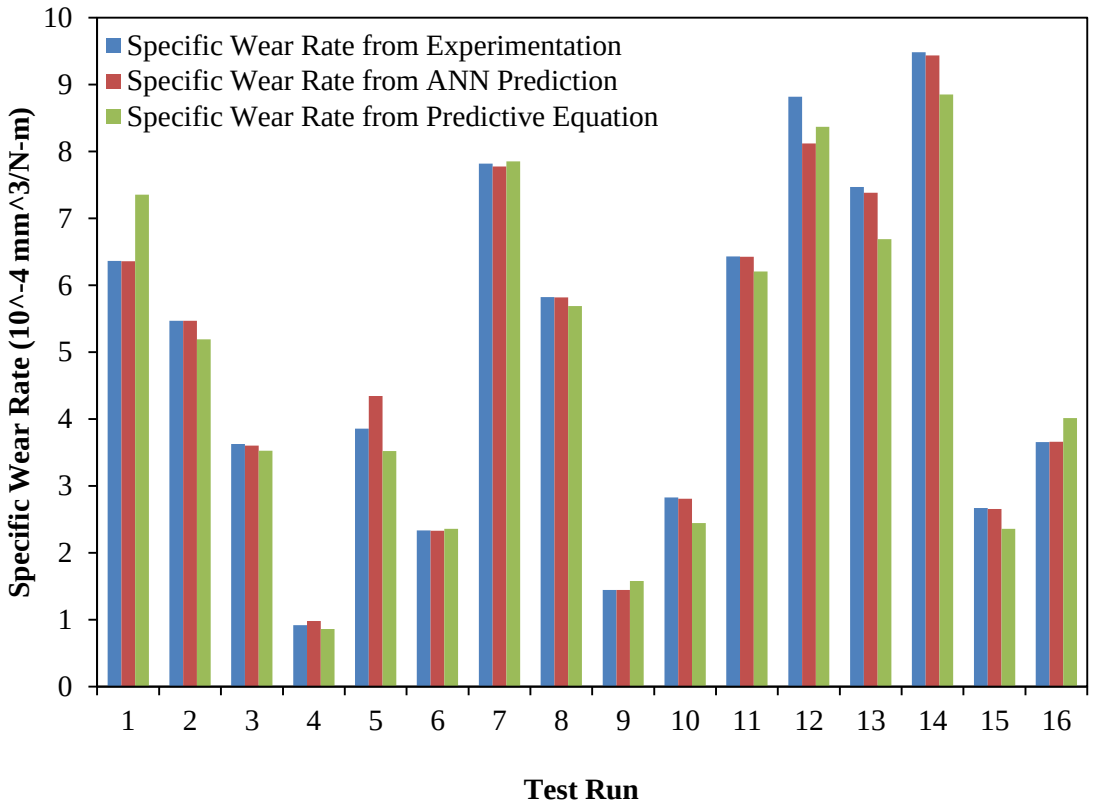

Figure 5.6: Comparison of the specific wear rates of epoxy-SPF composites obtained from different methods.

Figure 5.6 presents a comparision between the specific wear rates obtained from experiment with those obtained from predictive equation and ANN prediction. While the error associated with ANN prediction mostly lies in the range of 0-5%, the results obtained from the proposed equation lie in the range of 0-15%. Thus, it can be concluded that both predictive equation and ANN can be used for estimation of the specific wear rate although ANN prediction appears to be in better agreement with the experimental results.

Chapter Summary

This chapter has provided:

- The results of specific wear tests for epoxy-SPF composites.
- The analysis of experimental results using Taguchi's L_{16} orthogonal array.
- Surface morphologies of worn-out composites using SEM.
- Effect of various input parameters on the specific wear rate.
- Simulated wear prediction under different test conditions within and beyond the range of experiment using ANN.

The next chapter provides the thermal and acoustic properties of the samples under consideration.

*****

CHAPTER 6

Results and Discussion: III
Acoustic and Thermal Characterization

Chapter 6

Results and Discussion: III
Acoustic and Thermal Characterization

This chapter describes the effects of short palmyra fiber content on the acoustic and thermal behavior of the epoxy composites under study. Attempt has been made to find the sound absorption coefficient and the thermal conductivity of the composites with different weight percentages. Further, the effects of fiber content on the coefficient of thermal expansion (CTE) and glass transition temperature (T_g) of the composites have been studied.

6.1 Effects of SPF Content and Sample Thickness on the Sound Absorption Behavior

The acoustic absorption behavior of the epoxy composites under study are analyzed with the help of sound absorption coefficient (ratio of absorbed sound intensity to the initial sound intensity) which is found by using impedance tube test method as per the ASTM E 1050 standards. The values of sound absorption coefficient for any material varies from 0 to 1, where 0 signifies total reflectivity of sound waves and 1 signifies total absorption of the sound waves. In the first set of experiments, the frequency is varied from 125 Hz to 4000 Hz keeping the thickness of the composites constant at 3mm. In the second set of experiments, the frequency is kept constant at 4000 Hz while the thickness is varied from 5 mm to 25 mm and the variation of the sound absorption coefficient is studied. Table 6.1 shows the effects of SPF content on the sound absorption coefficient at varying frequency levels. From the Figure 6.1, it is clearly seen that as the fiber content increases from 2 wt. % to 14 wt. %, the sound absorption coefficient also increases. At a frequency of 125 Hz, the sound absorption coefficient of the composite with 2 wt. % fiber is found to be 0.048 which increases to 0.121 for the composite with 14 wt. % of fiber content. Similarly, at 4000 Hz the maximum sound absorption coefficient for the composite with 14 wt. % fiber

is found to be 0.698 which suggests that these composites can be successfully used as sound insulating materials.

Table 6.1: Effect of SPF content on the sound absorption coefficient

SPF Content (wt. %)	**Frequency (Hz)**							
	125	250	500	1000	1500	2000	3000	4000
2	0.048	0.073	0.112	0.128	0.143	0.168	0.272	0.389
8	0.056	0.088	0.142	0.171	0.180	0.224	0.406	0.503
10	0.069	0.111	0.174	0.231	0.257	0.336	0.524	0.621
14	0.121	0.138	0.236	0.296	0.351	0.476	0.578	0.698

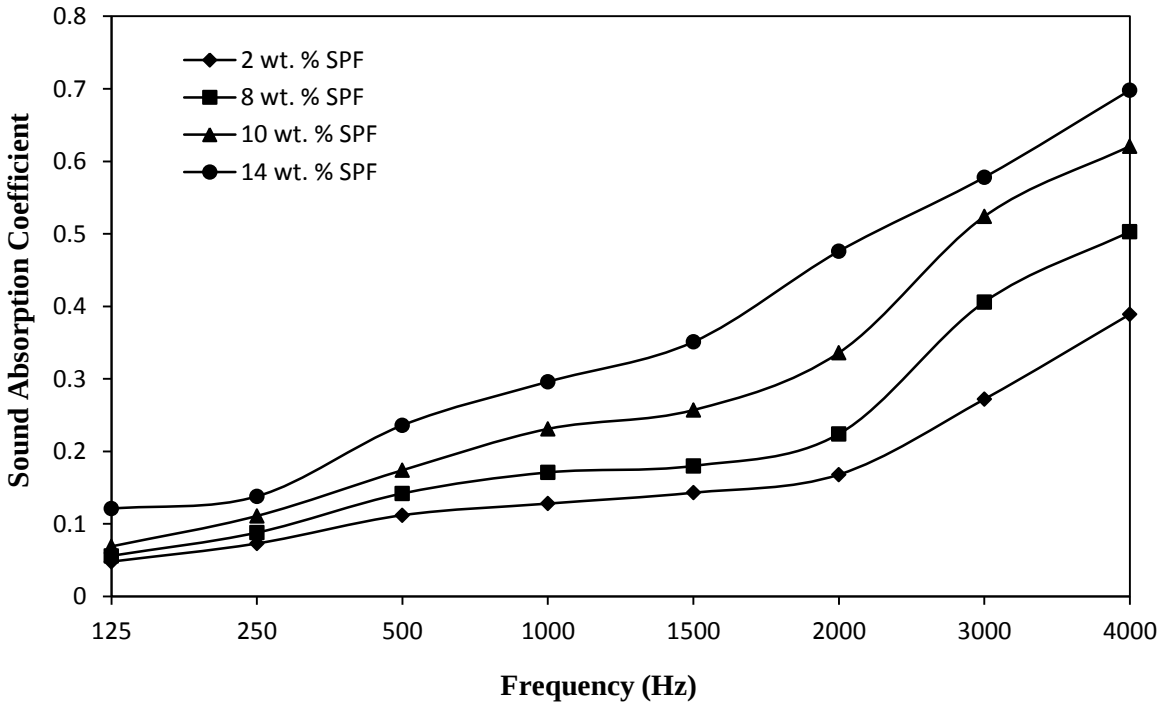

Figure 6.1: Effect of SPF content on sound absorption characteristics

Table 6.2: Effect of composite thickness on the acoustic absorption coefficient

SPF Content (wt. %)	**Thickness (mm)**				
	5	10	15	20	25
2	0.391	0.401	0.435	0.482	0.496
8	0.512	0.563	0.598	0.632	0.645
10	0.653	0.686	0.721	0.768	0.778
14	0.702	0.723	0.758	0.796	0.812

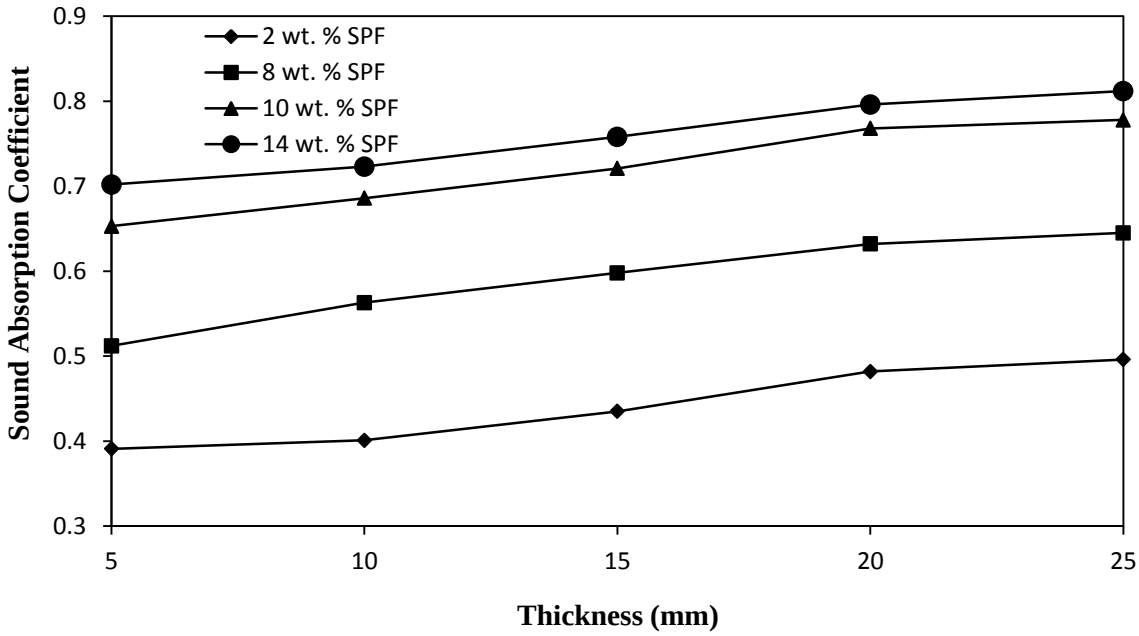

Figure 6.2: Effect of thickness on sound absorption characteristics

Absorption of sound energy occurs in a material when the sound energy interacts with different particles of the material which are of varying density, thermo-physical properties and compressibility. As a result of this interaction, the energy loss occurs and this amount of absorption can be measured by the sound absorption coefficient of that material. The effects of thickness on the sound absorption behavior of epoxy-SPF composites are tabulated in Table 6.2 and the variation is graphically shown in Figure 6.2. From the figure it can be clearly observed that as the thickness of the composite increases, the sound

absorption coefficient also increases. However, beyond a certain thickness, the sound absorption coefficient almost remains constant because the penetrating power of the sound wave gradually decreases.

6.2 Effects of SPF Content on the Thermal Conductivity, Glass Transition Temperature and Coefficient of Thermal Expansion of the Composites

6.2.1 Effects of SPF Content on the Effective Thermal Conductivity

In the present investigation, *Unitherm* 2022 thermal conductivity tester has been used to find out the effective thermal conductivity experimentally. The experimental values are then compared with those obtained from different established theoretical models. The simplest model among all is the Rule of Mixture (ROM) which is used to mathematically find out the effective thermal conductivity of a composite consisting of two components. The arrangement can be in series or parallel depending on the direction of heat flow. The following equations 6.1 and 6.2 give the effective thermal conductivity of a two component composite sample in series [199] and parallel [200] combination respectively.

$$\frac{1}{k_c} = \frac{(1-\phi)}{k_m} + \frac{\phi}{k_f} \tag{6.1}$$

$$k_c = (1-\phi)k_m + (\phi \times k_f) \tag{6.2}$$

Where, k_c denotes the effective thermal conductivity of the composite, k_f represents thermal conductivity of the fiber material, k_m the thermal conductivity of the matrix material and ϕ denotes the volume fraction of fiber in the composite.

Maxwell's equation for effective thermal conductivity [201] has also been used in the present investigation for comparison purpose with experimental values and values obtained from Rule of Mixture. The Maxwell's equation is given by:

$$k_c = k_m \left[\frac{k_f + 2k_m + 2\phi(k_f - k_m)}{k_f + 2k_m - 2\phi(k_f - k_m)} \right] \quad (6.3)$$

Where, k_c denotes the thermal conductivity of the composite material, k_f is given by the thermal conductivity of the fiber material and k_m represents the thermal conductivity of the matrix material. Table 6.3 represents the effective thermal conductivity found from various methods i.e. experimental value, Maxwell's model and Rule of Mixture.

Table 6.3: Effective thermal conductivity of epoxy-SPF composites

SPF Content (wt. %)	**SPF Content (vol. %)**	**Effective Thermal Conductivity (W/mK)**		
		Rule of Mixture (ROM)	Maxwell's Model	Experimental value
0	0	0.363	0.363	0.363
2	2.13	0.356	0.352	0.338
8	8.49	0.337	0.322	0.303
10	10.60	0.333	0.312	0.291
14	14.81	0.321	0.294	0.283

From the Table 6.3, it can be clearly observed that addition of short palmyra fiber to the neat epoxy has enhanced the thermal insulating properties as can be inferred from the gradually decreasing thermal conductivity with increasing SPF content. With addition of just 2.13 vol. % of SPF, the thermal conductivity of the neat epoxy reduced to 0.338 W/mK from 0.363 W/mK. Further with incorporation of 14.81 vol. % of SPF, the thermal conductivity reduced to 0.283 W/mK suggesting the use of these composites as insulation materials. Figure 6.3 shows the graphical representation of the variation of effective thermal conductivity of the epoxy-SPF composites with different fiber content.

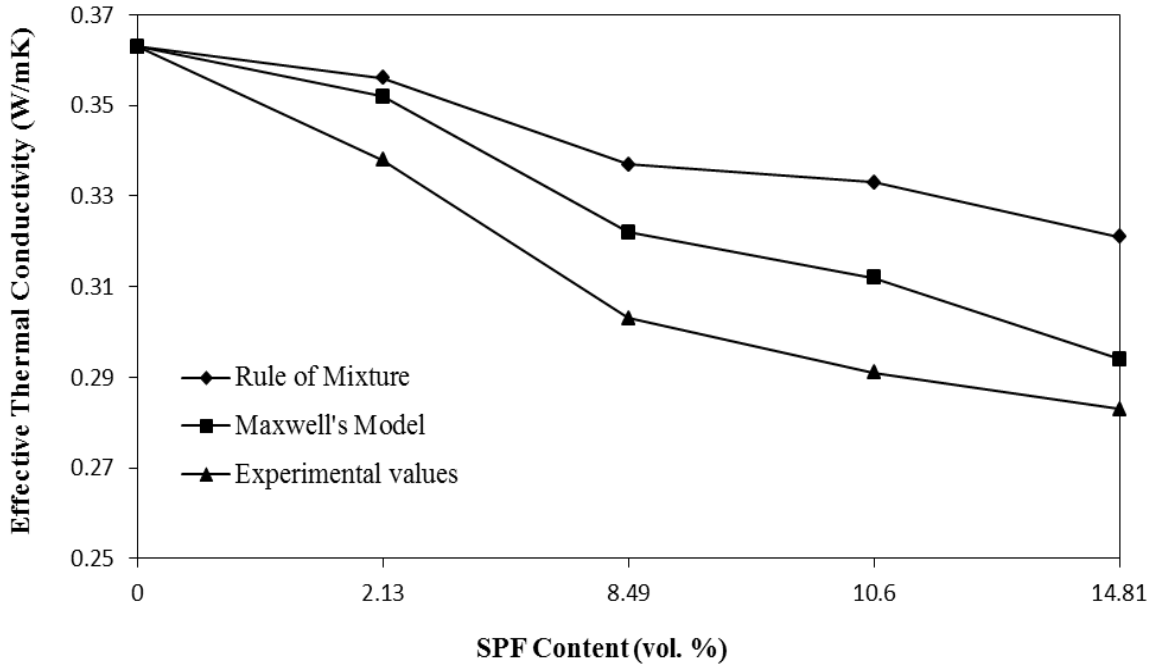

Figure 6.3: Variation of effective thermal conductivity with SPF content

From the Figure 6.3 it can be observed that the values of effective thermal conductivity obtained experimentally are less than the values obtained by using Maxwell's model and Rule of Mixture. This can be attributed to the fact that in actual practice, a number of voids or air pockets are present within the matrix body which are generated during fabrication of the composite. Air having a very low thermal conductivity, reduces the effective thermal conductivity of the sample.

6.2.2 Effects of SPF Content on the Glass Transition Temperature

A Perkin Elmer DSC 7 thermal mechanical analyzer has been used in the present investigation to find out the glass transition temperature (T_g) of the samples. Figure 6.4 shows the effect of SPF content on the glass transition temperature of the composites. It can be observed that as the SPF content increases, the T_g of the neat epoxy increases from 98.0 ^{0}C at 0 vol. % of SPF content to 109.0 ^{0}C at 14.81 vol. % of SPF content suggesting an increase of about 11 ^{0}C. This increase in the glass transition temperature of the composite samples can be attributed to the increase in the interaction between the matrix and the reinforcing material which prevents the movement of the epoxy molecules. An enhanced T_g permits the safe application of these composites in high temperature area without undergoing any change of state.

Table 6.4: Effect of SPF content on T_g and CTE of the composite samples

SPF Content (vol. %)	**T_g (^{0}C)**	**CTE (ppm/^{0}C)**
0	98.0	66.0
2.13	100.2	65.8
8.49	104.8	65.5
10.60	106.3	64.7
14.81	109.0	64.3

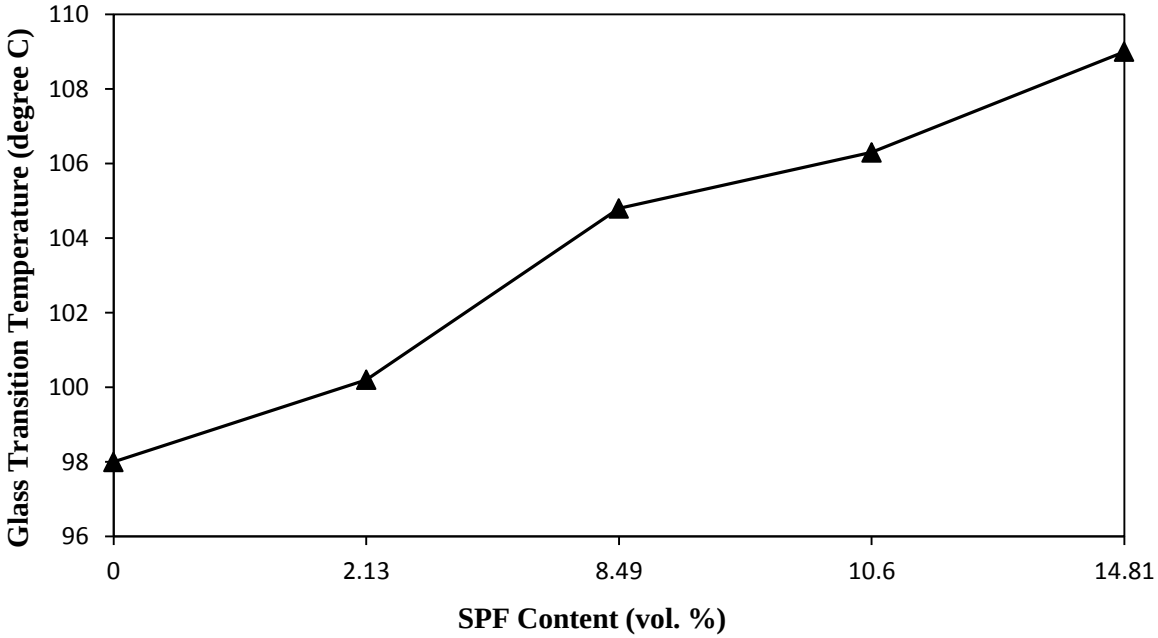

Figure 6.4: Effect of SPF content on T_g of neat epoxy

6.2.3 Effects of SPF Content on the Coefficient of Thermal Expansion

Figure 6.5 presents the change in coefficient of thermal expansion (CTE) with SPF content which is found out using a thermal mechanical analyzer. It can be observed that with addition of 2.13 vol. % of SPF to the neat epoxy, the coefficient of thermal expansion decreases from 66 ppm/^{0}C to 65.8 ppm/^{0}C which further reduces to 64.3 ppm/^{0}C at 14.81 vol. % of SPF content.

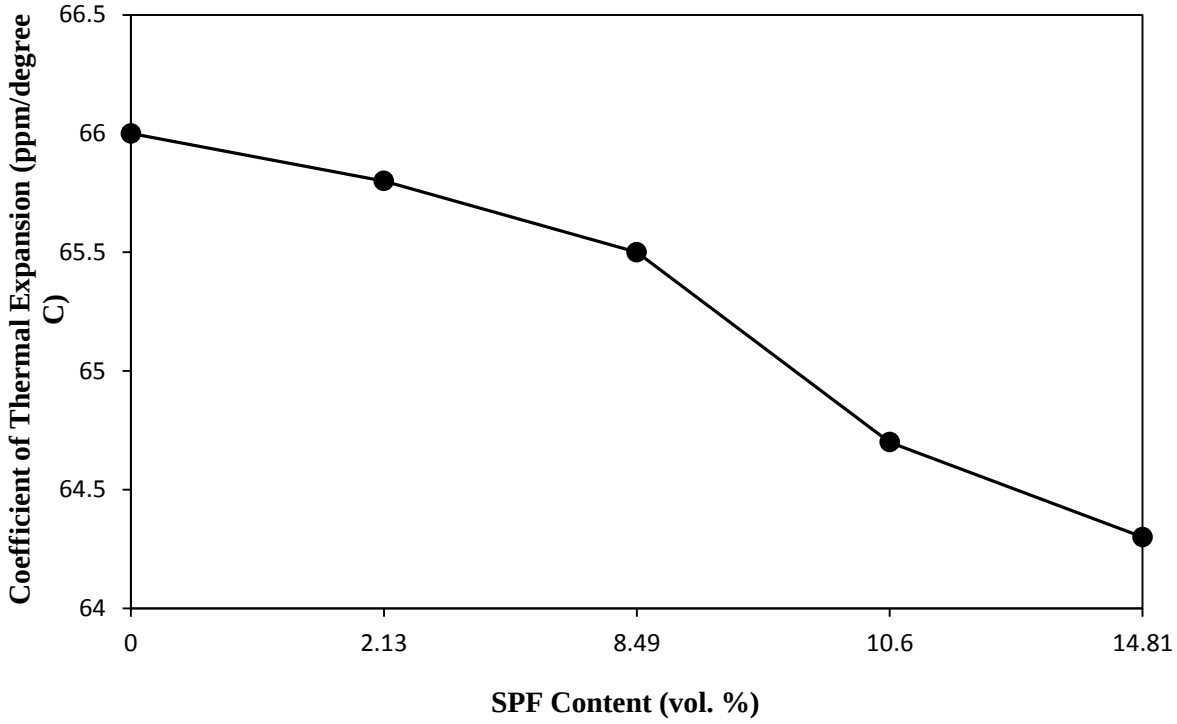

Figure 6.5: Effects of SPF content on the CTE of neat epoxy

This decrease in the coefficient of thermal expansion can be attributed to the decrease in the movement of epoxy molecules due to addition of short palmyra fibers to the neat epoxy. A decreased CTE suggests that less thermal stresses are induced in the composite when it is subjected to high temperature applications.

Chapter Summary

This chapter has provided:

- The results of impedance tube test to find out the sound absorption coefficient of the composite samples under study.
- Effects of SPF content and sample thickness on the sound absorption coefficient.
- Results of effective thermal conductivity found from the experiment and a comparison between the experimental values and values obtained by using ROM and Maxwell's model.
- Effects of SPF content on the CTE and T_g of the composite samples under study.

The next chapter provides the summary of the research investigation and the inferences drawn from it. Some applications of this new class of composite has been suggested which is followed by some ideas for future investigation.

*****

CHAPTER 7

Summary and Conclusions

Chapter 7

Summary and Conclusions

The research reported in this thesis broadly consists of four parts:

- The first part has provided the detailed description of the materials used and experiments conducted during the research.

- The second part presents the characteristics of the epoxy-SPF composites in regard to their physical and mechanical properties like density, void fraction, tensile, flexural strength and micro-structural features.

- The third part of this thesis reports on the sliding wear performance of these epoxy-SPF composites under different test conditions. Here the effects of fiber reinforcement on the wear characteristics of the samples are studied. An empirical correlation has also been proposed for estimating the specific wear rate.

- The last part of the thesis reports on the thermal and acoustic behavior of the epoxy-SPF composite samples under this study. The effects of increasing the SPF content on the thermal conductivity of the samples are studied. Further, its impact on the sound absorbing characteristics has also been discussed in detail in this part.

7.1 Summary of Research Findings

A new composite material's performance is often determined by its response under various mechanical, physical, tribological and thermal conditions as it gets very much essential for selecting materials of appropriate composition for application in a particular area. Hence, in the current investigation, an abundance of property information has been provided for a set of epoxy-SPF composites by processing them through hand-lay-up technique and by carrying out various physical, mechanical, tribological, acoustic and thermal tests on them under controlled laboratory conditions.

It is observed that by reinforcing short palmyra fibers into the neat epoxy resin, its effects, as desired are achieved in the form of enhanced mechanical, physical, tribological, thermal and acoustic properties. When the concentration of SPF in the neat epoxy is increased, the specific wear rate decreased gradually and at the same time a reduction in the effective thermal conductivity is also observed as palmyra fiber is insulative in nature. This is accompanied by increase in both tensile and flexural strength. Further, the sound absorption coefficient also increased by a huge margin as the SPF concentration in the neat epoxy increased. The effects of SPF content on the coefficient of thermal expansion and glass transition temperature of the composites are also found to be significant.

7.2 Conclusions

This investigation on the processing and characteristics of short palmyra fiber reinforced epoxy composites has led us to the following conclusions:

1. Successful fabrication of epoxy composites reinforced with short palmyra fibers (SPF) is possible through simple hand-lay-up technique.

2. Incorporation of SPF into the neat epoxy has modified its tensile and flexural strength as well as the micro-hardness. It has been observed that with the addition of SPF to neat epoxy, the strength properties improved considerably.

3. FTIR and XRD tests of the samples reveal their molecular orientation and it is concluded that the raw palmyra fiber exhibits about 29% crystallinity indicating its large amorphous nature.

4. Successful analysis of control factors affecting the sliding wear rate is carried out using Taguchi's L_{16} orthogonal array which is followed by ANN prediction of the specific wear rate within and beyond the scope of experimental data. From the dry sliding wear test results it is observed that the specific wear rate of the epoxy-SPF composites is mostly affected by the fiber content of the samples which is followed by the sliding velocity. The wear rate of the sample is found to be least at 12 wt. % of SPF content and 63 cm/sec of sliding velocity.

5. From the impedance tube test method it is found that as the SPF content in the sample is increased from 2 wt.% to 14 wt. %, the acoustic absorption coefficient also increased from 0.389 to 0.698 suggesting that these composites possess fairly good acoustic insulation properties. Further, with increase in the thickness of the composites, the acoustic absorption coefficient also increased.

6. The investigation revealed a decrease in the effective thermal conductivity of the epoxy-SPF composites from 0.363 W/m-K at 0 wt. % of SPF content to 0.283 W/m-K at 14 wt. % of SPF content. Further, a drop in the coefficient of thermal expansion is observed which is accompanied by a simultaneous increase in the glass transition temperature of the epoxy-SPF composites under study.

7. With a moderate strength, decreased wear rate, high coefficient of sound absorption and lowered thermal conductivity, the epoxy-SPF composites fabricated in the present investigation can be successfully used for applications such as building insulation materials, food containers, interior of automobiles, interior wall of halls where sound absorption in required, thermos flasks, packaging industries, rollers of conveyor belts, brake pads, etc.

7.3 Scope for Future Research

The current investigation leaves a wide scope for future research for exploring other characteristics of these composites. Few are suggested below:

- Exploring the effects of alkaline treatment of the fibers on the strength, acoustic, wear and thermal properties of the composites.
- Use of long fiber and to study its strength properties.
- Possible incorporation of particulates in order to develop a hybrid composite.
- Determination of optimal composite thickness for maximum absorption of sound.
- Development of theoretical models for effective thermal conductivity of the composites.
- Analyzing the cost of these composites for accessing their economic viability.

*****

References

References

[1] H. P. S. Abdul Khalil, M. A. Tehrani, Y. Davoudpour, A. H. Bhat, M. Jawaid, and A. Hassan, "Natural Fiber Reinforced Poly(Vinyl Chloride) Composites: A Review," *Journal of Reinforced Plastics and Composites*, vol. 32, no. 5, pp. 330-356, 2013.

[2] A. A. Abdulmajeeda, T. O. Narhia, P. K. Vallittu, and L. V. Lassilla, "The Effect Of High Fiber Fraction On Some Mechanical Properties Of Unidirectional Glass-Reinforced Composites," *Dental Materials*, vol. 27, pp. 313-321, 2011.

[3] S. Garoushi, P. K. Vallittu, and L. V. Lassilla, "Short Glass Fiber Reinforced Restorative Composite Resin With Semi-Inter Penetrating Polymer Network Matrix," *Dental Materials*, vol. 23, pp. 1356-1362, 2007.

[4] N. G. Karsli, and A. Aytac, "Tensile and Thermos-Mechanical Properties of Short Carbon Fiber Reinforced Polyamide 6 Composites," *Composites Part B: Engineering*, vol. 51, pp. 270-275, 2013.

[5] N. Oya, and H. Hamada, "Effect of Reinforcing Fiber Properties on Various Mechanical Properties of Unidirectional Carbon/Epoxy Laminates," *Science and Engineering of Composite Materials*, vol. 5, pp. 105-129, 1996.

[6] N. Oya, and D. J. Johnson, "Longitudinal Compressive Behavior And Microstructure Of PAN-Based Carbon Fibers," *Carbon*, vol. 39, pp. 635-645, 2001.

[7] M. Shioya, and M. Nakatani, "Compressive Strength of Single Carbon Fiber and Composite Strands," *Compo Sci Technol*, vol. 60, pp. 219-229, 2000.

[8] Sudarisman, and I. J. Davies, "Flexural Failure Of Unidirectional Hybrid Fiber-Reinforced Polymer Composites Containing Different Grades of Glass Fiber," *Advanced Materials Research*, vol. 41-42, pp. 357-362, 2008.

[9] Sudarisman, and I. J. Davies, "Influence Of Compressive Pressure, Vacuum Pressure, And Holding Temperature Applied during Autoclave Curing on the Microstructure of Unidirectional CFRP Composites," *Advanced Materials Research*, vol. 41-42, pp. 323-328, 2008.

[10] P. W. Manders, and M. G. Bader, "The Strength of Hybrid Glass/Carbon Fiber Composites," *Journal of Materials Science*, vol. 16, pp. 2233-2245, 1981.

[11] C. Dong, and I. J. Davies, "Flexural and Tensile Strengths of Unidirectional Hybrid Epoxy Composites Reinforced by S-2 Glass and T700S Carbon Fibers," *Materials and Design*, vol. 54, pp. 955-966, 2014.

[12] N. Encinas, M. Lavat-Gil, R.G. Dillingham, J. Abenojar, and M.A. Martinez, "Cold Plasma Effect on Short Glass Fiber Reinforced Composites Adhesion Properties," *International Journal of Adhesion and Adhesives*, vol. 48, pp. 85-91, 2014.

[13] I. Sridhar, P. P. Adie, and D. N. Ghista, "Optimal Design of Customized Hip Prosthesis Using Fiber Reinforced Polymer Composites," *Materials and Design*, vol. 31, pp. 2767-2775, 2010.

[14] S. Kumar, K. V. V. S. Murthy Reddy, A. Kumar, and G. Rohini Devi, "Development and Characterization of Polymer-Ceramic Continuous Fiber Reinforced Functionally Graded Composites for Aerospace Application," *Aerospace Science and Technology*, vol. 26, pp. 185-191, 2013.

[15] M. D. Shamsuddoha, M. D. M. Islam, T. Aravinthan, A. Manalo, and L. Lau, "Effectiveness Of Using Fiber-Reinforced Polymer Composites For Underwater Steel Pipeline Repairs," *Composite Structures*, vol. 100, pp. 40-54, 2013.

[16] L. Cercone, and J. D. Lockwood, "Review Of FRP Composite Materials For Pipeline Repair," *Pipelines*, pp. 1001-1013, 2005.

[17] M. Ramesh, K. Palanikumar, and K. Hemachandra Reddy, "Comparative Evaluation on Properties of Hybrid Glass Fiber-Sisal/Jute Reinforced Epoxy Composites," *Procedia Engineering*, vol. 51, pp. 745-750, 2013.

[18] G. Marom, S. Fischer, F. R. Tuler, and H. D. Wagner, "Hybrid Effects in Composites: Conditions for Positive or Negative Effects Versus Rule-Of-Mixtures Behavior," *Journal of Materials Science*, vol. 13, pp. 1419-1426, 1978.

[19] B. Z. Jang, "Advanced Polymer Composites: principles and applications," *ASM International*, 1994.

[20] L. Fan, Z. Dang, C.W. Nan, and M. Li. *Electrochimica Acta*, vol. 48, no. 2, pp. 205-297, 2002.

[21] T. D. Kim, N. L. Oh, S. T. Oh, and I. H. Moon. *Materials Letters*, vol. 51, no. 5, pp. 420, 2001.

[22] R. Gracia, R. E. Evans, and R. J. Palmer. *Toughened Composites*, STP 937, N.J. Johnson, Ed. ASTM, pp. 397-412.

[23] J. Bijwe, C. M. Logani, and U. S. Tewari, "Influence of Fillers and Fiber Reinforcement on Abrasive Wear Resistance of Some Polymeric Composites," *Wear*, vol. 138, pp. 77-92, 1990.

[24] J. Wang, M. Gu, B. Songhao, and S. Ge, "Investigation Of The Influence Of Mos_2 Filler On The Tribological Properties Of Carbon Fiber Reinforced Nylon 1010 Composites," *Wear*, vol. 255, pp. 774-779, 2003.

[25] M. J. John, and R. D. Anandjiwala, "Recent Developments in Chemical Modification And Characterization Of Natural Fiber-Reinforced Composites," *Polymer Composites*, vol. 29, no. 2, pp.187-207, 2008.

[26] D. N. Sahieb, and J. P. Jog, "Natural Fiber Polymer Composites: A Review," *Advances in Polymer Technology*, vol. 18, no. 4, pp. 351-363, 1999.

[27] A. R. Sanadi, S. V. Prasad, and P. K. Rohatgi, "Sun Hemp Fiber Reinforced Polyesters," *Journal of Material Science*, vol. 21, pp. 4299-4304, 1986.

[28] K. Jayaraman, "Manufacturing Sisal-Polypropylene Composites with Minimum Fiber Degradation," *Composites Science and Technology*, vol. 63, pp. 367-374, 2003.

[29] M. Z. Rong, M. Q. Zhang, Y. Liu, G. C. Yang, and H. M. Zeng, "The Effect Of Fiber Treatment On The Mechanical Properties Of Unidirectional Sisal Reinforced Epoxy Composites," *Composite Science and Technology*, vol. 61, pp. 1437-1442, 2001.

[30] J. Rout, M. Misra, and A. K. Mohanty, "Surface Modification Of Coir Fibers I – Studies On Graft Copolymerization Of Methyl Methacrylate On To Chemically Modified Coir Fiber," *Polymer for Advanced Technologies*, vol. 10, pp. 336-344, 1999.

[31] J. Rout, S. S. Tripathy, S. K. Nayak, M. Misra, and A. K. Mohanty, "Scanning Electron Microscopy Study Of Chemically Modified Coir Fibers," *Journal of Applied Polymer Science*, vol. 79, pp. 1169-1177, 2001.

[32] T. Nishino, K. Hirao, M. Kotera, K. Nakamae, and H. Inagaki, "Kenaf Reinforced Natural Degradable Composites," *Composites Science and Technology*, vol. 63, pp. 1281-1286, 2003.

[33] A. K. Mohanty, M. A. Khan, and G. Hinrichsen, "Influence Of Chemical Surface Modification on the Properties of Biodegradable Jute Fabrics-Polyester Amide Composite," *Composites Part A: Applied Science and Manufacturing*, vol. 31, no. 2, pp. 143-150, 2000.

[34] A. K. Mohanty, M. A. Khan, and G. Hinrichsen, "Surface Modification of Jute and Its Influence on Performance Of Biodegradable Jute-Fabric/Biopol Composites," *Composites Science and Technology*, vol. 66, no. 7, pp. 115-1124, 2000.

[35] K. Oksman, M. Skrifvars, and J. F. Selin, "Natural Fibers as Reinforcement in Polylactic Acid (PLA) Composites," *Composites Science and Technology*, vol.63, pp. 1324-1327, 2003.

[36] M. Shibata, K. Ozawa, N. Teramoto, R. Yosomiya, and H. Takeishi, "Natural Composites Made From Short Abaca Fiber And Natural Degradable Polyesters," *Macromolecular Material Engineering*, vol. 208, pp. 35-43, 2003.

[37] J. Ganster, and H. P. Fink, "Novel Cellulose Fiber Reinforced Thermoplastic Materials," *Cellulose*, vol. 13, pp. 271-280, 2006.

[38] S. V. Joshi, L. T. Drzal, A. K. Mohanty, and S. Arora, "Are Natural Fiber Composites Environment Superior To Glass Fiber Reinforced Composites," *Composites Part A: Applied Science and Manufacturing*, vol. 35, pp. 371-376, 2004.

[39] M. Z. Rong, and M. Q. Zhang, "The Effect Of Fiber Treatment On Mechanical Properties Of Unidirectional Sisal-Reinforced Epoxy Composites," *Composites Science and Technology*, vol. 61, pp. 1437-1447, 2001.

[40] A. K. Bledzki, H. P. Fink, and K. Specht, "Unidirectional Hemp And Flax EP And PP Composites: Influence Of Defined Fiber Treatments," *Journal Of Applied Polymer Science*, vol. 93, pp. 2150-2156, 2001.

[41] T. Van de Weyenberg, B. Chi Truong, I. Vangrimde, "Verpoest-Improving the Properties of UD Flax Fiber Reinforced Composites by Applying an Alkaline Fiber Treatment," *Composites Part A: Applied Science and Manufacturing*, vol. 37, no. 9, pp.1368-1376, 2006.

[42] R. Kozlowskiy, and M. Wladyka-Przybylak, "Flammability and Fire Resistance of Composites Reinforced by Natural Fibers," *Polymers for Advanced Technologies*, vol. 19, pp. 446-453, 2008.

[43] H. P. S. Abdul Khalil, and H. D. Rozman, "Rice Husk Polyester Composites: The Effect of Chemical Modification of Rice Husk on the Mechanical and Dimensional Stability Properties," *Polymer Plastics Technology and Engineering*, vol. 39, pp. 757-781, 2000.

[44] H. Takagi, and Y. Ichihara, "Effect Of Fiber Length On Mechanical Properties Of Green Composites Using A Starch-Based Resin And Short Bamboo Fibers," *JSME International Journal A*, vol. 47, no. 4, pp. 551-555, 2004.

[45] H. Takagi, "Natural Degradation Behavior Of Starch-Based "Green" Composites Reinforced by Manila Hemp Fibers," In: *Proceedings of 3rd International Conference on Eco-Composites*, Stockholm, vol. 14, pp. 1-6, 2005.

[46] L. Jiang, and G. Hinrichsen, "Flax And Cotton Fiber Reinforced Natural Degradable Polyester Amide Composites," *Die Angewandte Makromolekulare Chemie*, vol. 268, pp. 18-21, 1999.

[47] N. Chand, and D. Jain, "Effect of Sisal Fiber Orientation on Electrical Properties of Sisal Fiber Reinforced Epoxy Composites," *Composites Part A*, vol. 36, pp. 594-605, 2005.

[48] K. Joseph, and S. Thomas, "Tensile Properties Of Short Sisal Fiber Reinforced Polyethylene Composites," *Polymer*, vol. 37, pp. 5139-5149, 1996.

[49] N. Chand, and U. K. Dwivedi, "Effect Of Coupling Agent On Abrasive Wear Behavior Of Chopped Jute Fiber Reinforced PP Composites," *Wear*, vol. 261, pp. 1057-1063, 2006.

[50] A. M. Eleiche, and G. M. Amin, "The Effect of Unidirectional Cotton Fiber Reinforcement on the Friction and Wear Characteristics of Polyester," *Wear*, vol. 112, pp. 67-78, 1986.

[51] R. Kahraman, S. Abbasi, and B. Abu-Sharkh, "Influence Of Epolene G-3003 As A Coupling Agent On The Mechanical Behavior Of Pal-Fiber Polypropylene Composites," *International Journal of Polymeric Materials*, vol. 54, no. 6, pp. 483-503, 2005.

[52] K. G. Satyanarayana, K. Sukumaran, P. S. Mukherjee, C. Pavithran, and S. G. K. Pillai, "Natural Fiber-Polymer Composites," *Cement and Concrete Composites*, vol. 12, no. 2, pp. 117-136, 1990.

[53] K. G. Satyanarayana, K. Sukumaran, A. G. Kulkarni, S. G. K. Pillai, and P. K.K Rohatgi, "Fabrication And Properties Of Natural Fiber Reinforced Polyester Composites," *Composites*, vol. 17,no. 4, pp. 329-333, 1986.

[54] T. M. Gowda, A. C. B. Naidu, and R. Chhaya, "Some Mechanical Properties Of Untreated Jute Fabric-Reinforced Polyester Composites," *Composites Part A: Appleid Science and Manufacturing*, vol. 30, no. 3, pp. 277-284, 1999.

[55] L. A. Pothan, S. Thomas, and Z. Oommen, "Dynamic Mechanical Analysis Of Banana Fiber Reinforced Polyester Composites," *Composites Science and Technology*, vol. 63, no. 2, pp. 267-293, 2003.

[56] T. Corbiere-Nicollier, B. G. Laban, L. Lundquist, Y. Leterrier, J. Manson, and O. Jolliet, "Life Cycle Assessment Of Biofibers Replacing Glass Fibers As Reinforcement In Plastics," *Resources, Conservation and Recycling*, vol. 33, no. 4, pp. 267-287, 2001.

[57] L. A. Pothan, S. Thomas, and N. R. Neelakantan, "Short Banana Fiber Reinforced Polyester Composites: Mechanical, Failure And Aging Characteristics," *Journal of Reinforced Plastics and Composites*, vol. 16, no. 8, pp. 744-765, 1997.

[58] K. Joseph, S. Thomas, and C. Pavithran, "Viscoelastic Properties Of Short Sisal Fiber Filled Low Density Polyethylene Composites: Effect Of Fiber Length And Orientation," *Materials Letters*, vol. 15, pp. 224-228, 1992.

[59] J. George, S. S. Bhagawan, and S. Thomas, "Thermogravimetric And Dynamic, Mechanical Thermal Analysis Of Pineapple Fiber Reinforced Polyethylene Composites," *Journal of Thermal Analysis and Calorimetry*, vol. 47, no. 4, pp. 1121-1140, 1996.

[60] A. Amash, and P. Zugenmaier, "Morphology And Properties Of Isotropic And Oriented Samples Of Cellulose Fiber-Polypropylene Composites," *Polymer*, vol. 41, no. 4, pp. 1589-1596, 2000.

[61] S. Luo, and A. N. Netravali, "Mechanical And Thermal Properties Of Environmentally Friendly Green Composites Made From Pineapple Leaf Fibers And Poly (Hydroxybutyrate-Co-Valerate) Resin," *Polymer Composites*, vol. 20, no. 3, pp. 367-378, 1999.

[62] M. N. Cazaurang-Martinez, P. J. Herrera-Franco, P. I. Gonzalez-Chi, and M. Aguilar-Vega, "Physical And Mechanical Properties Of Henequen Fibers*," Journal of Applied Polymer Science*, vol. 43, no. 4, pp. 749-756, 1991.

[63] A. C. Karmaker, and J. P. Schneider, "Mechanical Performance Of Short Jute Fiber Reinforced Polypropylene," *Journal of Material Science Letters*, vol. 15, no. 3, pp. 201-202, 1996.

[64] A. K. Srivastav, M. K. Behera, and B. C. Ray, "Loading Rate Sensitivity Of Jute/Glass Hybrid Reinforced Epoxy Composites: Effect Of Surface Modifications," *Journal of Reinforced Plastics and Composites*, vol. 26, no. 9, pp. 851-860, 2007.

[65] S. Shibata, Y. Cao, and I. Fukumoto, "Press Forming Of Short Natural Fiber Reinforced Biodegradable Resin: Effect Of Fiber Volume And Length On Flexural Properties*," Polymer Testing*, vol. 24, no. 8, pp. 1005-1011, 2005.

[66] S. M. Sapuan, A. Leenie, M. Harimi, and Y. K. Beng, "Mechanical Properties of Woven Banana Fiber Reinforced Epoxy Composites," *Materials and Design*, vol. 27, no. 8, pp. 689-693, 2006.

[67] K. K. Chawla, and A. C. Bastos, "The Mechanical Properties of Jute Fibers and Polyester/Jute Composites*," In: Proceedings of the third international conference on mechanical behavior of materials. Cambridge, UK: Pergamon Press*, pp. 191-196, 1979.

[68] D. G. Hepworth, R. N. Hobson, D. M. Bruce, and J. W. Farrent, "The Use Of Unretted Hemp Fiber In Composite Manufacture," *Composites Part a: Applied Science and Manufacturing*, vol. 31, no. 11, pp. 1279-1283, 2000.

[69] L. B. Harriette, M. Jorg, and M. J. A, "Van Den Oever. Mechanical Properties Of Short Flax Fiber Reinforced Compounds," *Composites Part A: Applied Science and Manufacturing*, vol. 37, no. 10, pp. 1591-1604, 2006.

[70] S. N. Monteiro, L. A. H. Terrones, and J. R. M. D'Almeida, "Mechanical Performance Of Coir Fiber/Polyester Composites," *Polymer Testing*, vol. 27, no. 5, pp. 591-595, 2006.

[71] C. Santulli, "Post-Impact Damage Characterization On Natural Fiber Reinforced Composites Using Acoustic Emission," *NDT & E International*, vol. 34, no. 8, pp. 531-536, 2008.

[72] C. Pavithran, P. S. Mukherjee, M. Brahmakumar, and A. D. Damodaran, "Impact Properties Of Natural Fiber Composites," *Journal of Materials Science Letters*, vol. 6, no. 8, pp. 882-884, 1987.

[73] B. C. Tobias, "Tensile and Impact Behavior of Natural Fiber Reinforced Composite Materials," *In: Proceedings of Advanced Composites' 93: International Conference on Advanced Composite Materials; Australia*, pp. 623-627, 1993.

[74] V. S. Godbole, and S. C. Lakkad, "Effect Of Water Absorption On The Mechanical Properties Of Bamboo," *Journal of Materials Science Letters*, vol. 5, no. 3, pp. 303-304, 1986.

[75] X. Chen, Q. Guo, and Y. Mi, "Bamboo Fiber Reinforced Polypropylene Composites: A Study Of The Mechanical Properties," *Journal of Appleid Polymer Science*, vol. 69, no. 10, pp. 1891-1899, 1998.

[76] A. K. Chaurasiya, I. Chakraborty, and J. Saha, "Value Addition Of Palmyra Palm And Studies On The Storage Life," *Journal of Food Science Technology*, vol. 51, no. 4, pp. 768–773, 2014.

[77] R. Velmurugan, and V. Manikandan, "Mechanical Properties Of Palmyra/Glass Fiber Hybrid Composites," *Composites Part A: Applied Science and Manufacturing*, vol. 38, pp. 22216–2226, 2007.

[78] N. Venkateshwaran, A. Elaya Perumal, A. Alavudeen, and M. Thiruchitrambalam, "Mechanical and Water Absorption Behavior of Banana/Sisal Reinforced Hybrid Composites," *Materials and Design*, vol. 32, pp. 4017–4021, 2011.

[79] D. Shanmugam, and M. Thiruchitrambalam, "Static And Dynamic Mechanical Properties Of Alkali Treated Unidirectional Continuous Palmyra Palm Leaf Stalk Fiber/Jute Fiber Reinforced Hybrid Polyester Composites," *Materials and Design*, vol. 50, pp. 533–542, 2013.

[80] Adavi Balakrishna, Damera Nageswara Rao, and Adapa Swamy Rakesh, "Characterization and Modeling of Process Parameters on Tensile Strength of Short and Randomly Oriented Borassus Flabellifer (Asian Palmyra) Fiber Reinforced Composite," *Composites: Part B*, vol. 55, pp. 479–485, 2013.

[81] Zawawi Dauda, Mohd. Zainuri, Mohd. Hatta, and Halizah Awang, "Oil Palm Leaf And Corn Stalk – Mechanical Properties And Surface Characterization," *Procedia - Social and Behavioral Sciences*, vol. 195, pp. 2047 – 2050, 2015.

[82] Nadendla Srinivasababua, J. Suresh Kumar, and K. Vijaya Kumar Reddy, "Manufacturing and Characterization of Long Palmyra Palm/Borassus Flabellifer Petiole Fiber Reinforced Polyester Composites," *Procedia Technology: 2nd International Conference on Innovations in Automation and Mechatronics Engineering 2014*, vol. 14, pp. 252 – 259, 2014.

[83] Waranyou Sridach, "Pulping And Paper Properties Of Palmyra Palm Fruit Fibers," *Songklanakarin Journal of Science and Technology*, vol. 32, no. 2, pp. 201-205, 2010.

[84] Ahmed Ali, Djibrilla Alhadji, Clergé Tchiegang, and Clément Saïdou, "Physico-Chemical Properties Of Palmyra Palm *(Borassus Aethiopum* Mart.*)* Fruits From Northern Cameroon," *African Journal of Food Science*, vol. 4, no. 3, pp. 115-119, 2010.

[85] V. Manikandan, and R. Velmurugan, "Utilization Of Bioresources Such As Coir-Pith, Saw Dust And Palmyra Fiber As Reinforcement Material In Polyester Matrix," *Materials Science: an Indian Journal*, vol. 7, no. 2, pp. 94-99, 2011.

[86] V. K. Doko, E. C. Adjovi, C. Delisee, and P. Galimard, "Comparative Study Of The Formulation And Physical And Mechanical Features Of Cement Matrix Composite Rein-Forced With Plant Biomass: The Case Of Fibers *Borassus Ae-Thopium Mart* And Rice Husk," *International Journal of Advance Research*, vol. 1, no. 2, pp. 16-22, 2013.

[87] H. Byrne, "On the Use of the Timber of the Palmyra Palm in the Construction of Bridges," *Minutes of the Proceedings of the Institution of Civil Engineers*, vol. 22, pp. 58-61, 1863.

[88] M. F. Attom, N. M. Al-Akhras, and A. I. H. Malkawi, "Effect Of Fibres On The Mechanical Properties Of Clayey Soil," *Proceedings of the Institution of Civil Engineers - Geotechnical Engineering*, vol. 162, no. 5, pp. 277-282, 2009.

[89] C. Mahesh, B. Kondapanaidu, K. Govindarajulu, and V. Balakrishnamurthy, "Experimental Investigation Of Thermal And Mechanical Properties Of Palmyra Fiber Reinforced Polyester Composites With And Without Chemical Treatment And Also Addition Of Chalk Powder," International *Journal of Engineering Trends and Technology*, vol. 5, no. 5, pp. 259-271, 2013.

[90] Narayan C. Nayak, and Antaryami Mishra, "Development And Mechanical Characterization Of Palmyra Fruit Fiber Reinforced Epoxy Composites," *Journal of Production Engineering*, vol. 16, no. 2, pp. 69-72, 2013.

[91] B. M. Dabade, G. Ramachandra Reddy, S. Rajesham, and C. Udaya Kiran, "Effect Of Fiber Length And Fiber Weight Ratio On Tensile Properties Of Sun Hemp And Palmyra Fiber Reinforced Polyester Composites," *Journal Of Reinforced Plastics And Composites*, vol. 25, no. 16, pp. 1733-1738, 2006.

[92] M. Thiruchitrambalam, and D. Shanmugam, "Influence Of Pre-Treatments On The Mechanical Properties Of Palmyra Palm Leaf Stalk Fiber–Polyester Composites," *Journal of Reinforced Plastics and Composites*, vol. 31, no. 20, pp. 1400–1414, 2012.

[93] D. Shanmugam, M. Thiruchitrambalam, and R. Thirumurugan, "Continuous Unidirectional Palmyra Palm Leaf Stalk Fiber/Glass—Polyester Composites: Static And Dynamic Mechanical Properties," *Journal of Reinforced Plastics and Composites*, vol. 33, no. 9, pp. 836–850, 2014.

[94] V. Arumuga Prabu, V. Manikandan, R. Venkatesh, P. Vignesh, S. Vignesh, K. Siva Sankar, P. Sripathy, and E. Subburaj, "Influence Of Redmud Filler On Palmyra Fruit And

Palmyra Fiber Waste Reinforced Polyester Composite: Hardness, Tensile And Impact Studies," *Materials Physics and Mechanics*, vol. 24, pp. 41-49, 2015.

[95] Budrun Neher, Md. Mahbubur Rahman Bhuiyan, Humayun Kabir, Md. Rakibul Qadir, Md. Abdul Gafur, and Farid Ahmed, "Study Of Mechanical And Physical Properties Of Palm Fiber Reinforced Acrylonitrile Butadiene Styrene Composite," *Materials Sciences and Applications*, vol. 5, pp. 39-45, 2014.

[96] Budrun Neher, Md. Abdul Gafur, Muhammad Abdullah Al-Mansur, Md. Mahbubur Rahman Bhuiyan, Md. Rakibul Qadir, and Farid Ahmed, "Investigation Of The Surface Morphology And Structural Characterization Of Palm Fiber Reinforced Acrylonitrile Butadiene Styrene (Pf-Abs) Composites," *Materials Sciences and Applications*, vol. 5, pp. 378-386, 2014.

[97] P. Sudhakara, A. P. Kamala Devi, C. Venkata Prasad, K. Obi Reddy, L. Dong Woo, B. S. Kim, and J. I. Song, "Thermal, Mechanical, And Morphological Properties Of Maleated Polypropylene Compatibilized Borassus Fruit Fiber/Polypropylene Composites," *Journal of Applied Polymer Science*, DOI: 10.1002/app.38135, pp. 976-982, 2013.

[98] K. Ngargueudedjim, N. Allarabeye, K. Charlet, J. F. Destrebecq, R. Moutou Pitti, J. L. Robert, "Mechanical Caracteristics Of Fiber Palmyra," *The Global Journal of Researches in Engineering*, vol. 15, no. 3, 2015.

[99] S. A. S. Goulart, T. A. Oliveira, A. Teixeira, P. C. Miléo, D. R. Mulinari, "Mechanical Behaviour Of Polypropylene Reinforced Palm Fibers Composites," *Procedia Engineering*, vol. 10, pp. 2034–2039, 2011.

[100] G. W. Stachowiak, and A. W. Batchelor, "Engineering Tribology," 2nd Edition, *Jordan Hill, Oxford: Butterworth-Heinemann*, 2001.

[101] J. M. Ziman, "Electrons In Metals- A Short Guide To The Fermi Surface," *Taylor and Francis, London*, 1963.

[102] C. S. Yust, and R. S. Crouse, "Melting at Particle Impact Sites during Erosion of Ceramics," *Wear*, vol. 51, pp. 193-196, 1978.

[103] N. Soda, Y. Kimura, and A. Tanaka, "Wear Of Some F.C.C Metals During Unlubricated Sliding Part 1: Effects Of Velocity And Atmospheric Pressure," *Wear*, vol. 33, pp. 1-16, 1975.

[104] G. W. Rengstorff, K. Miyoshi, and D. H. Buckley, "Interaction Of Sulphuric Acid Corrosion And Mechanical Wear Of Iron," *ASLE Transactions*, vol. 29, pp. 43-51, 1986.

[105] J. Sato, "Recent Trends Of Fretting Wear," *Transactions JSLE*, vol. 30, pp. 853-858, 1985.

[106] J. Halling, "Principles Of Tribology," *The Macmillian Press Ltd*, 1975.

[107] J. A. Williams, "Engineering Tribology," *Oxford University Press*, 1995.

[108] I. M. Hutchings, 'Tribology: Friction And Wear Of Engineering Materials," *Edward Arnold*, 1992.

[109] B. J. Briscoe, "The Tribology Of Composite Materials: A Preface," *Advances in Composite Tribology, Composite Materials Series*, vol. 8, pp. 3-15, 1993.

[110] K. Friedrich, "Wear Performance of High Temperature Polymers and Their Composites," *Application of High Temperature Polymers*, vol. 2, pp. 221-246, 1997.

[111] Z. Jiang, A. G. Lada, K. S. Alois, F. Klaus, and Z. Zhang, "Study On Friction And Wear Behavior Of Polyphenylene Sulfide Composites Reinforced By Short Carbon Fibers And Sub-Micro Tio2 Particles," *Composites Science and Technology*, vol. 68, pp. 734-742, 2008.

[112] L. Chang, Z. Zhang, C. Breidt, and K. Friedrich, "Tribological Properties Of Epoxy Nano Composites I: Enhancement Of The Wear Resistance By Nano-Tio2 Particles," *Wear*, vol. 258, pp. 141-148, 2005.

[113] A. Satapathy, and A. Patnaik, "Analysis Of Dry Sliding Wear Behavior Of Red Mud Filled Polyester Composites Using The Taguchi Method," *Journal of Reinforced Plastics and Composites*, vol. 29, pp. 2883-2897, 2008.

[114] B. Z. Jang, "Advanced Polymer Composites: Principles And Application," *ASM International*, 1994.

[115] K. Jungil, P. H. Kang, and Y. C. Nho, "Positive Temperature Coefficient Behavior of Polymer Composites Having a High Melting Temperature," *Journal of Applied Polymer Science*, vol. 92, pp. 394-401, 2004.

[116] M. Cirino, K. Friedrich, and R. B. Pipes, "The Abrasive Wear Behavior Of Continuous Fiber Polymer Composites," *Journal of Materials Science*, vol. 22, pp. 2481-2492, 1987.

[117] M. Cirino, K. Friedrich, and R. B. Pipes, "Evaluation of Polymer Composites for Sliding and Abrasive Wear Application," *Composites*, vol. 19, pp. 383-392, 1988.

[118] K. Friedrich, J. Karger Kocsis, and Z. Lu, "Effects of Counterpart Roughness and Temperature on the Friction and Wear of PEEK Composites," *Wear*, vol. 148, pp. 235-247, 1991.

[119] K. Friedrich, Z. Lu, and A. M. Hager, "Overview on Polymer Composites for Friction and Wear Application," *Theoretical and Applied Fracture Mechanics*, vol. 19, pp. 1-11, 1993.

[120] N. S. El Tayeb, and R. M. Gadelrab, "Friction and Wear Properties of E-Glass Fiber Reinforced Epoxy Composites under Different Sliding Contact Conditions," *Wear*, vol. 192, pp. 112-117, 1996.

[121] A. Rout, and A. Satapathy, "Analysis Of Dry Sliding Wear Behavior Of Rice Husk Filled Epoxy Composites Using Design Of Experiment And ANN," *Procedia Engineering*, vol. 38, pp. 1218-1232, 2012.

[122] B. Shivamurthy, K. Udaya Bhat, and S. Anandhan, "Mechanical and Sliding Wear Properties of Multi-Layered Laminates from Glass Fabric/Graphite/Epoxy Composites," *Materials and Design*, vol. 44, pp. 136-143, 2013.

[123] L. A. Gyurova, and K. Friedrich, "Artificial Neural Networks for Predicting Sliding Friction and Wear Properties of Polyphenylene Sulfide Composites," *Tribology International*, vol. 44, pp. 603-609, 2011.

[124] L. A. Gyurova, "Sliding Friction And Wear Of Polyphenylene Sulfide Matrix Composites: Experimental And Artificial Neural Network Approach," *Ph.D. Thesis, Institutfuer Verbundwerkstoffe Gmbh: Kaiserslautern, Germany*, 2010.

[125] Z. Jia, and Y. Yang, "Self-Lubricating Properties Of PTFE/Serpentine Nano Composite Against Steel At Different Loads And Sliding Velocities," *Composites: Part B*, vol. 43, pp. 2072-2078, 2012.

[126] A. Abdelbary, M. N. Abouelwafa, I. El Fahham, and A. H. Hamdy, "The Influence Of Surface Crack On The Wear Behavior Of Polyamide 66 Under Dry Sliding Condition," *Wear*, vol. 271, pp. 2072-2078, 2012.

[127] V. K. Srivastava, and J. P. Pathak, "Friction and Wear Properties of Bushing Bearing of Graphite Filled Short Glass Composites in Dry Sliding," *Wear*, vol. 197, pp. 145-150, 1996.

[128] A. Umeda, J. Sugimura, and Y. Yamamoto, "Characterization of Wear Particles and Their Relations with Sliding Conditions," *Wear*, vol. 216, pp. 220-228, 1998.

[129] G. Xian, and Z. Zhang, "Sliding Wear Polyitherimide Matrix Composites I: Influence Of Short Carbon Fiber Reinforcement," Wear, vol. 258, pp. 783-788, 2005.

[130] G. Xian, and Z. Zhang, "Sliding Wear Of Polyitherimide Matrix Composites II: Influence Of Graphite Flakes," *Wear*, vol. 258, pp. 783-788, 2005.

[131] P. K. Bajpai, I. Singh, and J. Madaan, "Friction And Adhesive Wear Performance Of Natural Fiber Reinforced Polypropylene Composites," *Proceedings of The Institution of Mechanical Engineers Part J: Journal of Engineering Tribology*, DOI: 10.1177/1350650112461868, 2012.

[132] P. K. Bajpai, I. Singh, and J. Madaan, "Comparative Studies Of Mechanical And Morphological Properties Of PLA And PP Based Natural Fiber Composites," *Journal of Reinforced Plastics and Composites*, vol. 31, no. 24, pp. 1712-1724, 2012.

[133] H. Unal, and A. Mimaroglu, "Friction And Wear Performance Of Polyamide 6 And Graphite And Wax Polyamide 6 Composites Under Dry Sliding Conditions," *Wear*, vol. 289, pp. 132-137, 2012,

[134] G. Zhao, I. Hussainova, M. Antonov, Q. Wang, and T. Wang, "Friction and Wear Of Fiber Reinforced Polyamide Composites," *Wear*, vol. 301, pp. 122-129, 2013.

[135] P. K. Bajpai, I. Singh, and J. Madaan, "Tribological Behavior of Natural Fiber Reinforced PLA Composites," *Wear*, vol. 297, pp. 829-840, 2013.

[136] Sezgin Ersoy, and Haluk Kucuk, "Investigation of Industrial Tea-Leaf-Fibre Waste Material for Its Sound Absorption Properties," *Applied Acoustics*, vol. 70, pp. 215–220, 2009.

[137] Umberto Berardi, and Gino Iannace, "Acoustic Characterization Of Natural Fibers For Sound Absorption Applications," *Building and Environment. http://dx.doi.org/10.1016/j.buildenv.2015.05.029.* Article in Press, 2015.

[138] S. Prabhakarana, V. Krishnaraj, M. Senthil kumar, and R. Zitouned, "Sound and Vibration Damping Properties of Flax Fiber Reinforced Composites," *Procedia Engineering*, vol. 97, pp. 573 – 581, 2014.

[139] Hasan Koruk, and Garip Genc, "Investigation of the Acoustic Properties of Bio Luffa Fiber and Composite Materials," *Materials Letters*, vol. 157, pp. 166–168, 2015.

[140] Mohammad Hosseini Fouladi , Md. Ayub, and Mohd Jailani Mohd Nor, "Analysis Of Coir Fiber Acoustical Characteristics," *Applied Acoustics*, vol. 72, pp. 35–42, 2011.

[141] Con Wassilieff, "Sound Absorption of Wood-Based Materials," *Applied Acoustics*, vol. 48, no. 4, pp. 339-356, 1996.

[142] K. O. Ballagh, "Acoustical Properties of Wool," *Applied Acoustics*, vol. 48, no. 2, pp. 101-120, 1996.

[143] Han Seung Yang, Dae Jun Kim, and Hyun Joong Kim, "Rice Straw–Wood Particle Composite For Sound Absorbing Wooden Construction Materials," *Bioresource Technology*, vol. 86, pp. 117–121, 2003.

[144] Yang Wei Dong, and Li Yan, "Sound Absorption Performance of Natural Fibers and Their Composites," *Science China*, vol. 55, no. 8, pp. 2278-2283, 2012.

[145] G. Thilagavathi, E. Pradeep, T. Kannaian, and L. Sasikala, "Development of Natural Fiber Nonwovens for Application as Car Interiors for Noise Control," *Journal of Industrial Textiles*, vol. 39, no. 3, pp. 267-278, 2010.

[146] Hai fan Xiang, Dong Wang, Hui chao Liua, Ning Zhaoa, and Jian Xu, "Investigation On Sound Absorption Properties Of Kapok Fibers," *Chinese Journal of Polymer Science*, vol. 31, no. 3, pp. 521−529, 2013.

[147] Elammaran Jayamania, Sinin Hamdan, Md. Rezaur Rahman, and Muhammad Khusairy Bin Bakri, "Investigation of Fiber Surface Treatment on Mechanical, Acoustical and Thermal Properties of Betelnut Fiber Polyester Composites," *Procedia Engineering*, vol. 97, pp. 545 – 554, 2014.

[148] M. J. Swift, P. Brisi, and K. V. Horoshenkov, "Acoustic Absorption In Re-Cycled Rubber Granulate," *Applied Acoustics*, vol. 57, pp. 203-212, 1999.

[149] Zhou Hong, Li Bo, Huang Guangsu, and He Jia, "A Novel Composite Sound Absorber With Recycled Rubber Particles," *Journal of Sound and Vibration*, vol. 304, pp. 400–406, 2007.

[150] Hong Zhou, Bo Li, and Guangsu Huang, "Sound Absorption Characteristics of Polymer Microparticles," *Journal of Applied Polymer Science*, vol. 101, pp. 2675–2679, 2006.

[151] R. Verdejo, R. Stämpfli, M. Alvarez Lainez, S. Mourad, M. A. Rodriguez Perez, P. A. Brühwiler, and M. Shaffer, "Enhanced Acoustic Damping in Flexible Polyurethane Foams Filled with Carbon Nanotubes," *Composites Science and Technology*, vol. 69, pp. 1564–1569, 2009.

[152] Sheng Jiang, Yunyan Xu, Huiping Zhang, Chris Branford White, and Xiong Yan, "Seven-Hole Hollow Polyester Fibers As Reinforcement in Sound Absorption Chlorinated Polyethylene Composites," *Applied Acoustics*, vol. 73, pp. 243–247, 2012.

[153] J. Henning, and W. Knappe, "Anisotropy of Thermal Conductivity in Stretched Amorphous Linear Polymers and In Strained Elastomers," *Journal of Polymer Science Part C*, vol. 6, pp. 167-174, 1964.

[154] D. Hansen, and C. Ho, "Thermal Conductivity of High Polymers," *Journal of Polymer Science Part A*, vol. 3, pp. 659-670, 1965.

[155] S. Peng, and R. Landel, "Induced Anisotropy of Thermal Conductivity of Polymer Solids under Large Strain," *Journal of Applied Polymer Science*, vol. 19, pp. 49–68, 1975.

[156] C. L. Choy, and K. Young, "Thermal Conductivity of Semi Crystalline Polymers – A Model," *Polymer*, vol. 18, pp. 769-776, 1977.

[157] I. Tavman, "Thermal Anisotropy of Polymers as a Function of Their Molecular Orientation, Experimental Heat Transfer, Fluid Mechanics, and Thermodynamics," *Elsevier*, pp. 1562-1568, 1991.

[158] A. Griesinger, W. Hurler, and M. Pietralla, "A Photothermal Method With Step Heating For Measuring The Thermal Diffusivity Of Anisotropic Solids," *International Journal of Heat and Mass Transfer*, vol. 40, pp. 3049-3058, 1997.

[159] N. M. Sofian, M. Rusu, R. Neagu, and E. Neagu, "Metal Powder-filled Polyethylene Composites. V. Thermal Properties," *Journal of Thermoplastic Composite Materials*, vol. 14, no. 1, pp. 20–33, 2001.

[160] Y. P. Mamunya, V. V. Davydenko, P. Pissis, and E. V. Lebedev, "Electrical and Thermal Conductivity of Polymers Filled with Metal Powders," *European Polymer Journal*, vol. 38, pp. 1887–1897, 2002.

[161] H. S. Tekce, D. Kumlutas, and I. H. Tavman, "Determination of the Thermal Properties of Polyamide-6 (Nylon-6)/Copper Composite by Hot Disk Method," *In Proceedings of the 10th Denizli Material Symposium*, pp. 296–304, 2004.

[162] L. S. Luyt, J. A. Molefi, and H. Krump, "Thermal, Mechanical and Electrical Properties of Copper Powder Filled Low-Density and Linear Low-Density Polyethylene Composites," *Polymer Degradation and Stability*, vol. 91, pp. 1629-1636, 2006.

[163] I. H. Tavman, "Thermal and Mechanical Properties of Aluminum Powder filled High-density Polyethylene Composites," *Journal of Applied Polymer Science*, vol. 62, pp. 2161–2167, 1996.

[164] K. Sanada, Y. Tada, and Y. Shindo, "Thermal Conductivity Of Polymer Composites With Close-packed Structure of Nano and Micro Fillers," *Composites: Part A*, vol. 40, pp. 724-730, 2009.

[165] A. Agrawal, and A. Satapathy, "A Numerical Study on Heat Conductivity Characterization of Aluminium Filled Polypropylene Composites," *Advanced Material Research*, vol. 585, pp. 14-18, 2012.

[166] D. Veyret, S. Cioulachtjian, L. Tadrist, and J. Pantoloni, "Effective Thermal Conductivity Of A Composite Material: A Numerical Approach," *ASME Journal of Heat Transfer*, vol. 115, pp. 866-871, 1993.

[167] D. Kumlutas, and I. H. Tavman, "A Numerical and Experimental Study on Thermal Conductivity of Particle Filled Polymer Composites," *Journal of Thermoplastic Materials*, vol. 19, pp. 441-455, 2006.

[168] A. Boudenne, L. Ibos, M. Fois, E. Gehin, and J. C. Majeste, "Thermophysical Properties Of Polypropylene/Aluminium Composites," *Journal of Polymer Composite: Part B: Polymer Physics*, vol. 42, pp. 722-732, 2004.

[169] A. Bjorneklett, L. Halbo, and H. Kristiansen, "Thermal Conductivity of Epoxy Adhesives Filled with Silver Particles," *International Journal of Adhesion and Adhesives*, vol. 12, pp. 99–104, 1992.

[170] H. Tu, and L. Ye, "Thermal Conductive PS/Graphite Composites," *Polymer Advance Technology*, vol. 20, pp. 21–27, 2009.

[171] Z. Liu, Q. Guo, J. Shi, G. Znai, and L. Liu, "Graphite Blocks with High Thermal Conductivity Derived from Natural Graphite Flake," *Carbon*, vol. 46, pp. 414-421, 2008.

[172] S. Ganguli, A. K. Roy, and D. P. Anderson, "Improved Thermal Conductivity For Chemically Functionalized Exfoliated Graphite/Epoxy Composites," *Carbon*, vol. 46, pp. 806–817, 2008.

[173] G. G. Tibbetts, M. L. Lake, K. L. Strong, and B. P. Rice, "A Review of the Fabrication and Properties of Vapor-Grown Carbon Nanofiber/Polymer Composites," *Composite Science and Technology*, vol. 67, pp. 1709–1718, 2007.

[174] Z. Han, and A. Fina, "Thermal Conductivity of Carbon Nanotubes and Their Polymer Nanocomposites: A Review," *Progress in Polymer Science*, vol. 36, pp. 914-944, 2011.

[175] Dong-Pyo Kim, M. Rusu, R. Neagu, and E. Neagu, "Fabrication and Properties of Thermal Insulating Glass Fiber Reinforced Composites from Low Temperature Curable Polyphosphate Inorganic Polymers," *Journal of Thermoplastic Composite Materials*, vol. 14, pp. 20-23, 2003.

[176] H. S. Schuster, D. Kumlutas, and I. H. Tavman, "Thermal Conductivities of Three dimensionally Woven Fabric Composites," *Denizli*, pp. 96–304, 2008.

[177] T. Zhidong, and L. Nielsen, "Thermal Conductivity of Carbon Nanotubes and Their Polymer Nanocomposites: A Review," 141449-1471, 2011.

[178] N. N. Yüksel, A. Avcı, and M. Kılıc, "The Temperature Dependence of Effective Thermal Conductivity of the Samples of Glass Wool Reinforced with Aluminium Foil," *International Communications in Heat and Mass Transfer*, vol. 37, pp. 675–680, 2010.

[179] J. Z. L. Hang, F. H. Li, "An Approach to Enhance Through-Thickness Thermal Conductivity of Polymeric Fiber Composites," *Polymer Testing*, vol. 25, pp. 527-531, 2013.

[180] Sharifah H. Aziz, and Martin P. Ansell, "The Effect of Alkalization and Fibre Alignment on The Mechanical And Thermal Properties Of Kenaf And Hemp Bast Fibre Composites: Part 1 – Polyester Resin Matrix," *Composites Science and Technology*, vol. 64, pp. 1219–1230, 2004.

[181] Maries Idicula, Abderrahim Boudenne, L. Umadevi, Laurent Ibos, Yves Candau, and Sabu Thomas, "Thermophysical Properties Of Natural Fibre Reinforced Polyester Composites," *Composites Science and Technology*, 66, pages 2719–2725, 2006.

[182] Thi-Thu-Loan Doan, Hanna Brodowsky, and Edith Ma¨der, "Jute Fibre/Polypropylene Composites II. Thermal, Hydrothermal And Dynamic Mechanical Behavior," *Composites Science and Technology*, vol. 67, pp. 2707–2714, 2007.

[183] I. S. Aji, E. S. Zainudin, A. Khalina, S. M. Sapuan, and M. D. Khairul, "Thermal Property Determination Of Hybridized Kenaf/PALF Reinforced HDPE Composite By

Thermogravimetric Analysis," *Journal of Thermal Anal Calorim*, vol. 109, pp. 893–900, 2012.

[184] Y. A. El-Shekeil, S. M. Sapuan, A. Khalina, E. S. Zainudin, and O. M. Al-Shuja'a, "Effect Of Alkali Treatment On Mechanical And Thermal Properties Of Kenaf Fiber-Reinforced Thermoplastic Polyurethane Composite," *Journal Thermal Anal Calorim*, vol. 109, pp. 1435–1443, 2012.

[185] P. Persico, D. Acierno, C. Carfagna, and F. Cimino, "Mechanical and Thermal Behaviour of Ecofriendly Composites Reinforced by Kenaf and Caroà Fibers," *International Journal of Polymer Science*, Vol. 2011, Article ID 841812, pp. 1-7, 2011.

[186] Jahangir A. Khan, Mubarak A. Khan, and M. Rabiul Islam, "A Study on Mechanical, Thermal and Environmental Degradation Characteristics of N,N-Dimethylaniline Treated Jute Fabric-reinforced Polypropylene Composites," *Fibers and Polymers*, vol. 15, no. 4, pp. 823-830, 2014.

[187] R. A. Braga, and P. A. A. Magalhaes Jr, "Analysis of the Mechanical and Thermal Properties of Jute and Glass Fiber as Reinforcement Epoxy Hybrid Composites," *Materials Science and Engineering C*, vol. 56, pp. 269–273, 2015.

[188] R. V. Silva, M. M. Ueki, D. Spinelli, W. W. Bose Filho, and J. R. Tarpani, "Thermal, Mechanical, and Hygroscopic Behavior of Sisal Fiber/Polyurethane Resin-based Composites," *Journal of Reinforced Plastics and Composites*, vol. 29, no. 9, pp.1399-1417, 2010.

[189] G Phiri, MC Khoathane, and ER Sadiku, "Effect Of Fibre Loading On Mechanical And Thermal Properties Of Sisal And Kenaf Fibre-Reinforced Injection Moulded Composites," *Journal of Reinforced Plastics and Composites*, vol. 33, no. 3, pp. 283–293, 2014.

[190] Andressa Cecília Milanese, Maria Odila Hilário Cioffi, and Herman Jacobus Cornelis Voorwald, "Thermal And Mechanical Behaviour Of Sisal/Phenolic Composites," *Composites: Part B*, vol. 43, pp. 2843–2850, 2012.

[191] Maria F. V. Marques, Juliana N. Lunz, Vinicius O. Aguiar Iryna Grafova, Marianna Kemell, Francesca Visentin, Andrea Sartori, and Andriy Grafov, "Thermal and Mechanical Properties of Sustainable Composites Reinforced with Natural Fibers," *Journal of Polymer Environment*, vol. 23, pp. 251–260, 2015.

[192] Sandhyarani Biswas, "Processing, Characterization and Wear Response of Particulate Filled Epoxy Based Hybrid Composites,"*A thesis submitted to NIT Rourkela*, 2010.

[193] J. Ever Barbero, "Introduction to Composite Materials Design," *Taylor & Francis, Philadelphia, PA*, 1999.

[194] Shanmugam D, **"**Studies On The Properties Of Palmyra Palm Leaf Stalk Fiber (Pplsf) Reinforced Polyester Composite Materials," *A thesis submitted to Anna University*, 2014.

[195] B. D. Agarwal, and L. J. Broutman, "Analysis and Performance of Fiber Composites: Second Edition," *John Wiley and Sons*, Inc, 1990.

[196] Z. Zhang, and K. Friedrich, "Artificial Neural Network Applied to Polymer Composites: A Review," *Composites Science and Technology*, vol. 63, no. 14, pp. 2029-2044, 2003.

[197] H. E. Kadi, "Modelling the Mechanical Behaviour of Fiber-reinforced Polymeric Composite Materials Using Artificial Neural Network- A Review," *Composite Structure*, vol. 73, no. 1, pp. 1-23, 2006.

[198] Z. Jiang, Z. Zhang, and K. Friedrich, "Prediction on Wear Properties of Polymer Composites with Artificial Neural Network," *Composites Science and Technology*, vol. 67, pp. 168-176, 2007.

[199] D. Kumlutas, I. H. Tavman, and M. T. Coban, "Thermal Conductivity of Particle Filled Polyethylene Composite Materials," *Composites Science and Technology*, vol. 63, no. 1, pp. 113-117, 2003.

[200] T. Lewis, and L. Nielsen, "Thermal Conductivity of Particulate Filled Polymers," *Journal of Applied Polymer Science*, vol. 29, pp. 3819-3825, 1973.

[201] J. C. Maxwell, "A Treatise on Electricity and Magnetism," *3rd edition New York: Dover*, vol. 2, pp. 263-269, 1954.

*****

Dissemination

List of Publications

1. **Somen Biswal** and Alok Satapathy, "Dry Sliding Wear Behavior of Epoxy Composite Reinforced With Short Palmyra Fibers," *5th National Conference on Processing and Characterization of Materials, IOP Conf. Series: Materials Science and Engineering*, 115, 012028 doi:10.1088/1757-899X/115/1/012028, 2016.

2. **Somen Biswal** and Alok Satapathy. "Preparation, Properties and Wear Performance Evaluation of Epoxy-Palmyra Fiber Composites," ***Journal of Polymer Composites,*** (Accepted on 21 June, 2016).

Conference Presentation

1. **Somen Biswal** and Alok Satapathy. Processing and Characterization of Epoxy Composites Reinforced with Short Palmyra Fiber. Proceedings of International Conference on Science, Technology and Management (ICSTM 2016), April, 2016, Bangkok, Thailand.

2. **Somen Biswal** and Alok Satapathy. Parametric Optimization of Sliding Wear Behavior of Epoxy Composites Reinforced with Short Palmyra Fibers. Proceedings of International Conference on Advancement in Polymeric Materials (APM 2016), February, 2016, CIPET Ahmedabad.

3. **Somen Biswal** and Alok Satapathy. Dry Sliding Wear Behavior of Epoxy Composite Reinforced With Short Palmyra Fibers. Proceedings of National Conference on Processing and Characterization of Materials (NCPCM 2015), December, 2015, NIT Rourkela.

Preparation, Properties and Wear Performance Evaluation of Epoxy-Palmyra Fiber Composites

Somen Biswal, Alok Satapathy
Department of Mechanical Engineering, National Institute of Technology, Rourkela 769008, India

This article presents a parametric analysis of dry sliding wear process undergone by a new class of composite material consisting of epoxy and short palmyra fibers (SPF). It is an attempt to explore the possibility of improving the dry sliding wear resistance of neat epoxy by reinforcing it SPF. Palmyra fiber is an inexpensive, strong, and naturally available fiber derived from the stalks of palmyra leaf. In the present investigation, epoxy-based composites with different weight proportions of SPF (0, 4, 8, and 12 wt%) are fabricated although the simple hand-lay-up route. The tensile, flexural, and micro-hardness properties of the samples are found out which is followed by a FTIR spectroscopy of the samples. The composite samples are then subjected to wear trials using a pin-on-disc test rig as per ASTM G 99-05 test standards under different operating conditions. The effects of various operational variables on the dry sliding wear behavior of these epoxy composites with and without SPF reinforcement are studied. The design of experiments approach using Taguchi's L16 orthogonal array is used for parametric analysis of the wear process. Significant parameters affecting the wear rate of epoxy are identified. This study revealed that while the fiber content and the sliding velocities have significant influence on the wear arte of the composites, the effects of sliding distance and normal load are ignorable. An optimal parameter setting for minimum specific wear rate is obtained. The morphologies of the worn surfaces are examined by scanning electron microscopy and possible wear mechanisms are identified. POLYM. COMPOS., 00:000–000, 2016. © 2016 Society of Plastics Engineers

INTRODUCTION

Natural fiber reinforced composites now-a-days are being used extensively because of many advantages offered by them. Unlike synthetic fibers, natural fibers are low cost, bio-degradable, eco-friendly, light weight, and easily available. Being completely renewable, natural fibers provide many advantages to the environment. Also the waste generated by these natural fibers is organic and, hence, can be used for other purposes such as electricity generation, house building material, and so forth. These advantageous properties of natural fibers have attracted researchers from all over the world to develop new materials based on them.

Considerable work by researchers have been reported in the past on natural fibers such as flax [1], oil palm [2], bamboo [3], kenaf [4], sisal [5], and so forth, and it has been found that these natural fibers can be potential substitutes for synthetic fibers. Few works are also available in the literature on polymer composites reinforced with palmyra fibers. Srinivasababu et al. [6] studied and characterized treated and untreated palmyra fiber reinforced polyester composites based on mechanical properties such as tensile, impact, and flexural strength. Wu et al. [7] characterized palmyra palm fiber-based poly butylene succinate composites on the basis of their mechanical and thermal behavior. Velmurugan et al. [8] investigated the mechanical properties of randomly oriented short palmyra/glass fiber hybrid composites. They also studied the water absorption capacity of these hybrid composites. Mahesh et al. [9] studied the mechanical and thermal properties of palmyra fiber composites with polyester as the matrix. Velmurugan et al. [10] investigated the tensile properties of epoxy composites reinforced with palmyra fiber.

A number of studies on friction and wear characteristics of natural fiber composites are also reported in recent past. Chand et al. [11] studied the influence of fiber orientation on the wear characteristics of sisal fiber reinforced composites with epoxy as the matrix material. It was found that the wear rate decreased considerably by addition of sisal fiber to the epoxy composites. It was also observed that the wear rate was minimum when the fibers were normally oriented and maximum wear was recorded when the fibers were oriented in longitudinal direction. Yousif et al. [2] studied and compared the mechanical and tribological properties of oil palm fiber reinforced polyester (OPRP) composites and chopped strand mat glass fiber reinforced (CGRP) composites. It was found that OPRP showed much better wear characteristics than CGRP. Similarly,

Correspondence to: S. Biswal; e-mail: somenbiswal7@gmail.com
DOI 10.1002/pc.24134
Published online in Wiley Online Library (wileyonlinelibrary.com).

Tong et al. [3] studied the sliding wear behavior of bamboo fiber against gray iron (HT200). It was seen that with increase in sliding velocity, the wear volume increased. It was observed that normal-oriented fiber specimens showed better wear characteristics than parallel-oriented fiber specimens. Chin et al. [4] studied the potentiality of kenaf fiber as reinforcement for application against wear. It was found that normal-oriented kenaf fiber specimens showed better wear characteristics than parallel-oriented specimens. It was also observed that presence of fiber served as a dominant factor over applied load and sliding velocity on the specific wear rate of the specimen. The wear mechanisms of the composites were predominated by micro-cracks and debonding in the fibrous regions and deformation in the resinous regions. Tayeb [12] studied sugarcane fiber reinforced polyester composites for tribological characterizations. He compared and found that sugarcane fiber reinforced polyester composites are more resistant toward wear than glass fiber reinforced polyester composites. The friction coefficient was also found to decrease with increase in load for chopped and unidirectional sugarcane fibers. It was also found that the wear rate decreased on increasing the fiber length up to a maximum of 5 mm and then again increased indicating the existence of a critical fiber length for minimum wear rate. Nirmal et al. [13] studied the effect of betelnut fiber on the adhesive wear of polyester composites. A superior wear performance was observed in anti-parallel oriented betelnut fiber followed by parallel orientation and normal orientation of the fiber. Siva et al. [14] studied the mechanical and tribological characteristics of woven coconut fibers and found the wear resistance to be maximum when a combination of silane treated glass fiber and coconut fiber was used. Chand et al. [15] studied the effect of silane coupling agent and applied load on the frictional and sliding wear behavior of sisal fiber reinforced polyester composites.

Most of the published works on palmyra fibers have reported on the strength properties of the composites and not on the effects of fibers on friction and wear behavior. Moreover, although a lot of work has been done on the wear characteristics of composites with other natural fibers, no work has been reported so far on epoxy-based composites reinforced with short palmyra fiber (SPF). In view of this, the present work includes the investigation of dry sliding wear behavior using a pin-on-disc set up for epoxy filled with SPF with an objective to find ways to use these locally available inexpensive fibers as a substitute for highly expensive synthetic fibers for wear resistance applications. Taguchi technique and Artificial Neural Network (ANN) have been used in an integrated manner in this work for parametric analysis of the wear process and to predict the sliding wear response of epoxy-palmyra fiber composites within and beyond the experimental limit.

EXPERIMENTAL DETAILS

Composite Fabrication

In the present work, Epoxy LY556 which belongs to the epoxide family has been used as the matrix material. Epoxy LY556 is a low-temperature curing resin, and it is mixed with hardener HY951 in the ratio of 10:1. The SPF used in the present work is extracted from the palmyra tree leaf stalk. The stalk after being cut from the tree is soaked in water for 10 days and is beaten to separate the cellulose and lignin present in the fiber. The fiber is then dried in the sunlight for 5 days until it dries out completely. The fiber is then cut into 2–3 mm in length with scissor. This fiber is thoroughly mixed with the epoxy resin (LY556) in different weight proportions (0, 4, 8, and 12 wt%). The dough (epoxy and SPF) is then slowly poured into the cylindrical glass moulds (9-mm dia and 100-mm length), coated beforehand with silicone-releasing agent. These are left to cure for 24 h after which the moulds are broken and specimens are released.

MECHANICAL CHARACTERIZATION

Tensile, Flexural, and Micro-Hardness

Generally, flat specimens are used to carry out the tensile test. The dimension of the specimen used to carry out the test is 150 mm $\times$ 20 mm $\times$ 3 mm and a uniaxial load is applied through both ends of the specimen. The tensile and flexural tests are carried out according to ASTM E 1309 standard. In the present research work, this test is carried out in the universal testing machine *Instron* 1195 at a crosshead speed of 10 mm/min and the results are used to calculate the strength of the composite. The test is repeated four times and the mean value is reported as the tensile and flexural strength of that specimen respectively.

In the present research work, a Vaiseshika micro-hardness tester is used to perform the micro-hardness test. A right pyramid form of diamond indenter with a square base having an angle of 136° between the opposite faces is forced into the material under a load F. The two diagonals X and Y of the indentation left on the surface of the material after removal of the load are measured and their arithmetic mean L is calculated.

FTIR Spectroscopy

In the present research work, Perkin Elmer FTIR spectrometer is used for analyzing the molecular structures present in the raw SPF and the epoxy-SPF composites under consideration. A hydraulic press is used to prepare the pellet shaped samples prior to performing the test.

 DOI 10.1002/pc

TABLE 1. Control factors and their selected levels of dry sliding wear

	Levels				
Control factors	1	2	3	4	Units
Sliding velocity (A)	63	125	190	250	cm/s
Normal load (B)	5	10	15	20	N
Sliding distance (C)	250	500	750	1000	m
Fiber content (D)	0	4	8	12	wt%

Sliding Wear Test

The samples are subjected to sliding wear test using a pin-on-disc type friction and wear monitoring test rig as per ASTM G 99-05. The counter body is a disc made of hardened ground steel (EN-32, hardness 72 HRC, surface roughness 0.6 μm*Ra*). The specimen is held stationary while the disc rotates. Normal load is applied through a lever mechanism. A series of tests are conducted with four sliding velocities of 63, 125,190, and 250 cm/s each under four different normal loads of 5, 10, 15, and 20 N. The material loss from the composite surface was measured using a precision electronic balance with accuracy ±0.1 mg and the specific wear rate (mm^3/N-m) was expressed on a volume loss basis as:

$$W_s = \Delta m/(\rho.\ t.\ V_s.\ F_n), \tag{1}$$

where Δm is the mass loss of the composite in the test duration (g), ρ is the density of the composite (g/mm^3), t is the test duration (s), V_s is the sliding velocity (cm/s), and F_n is the average normal load (N).

Taguchi Experimental Design

Taguchi experimental design is a very powerful tool to determine the degree of effect of various parameters on the output result. Selecting the control factors affecting the performance output in design of experiments is the most vital stage. In the initial stage, a number of factors are considered and subsequently the less important factors are eliminated leaving behind only the more important factors. In the present sliding wear test, four major factors have been considered such velocity, load, sliding distance, and fiber content each at four levels according to Taguchi's L_{16} orthogonal array as shown in Table 1. The experiments are conducted at room temperature. Use of Taguchi L_{16} reduced the number of experiments from $4^4 = 256$ conventional runs to just 16 runs thereby saving a lot of experimental time and cost. These experimental observations are again converted into signal-to-noise (S/N) ratios. The S/N ratio for minimum wear rate can be expressed as "smaller is better" which is calculated as logarithmic transformation of loss function as shown below:

$$\frac{S}{N} = -10\log\frac{1}{n}\left(\sum y^2\right), \tag{2}$$

where n is the number of observations and y is the observed data.

Prediction Using ANN

ANN is a very powerful tool for solving a huge variety of problems from various fields. It uses the basic principle of a biological neural system to predict the results. It was developed to simulate the strong learning, clustering, and reasoning capacity of biological neurons. With a strong learning capability and use of parallel computation and nonlinear mapping, neural networks can be successfully applied for identifying several nonlinear systems and control problems [16]. ANN is widely used in the field of classification and control of dynamic system, medical science, image and speech recognition, and so forth. In the present study, ANN serves as a very helpful tool for predicting the specific wear rate as it is very difficult to get a mathematical formulation for the wear behavior. This proposed approach not only yields a sufficient understanding of the effects of process parameters but also produces an optimal parameter setting to ensure that the composites exhibit the best wear performance characteristics. The details of this methodology are described by Kadi [17].

RESULTS AND DISCUSSION

Tensile, Flexural, and Micro-Hardness Test Results

The tensile strengths of the composite specimens are evaluated and the test results for various epoxy-SPF composites are presented in Fig. 1. It is found that with increase in the SPF content, tensile strength of the composite increases. With a reinforcement of 2 wt% of SPF, the tensile strength of the composite is found to be improved from 65MPa to 78MPa, which indicates an improvement of about 20%. With further addition of the

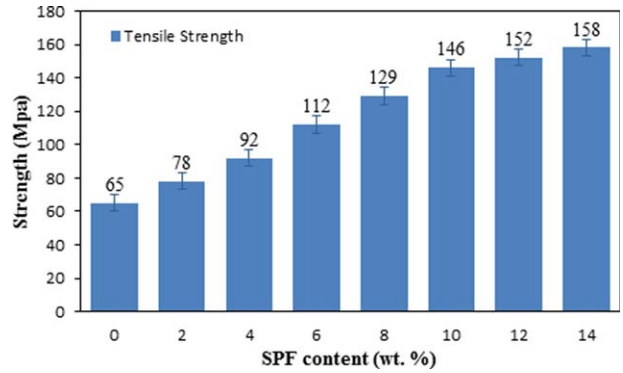

FIG. 1. Graphical representation of tensile strength. [Color figure can be viewed in the online issue, which is available at wileyonlinelibrary.com.]

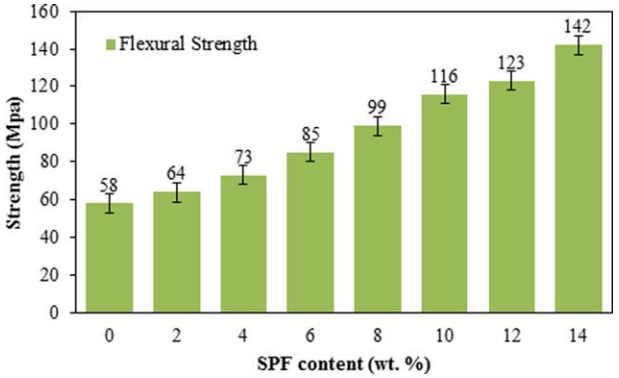

FIG. 2. Graphical representation of flexural strength. [Color figure can be viewed in the online issue, which is available at wileyonlinelibrary.com.]

SPF, the tensile strength increases steadily and registers a growth of about 143% at 14 wt% of SPF content. This can be attributed to the reason that with increase in fiber content, the axial load carrying capacity of the composite increases.

In the present work, the flexural strength values of the epoxy-SPF composites are evaluated and the variations are presented in Fig. 2. A gradual improvement in flexural strength is recorded in case of epoxy composite reinforced with SPF and this improvement is found to be proportional to the fiber content. It is found that while the flexural strength of neat hardened epoxy is about 58MPa, with the addition of just 2 wt% of SPF, it increases to about 64 MPa. Similarly, with incorporation of 14 wt% of SPF, the flexural strength of the composite improves by about 144% and attains a value of 142MPa.

The wear resistance of any material is dependent on the hardness of that material. In the present research work, the micro-hardness values of the epoxy-SPF composites with different SPF content have been obtained and are presented in Fig. 3. It is evident that with addition of SPF, micro-hardness of the composite is improved. With an addition of 2 wt% of SPF in the neat epoxy, the micro-hardness of the neat epoxy increases from 0.085 to 0.091 GPa which is an increase of about 7%. With further addition of fiber to

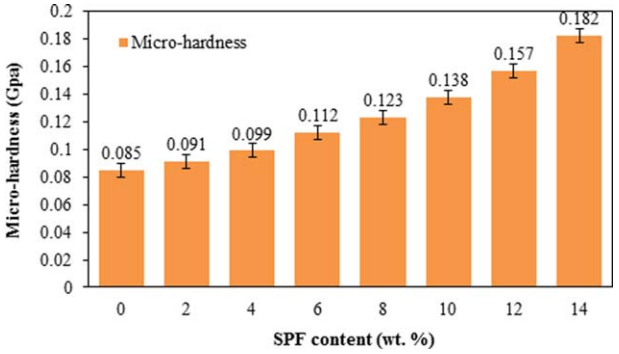

FIG. 3. Micro-hardness of SPF-epoxy composites. [Color figure can be viewed in the online issue, which is available at wileyonlinelibrary.com.]

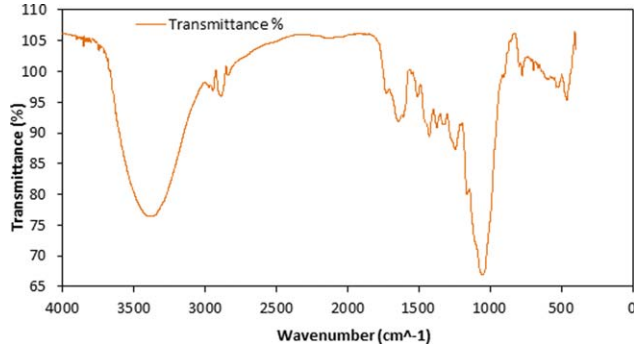

FIG. 4. FTIR spectroscopy of raw SPF. [Color figure can be viewed in the online issue, which is available at wileyonlinelibrary.com.]

the neat epoxy, the micro-hardness increases and at 14 wt% the composite micro-hardness value is reported as 0.182 GPa which indicates an increase of about 114% as compared to the hardness of neat epoxy.

FTIR Spectroscopy

The FTIR spectroscopy was carried out using the Perkin Elmer spectrometer on raw SPF and epoxy-SPF composites. The FTIR spectroscopy results for both raw SPF and epoxy-SPF composite are shown in Figs. 4 and 5, respectively. Figure 4 reveals nine major downward peaks. The band at 3374.02 cm^{-1} suggests the presence of amines and amides stretching (N-H bond). Peaks at 2887.95 and 2828.02 cm^{-1} suggests the presence of alkane (C-H) and aldehydes (H-C = O: C-H) stretching, respectively. Wavenumber 1645.81 cm^{-1} shows the presence of –C = C- stretching. Peak at 1514.82 cm^{-1} suggests the presence of nitro compounds. There is a major peak at 1053.08 cm^{-1} suggesting the presence of aliphatic amine stretching (C-N).

Figure 5 shows the FTIR analysis of the epoxy-SPF composites. The analysis revealed a many new peaks which were not present in Fig. 4. The wavenumber 3328.34 and 2967.30 cm^{-1} suggests the presence of alkynes and alkanes stretching respectively in the epoxy-SPF composite. Wavenumber 1607.74 cm^{-1} reveals the

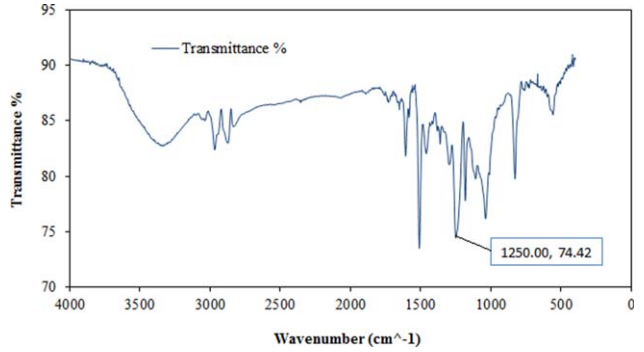

FIG. 5. FTIR spectroscopy of epoxy-SPF composite. [Color figure can be viewed in the online issue, which is available at wileyonlinelibrary.com.]

DOI 10.1002/pc

TABLE 2. Specific wear rates obtained for different test conditions with S/N ratios

Test run	Sliding velocity *A* (cm/s)	Normal load *B* (N)	Sliding distance *C* (m)	SPF content *D* (wt%)	Sp. wear rate (10^{-4} mm^3/N-m)	S/N ratio (dB)
1	63	5	250	0	6.3600	−16.0691
2	63	10	500	4	5.4690	−14.7582
3	63	15	750	8	3.6250	−11.1862
4	63	20	1000	12	0.9165	0.7574
5	125	5	500	8	3.8560	−11.7227
6	125	10	250	12	2.3320	−7.3546
7	125	15	1000	0	7.8180	−17.8619
8	125	20	750	4	5.8230	−15.3029
9	190	5	750	12	1.4440	−3.1913
10	190	10	1000	8	2.8280	−9.0296
11	190	15	250	4	6.4300	−16.1642
12	190	20	500	0	8.8180	−18.9074
13	250	5	1000	4	7.4690	−17.4652
14	250	10	750	0	9.4840	−19.5398
15	250	15	500	12	2.6660	−8.5172
16	250	20	250	8	3.6560	−11.2601

presence of 1° amines (N-H bend). Wavenumber 1250.00 cm^{-1} shows the presence of aliphatic amines (C-N stretch).

Sliding Wear Test Results

The specific wear rates and their corresponding S/N ratios obtained by Taguchi L_{16} orthogonal array for all the 16 experiments are presented in Table 2. From the Table 2, it is found that the overall mean of the S/N ratio is −12.4429 dB for epoxy-based composites reinforced with SPF. A commercial software Minitab 14 was used for the application of design of experiment. From the S/N ratio output, it is observed that among all the four factors considered for the analysis, the specific wear rate is mostly affected by the SPF content in the epoxy composite followed by the sliding velocity, sliding distance, and normal load. The analysis showed that at sliding velocity (*A*) of 63 cm/s, normal load (*B*) of 20 N, sliding distance (*C*)

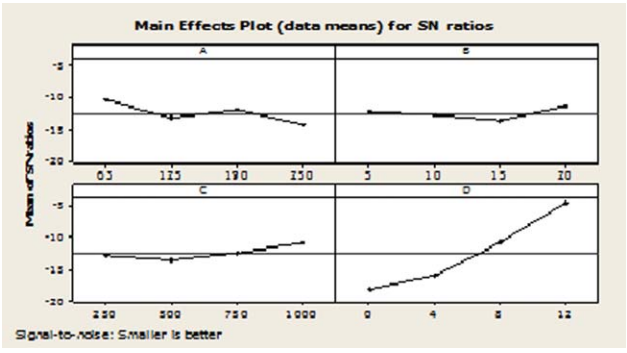

FIG. 6. Main effects plot for S/N ratios (with short palmyra fiber). [Color figure can be viewed in the online issue, which is available at wileyonlinelibrary.com.]

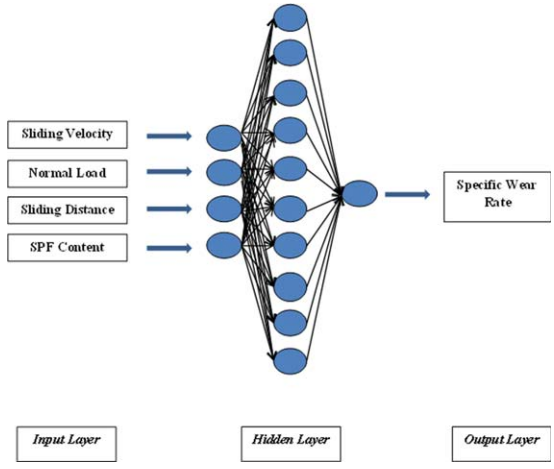

FIG. 7. The three layer neural network. [Color figure can be viewed in the online issue, which is available at wileyonlinelibrary.com.]

TABLE 3. Response table for minimum sliding wear for composite with short palmyra fiber

Level	*A*	*B*	*C*	*D*
1	−10.314	−12.112	−12.712	−18.095
2	−13.061	−12.671	−13.476	−15.924
3	−11.823	−13.432	−12.305	−10.800
4	−14.196	−11.178	−10.900	−4.576
Delta	3.882	2.254	2.577	13.518
Rank	2	4	3	1

TABLE 4. Input parameters selected during training

Input Parameters	Values
Number of input layer neuron (I)	4
Number of hidden layer neuron (H)	10
Number of output layer neuron (O)	1
No of epochs	1000000
Gradient value	1.00 e^{-14}
Validation check	100000

TABLE 5. Comparison of experimental results with ANN predicted values

Specific wear rate (10^{-4} mm^3/N-m)			
Test run	Experimental	ANN predicted	Error %
1	6.360	6.359136	0.013
2	5.469	5.468302	0.012
3	3.625	3.601238	0.655
4	0.917	0.942864	2.820
5	3.856	4.021859	4.301
6	2.332	2.328292	0.159
7	7.818	7.773308	0.571
8	5.823	5.818631	0.075
9	1.444	1.443930	0.004
10	2.828	2.805736	0.787
11	6.430	6.425846	0.064
12	8.818	8.512651	3.462
13	7.469	7.382000	1.520
14	9.484	9.433750	0.529
15	2.666	2.654097	0.446
16	3.656	3.660072	0.111

of 1000 m, and SPF content (D) of 12 wt%, the specific wear rate is minimum as shown in Fig. 6. The response table for S/N ratios is shown in Table 3.

ANN for Prediction

ANN is a very useful tool to predict the input and output pattern of nonlinear problems such as sliding wear. ANN technology can be effectively used for solving complex, nonlinear, and multidimensional problems because it is able to imitate the learning capability of human beings. As a result of this, ANN could predict the results effectively from the examples without using any formula and could even predict new results based on the trends obtained from the examples. In the present analysis, sliding velocity, normal load, sliding distance, and SPF content are taken as the four input parameters. The database is then divided into three categories, namely: (1) a validation category, which is required to define the ANN architecture and adjust the number of neurons for each layer; (2) a training category, which is exclusively used to adjust the network weights; and (3) a test category, which corresponds to the set that validates the results of the training protocol. The input variables are normalized so that it lies in the range 0–1. The output layer has one neuron which represents the specific wear rate. Different structures of ANN were tested by varying the number of neurons in the hidden layer and gradient value. Finally one structure with minimum error was selected for training. The optimized 3-layer neural network used in this simulation is shown in Fig. 7. The selected structure was trained rigorously by selecting maximum number of cycles. The Table 4 below shows the parameters during the training. The predicted values are compared with the experimental values and the results are shown in Table 5 with the associated error percentages.

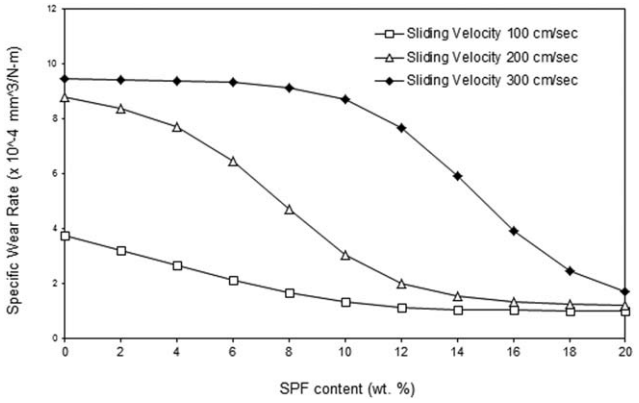

FIG. 8. ANN prediction of variation in specific wear rate with SPF content for SPF-Epoxy composites.

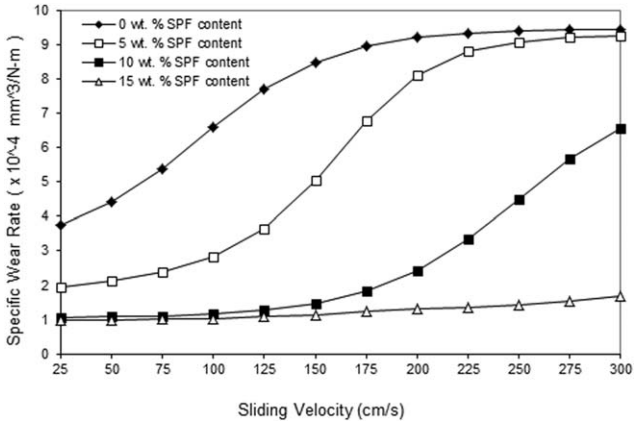

FIG. 9. ANN prediction of variation in specific wear rate with sliding velocity for SPF-Epoxy composites.

TABLE 6. Comparison of predicted and experimental values for sliding wear rate

Epoxy- SPF composites		
Specific wear rate (10^{-4}mm^3/N-m) (Predicted)	Specific wear rate (10^{-4}mm^3/N-m) (Experimental)	Error %
7.353	6.36	15.6
5.189	5.469	5.1
3.525	3.625	2.7
0.861	0.9165	6.0
3.521	3.856	8.6
2.357	2.332	1.0
7.849	7.818	0.3
5.685	5.823	2.3
1.577	1.444	9.2
2.441	2.828	13.6
6.205	6.43	3.4
8.369	8.818	5.0
6.685	7.469	10.4
8.849	9.484	6.6
2.357	2.666	11.5
4.012	3.656	9.7

DOI 10.1002/pc

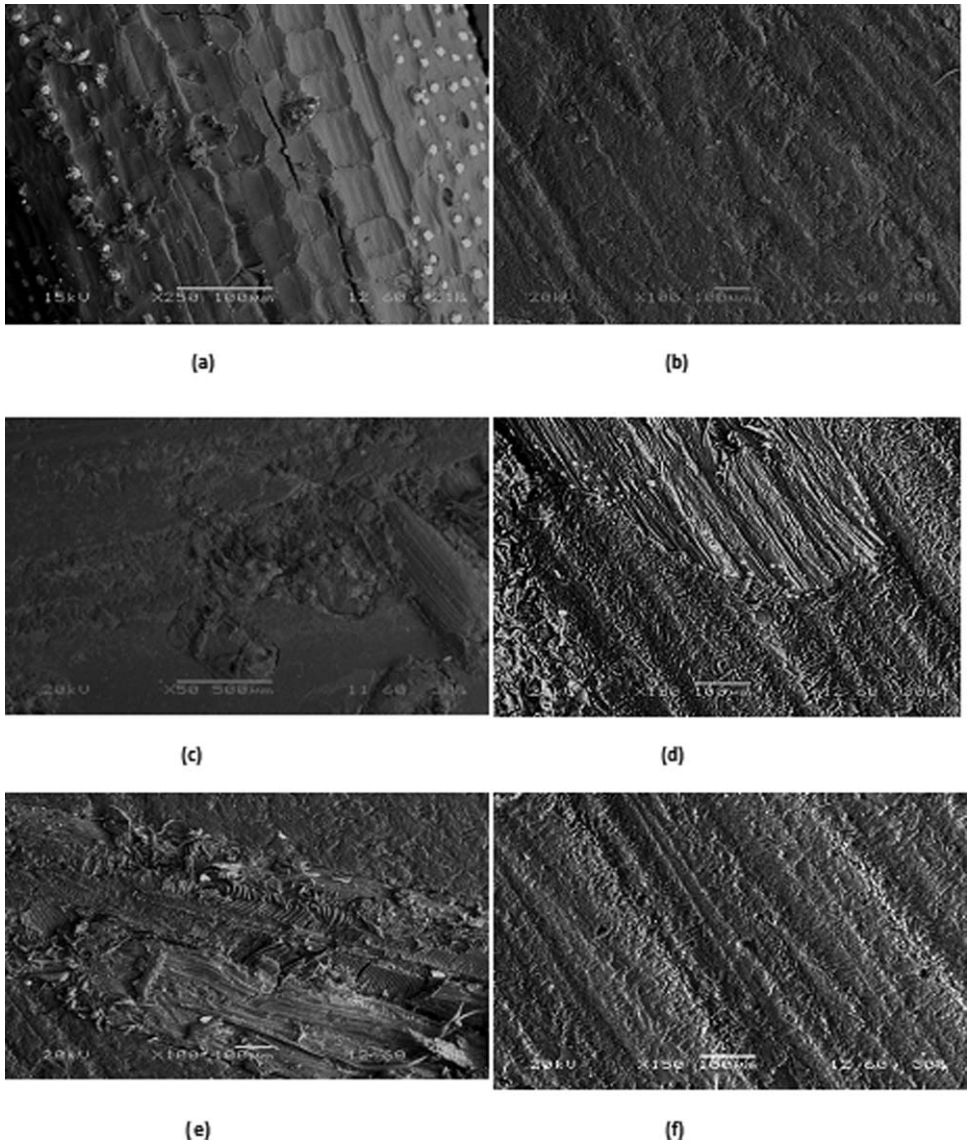

FIG. 10. Typical SEM images of SPF-Epoxy composites.

The Figs. 8 and 9 below shows the effect of two most dominant factors, that is, SPF content and sliding velocity on the specific wear rate of the specimens and a simulated specific wear rate has been predicted using ANN

From the Figs. 8 and 9 it can be concluded that while the specific wear rate reduced invariably with the increase in the SPF content, it increased with increase in the sliding velocity. The figure clearly indicates an improvement in the wear resistance with increase in SPF content. The increase in the wear rate with increase in the sliding wear velocity can be attributed to the fact that with increase in the sliding velocity, the interface temperature between the specimen and the counter surface of the pin-on-disc setup increases. As both the fiber and the epoxy matrix has different thermal expansion coefficient, it creates an interfacial stress. When this interfacial stress exceeds the bonding strength of the fiber and epoxy, cracks starts forming and more wear takes place.

Factor Settings for Minimum Specific Wear Rate

In the present research work to minimize the specific wear rate, an attempt has been made to find the optimal settings for the control factors. The specific wear rate can be predicted using a nonlinear regressive predictive equation showing the relationship between the specific wear rate and the individual control factors. This correlation is developed statically using the standard SYSTAT 7. To express the specific wear rate in terms of mathematical model, the following equation is suggested:

$$W_S = K_0 + K_1 \times A + K_2 \times B + K_3 \times C + K_4 \times D \qquad (3)$$

where, $\boldsymbol{W_s}$ denotes the specific wear rate in mm^3/N-m which is the performance output and $\boldsymbol{K_i}$ (i = 0,1,2,3 and 4) are the constants of the model. ***A*** represents the sliding velocity in cm/s, ***B*** represents the normal load (N), ***C***

denotes the sliding distance (m), and ***D*** represents the fiber content in wt%. Values of all the constants are calculated using the SYSTAT 7 software and the final expression for epoxy + SPF is given as follows:

$$W_S = 6.849 + 0.008 \times A - 0.541 \times D \quad (4)$$

The correlation coefficient (r^2) is found to be 0.988 for the epoxy-SPF composites which is quite high to confirm the correctness of the calculated constants and thus making it possible for further analysis. Table 6 shows the comparison between wear rates obtained from experiment and those of calculated from the predictive equation. The corresponding error percentages are also reported in the following table.

Morphology of the Specimen

Figure 10a presents the surface morphology of a typical palmyra fiber used in this investigation. It is clearly seen that the surface is uneven and exhibits a peculiar arrangement of hemispherical dots and bony ridges of different size and thickness. The surface features of epoxy SPF composite with a fiber content of 8 wt% is shown in Fig. 10b.

The worn surface morphology (sliding velocity of 63 cm/s and normal load of 5 N) of the same composite is presented in Fig. 10c in which local removal of the matrix layer as a result of the dry sliding wear is visible. Figure 10d presents the SEM image of a worn composite surface at relatively higher sliding speed of 190 cm/s. Removal of the upper matrix layer and protrusion of fibers beneath the epoxy resin are revealed. The direction of sliding is also clear in this micrograph. Figure 10e presents another typical worn surface of a composite with low fiber content (4 wt%). Formation of wear debris, surface cracks and signs of plastic are evident. But such features are not adequately seen in Fig. 10f which presents the worn surface morphology of an epoxy-SPF composite with fiber content as high as 12 wt%. Signs of plastic deformation are however clearly seen in the micrograph and the wear tracks, indicated by arrows.

CONCLUSIONS

1. Successful fabrication of SPF reinforced epoxy composites are possible and the results show that with the increase in SPF content, the sliding wear rate decreases considerably.
2. The effect of various factors such as sliding velocity, normal load, sliding distance, and SPF content can be successfully determined using Taguchi L16 experimental design. It was observed from the analysis that SPF content is the most dominant factor followed by sliding velocity. The analysis showed normal load as the least affecting factor for specific wear rate.
3. The work also illustrates the use of ANN for predicting the specific wear rate of SPF composites with increase in SPF content and sliding velocity beyond the experimental domain. The predicted and experimental values of wear rate exhibited good agreement, validating the remarkable capability of a well-trained neural network as far as the present work is concerned.

REFERENCES

1. M. Baiardo, E. Zini, and M. Scandola, *Compos. Part A*, **35**, 701 (2004).
2. B.F. Yousif and N.S.M. Tayeb, *Int. J. Precis. Technol.*, **1**, 213 (2009).
3. J. Tong, R.D. Arnell, and L.Q. Ren, *Wear*, **221**, 37 (1998).
4. C.W. Chin and B.F. Yousif, *Wear*, **267**, 1550 (2009).
5. P.K. Bajpai and J. Singh Iand Madaan, *Wear*, **297**, 829 (2013).
6. N. Srinivasababu, J.S. Kumar, and K.V.K. Reddy, *Proc. Technol.*, **14**, 252 (2014).
7. C.S. Wu, H.T. Liao, and J.J. Jhang, *Polym. Bull.*, **70**, 3443 (2013).
8. R. Velmurugan and V. Manikandan, *Compos. Part A*, **38**, 2216 (2007).
9. C. Mahesh, B. Kondapanaidu, K. Govindarajulu, and V. Balakrishna murthy, *Int. J. Eng. Trends Technol.*, **5**, 259 (2013).
10. G. Velmurugan, D. Vadivel, R. Arravind, S.P. Vengatesan, and A. Mathiazhagan, *Int. J. Mech. Ind. Eng.*, **2**, 2231 (2012).
11. N. Chand and U.K. Dwivedi, *Polym. Compos.*, **28**, 437 (2007).
12. N.S.M. Tayeb, *Wear*, **265**, 223 (2008).
13. U. Nirmal, B.F. Yousif, D. Rilling, and P.V. Brevern, *Wear*, **268**, 1354 (2010).
14. I. Siva, J.T.W. Jappes, and B. Suresha, *Polym. Compos.*, **33**, 723 (2012).
15. N. Chand and U.K. Dwivedi, *Polym. Compos.*, **29**, 280 (2008).
16. P.K. Padhi and A. Satapathy, *Tribol. Trans.*, **56**, 789 (2013).
17. H.E. Kadi, *Compos. Struct.*, **73**, 1 (2006).

 DOI 10.1002/pc

Dry sliding wear behavior of epoxy composite reinforced with short palmyra fibers

Somen Biswal and **Alok Satapathy**

Department of Mechanical Engineering, National Institute of Technology, Rourkela, 769008, India

somenbiswal7@gmail.com, alok@nitrkl.ac.in

Abstract. The present work explores the possibility of using palmyra fiber as a replacement for synthetic fiber in conventional polymer composites for application against wear. An attempt has been made in this work to improve the sliding wear resistance of neat epoxy by reinforcing it with short palmyra fibers (SPF). Epoxy composites with different proportions (0, 4, 8 and 12 wt. %) of SPF are fabricated by conventional hand lay-up technique. Dry sliding wear tests are performed on the composite samples using a pin-on-disc test rig as per ASTM G 99-05 standards under various operating parameters. Design of experiment approach based on Taguchi's L_{16} Orthogonal Arrays is used for the analysis of the wear. This parametric analysis reveals that the SPF content is the most significant factor affecting the wear process followed by the sliding velocity. The sliding wear behavior of these composites under an extensive range of test conditions is predicted by a model based on the artificial neural network (ANN). A well trained ANN has been used to predict the sliding wear response of epoxy based composites over a wide range.

1. Introduction

The use of various natural fibers as substitutes for synthetic functional fibers is increasing day-by-day owing to their several advantages like bio-degradability, renewability, low-cost and low-toxicity. These composites find several applications starting from household appliances to wear resistant components. A number of studies on friction and wear characteristics of natural fiber composites have been reported in recent past. Chand et. al. [1] studied the influence of fiber orientation on the wear characteristics of sisal fiber reinforced composites with epoxy as the matrix material. It was found that the wear rate decreased considerably by addition of sisal fiber to the epoxy composites. Yousif et. al. [2] studied and compared the mechanical and tribological properties of oil palm fiber reinforced polyester composites (OPRP) and chopped strand mat glass fiber reinforced composites (CGRP). Similarly, Tong et. al. [3] studied the sliding wear behavior of bamboo fiber against grey iron (HT200). Chin et. al. [4] studied the potential of kenaf fiber as reinforcement for application against wear. Tayeb [5] studied sugarcane fiber reinforced polyester composites for tribological characterizations. Nirmal et. al. [6] studied the effect of betelnut fiber on the adhesive wear of polyester composites. A superior wear performance was observed in anti-parallel oriented betelnut fiber followed by parallel orientation and normal orientation of the fiber. Siva et. al. [7] studied the mechanical and tribological characteristics of woven coconut fibers and found the wear resistance to be maximum when a combination of silane treated glass fiber and coconut fiber was used. Chand et. al. [8] studied the effect of silane coupling agent and applied load on the frictional and sliding wear

behavior of sisal fiber reinforced polyester composites. Most of the published works on palmyra fibers have reported on the strength properties of the composites and not on the effects of fibers on friction and wear behavior. Moreover, although a lot of work has been done on the wear characteristics of composites with other natural fibers, no work has been reported so far on epoxy based composites reinforced with short palmyra fiber. In view of this, the present work includes the investigation of dry sliding wear behavior using a pin-on-disc set up for epoxy filled with short palmyra fibers with an objective to find ways to use these locally available inexpensive fibers as a substitute for highly expensive synthetic fibers for wear resistance applications. Taguchi technique and Artificial Neural Network (ANN) have been used in an integrated manner in this work for parametric analysis of the wear process and to predict the sliding wear response of epoxy-palmyra fiber composites within and beyond the experimental limits.

2. Experimental details

2.1. Sliding Wear Test

In the present work Epoxy LY556 which belongs to the epoxide family has been used as the matrix material. Epoxy LY556 is a low-temperature curing resin and it is mixed with hardener HY951 in the ratio of 10:1. The short palmyra fiber (SPF) used in the present work is extracted from the palmyra tree leaf stalk and this fiber is thoroughly mixed with the epoxy resin (LY556) in four different weight proportions (0, 4, 8 and 12 wt%) to prepare composite samples. The samples are subjected to sliding wear test using a pin-on-disc type friction and wear monitoring test rig as per ASTM G 99-05. The counter body is a disc made of hardened ground steel (EN-32, hardness 72 HRC, surface roughness 0.6 μm *Ra*). The specimen is held stationary while the disc rotates. Normal load is applied through a lever mechanism. A series of tests are conducted with four sliding velocities of 63, 125,190 and 250 cm.s−1 each under four different normal loads of 5, 10, 15 and 20 N. The material loss from the composite surface is measured using a precision electronic balance with accuracy ±0.1 mg and the specific wear rate (mm^3/N-m) is expressed on a volume loss basis as:

$$W_S = \frac{\Delta m}{\rho \times t \times V_s \times F_n} \quad [1]$$

where Δm is the mass loss of the composite in the test duration (g), ρ is the density of the composite (g/mm^3), t is the test duration (s), Vs is the sliding velocity (cm.s−1), and Fn is the average normal load (N).

2.2. Taguchi Experimental Design

Taguchi experimental design is a very powerful tool to make parametric appraisal of any multi variable engineering process. In the present study for sliding wear test of epoxy-SPF composites, four major factors have been considered such as sliding velocity, applied load, sliding distance and fiber content each at four levels according to Taguchi's L_{16} orthogonal array as shown in Table 1. Use of Taguchi L_{16} reduced the number of experiments from 4^4= 256 conventional runs to just 16 runs thereby saving a lot of experimental time and cost. These experimental observations are again converted into signal-to-noise (S/N) ratios. The S/N ratio for minimum wear rate can be expressed as "smaller is better" which is calculated as logarithmic transformation of loss function as shown below:

$$\frac{S}{N} = -10 \log \frac{1}{n}\left(\sum y^2\right), \quad [2]$$

where n is the number of observations and y is the observed data.

Table 1. Control Factors and their Selected Levels for Dry Sliding Wear

Control factors	Levels				
	1	2	3	4	Units
Sliding velocity (A)	63	125	190	250	Cm/sec
Normal load (B)	5	10	15	20	N
Sliding distance (C)	250	500	750	1000	m
Fiber content (D)	0	4	8	12	Wt %

Table 2. Specific Wear Rates Obtained for Different Test Conditions with S/N Ratios

Test Run	Sliding Velocity A (cm/sec)	Normal Load B (N)	Sliding Distance C (m)	SPF Content D (wt %)	Sp. Wear Rate ($10^{-4}mm^3$/N-m)	S/N Ratio (dB)
1	63	5	250	0	6.3600	-16.0691
2	63	10	500	4	5.4690	-14.7582
3	63	15	750	8	3.6250	-11.1862
4	63	20	1000	12	0.9165	0.7574
5	125	5	500	8	3.8560	-11.7227
6	125	10	250	12	2.3320	-7.3546
7	125	15	1000	0	7.8180	-17.8619
8	125	20	750	4	5.8230	-15.3029
9	190	5	750	12	1.4440	-3.1913
10	190	10	1000	8	2.8280	-9.0296
11	190	15	250	4	6.4300	-16.1642
12	190	20	500	0	8.8180	-18.9074
13	250	5	1000	4	7.4690	-17.4652
14	250	10	750	0	9.4840	-19.5398
15	250	15	500	12	2.6660	-8.5172
16	250	20	250	8	3.6560	-11.2601

2.3. Prediction Using Artificial Neural Network

ANN is widely used in the field of classification and control of dynamic system, medical science, image and speech recognition, etc [9]. In the present study ANN serves as a very helpful tool for predicting the specific wear rate as it is very difficult to get a mathematical formulation for the wear behavior. This proposed approach not only yields a sufficient understanding of the effects of process parameters but also produces an optimal parameter setting to ensure that the composites exhibit the best wear performance characteristics. The details of this methodology are described by Kadi [10].

1. Results and discussion

1.1. Sliding Wear Test Results

The specific wear rates and their corresponding S/N ratios obtained by Taguchi L_{16} orthogonal array for all the 16 experiments are presented in Table 2. From the Table 2 it is found that the overall mean of the S/N ratio is -12.4429 dB for epoxy based composites reinforced with short palmyra fibers. A commercial software Minitab 14 was used for the application of design of experiment. From the S/N ratio output, it is observed that among all the four factors considered for the analysis, the specific wear rate is mostly affected by the SPF content in the epoxy composite followed by the sliding velocity, sliding distance and normal load. The analysis showed that at sliding velocity (A) of 63 cm/s, normal load (B) of 20 N, sliding distance (C) of 1000 m and SPF content (D) of 12 wt%, the specific wear rate is minimum as evident from the response table for S/N ratios (Table 3).

1.2. Artificial Neural Network for Prediction

ANN is a very useful tool to predict the input and output pattern of nonlinear problems such as sliding wear. In the present analysis sliding velocity, normal load, sliding distance and SPF content are taken as the four input parameters. The input variables are normalized so that it lies in the range 0-1. The output layer has one neuron which represents the specific wear rate. Different structures of ANN were tested by varying the number of neurons in the hidden layer, gradient value and friction coefficient value (*mu* value). Finally one structure with minimum error was selected for training. The selected structure was trained rigorously by selecting maximum number of cycles. The predicted values are compared with the experimental values and the results are shown in Table 4 with the associated error percentages.

The Figure 1-2 below shows the effect of two most dominant factors i.e. SPF content and sliding velocity on the specific wear rate of the specimens and a simulated specific wear rate has been predicted using ANN.

Table 3. Response Table for Minimum Sliding Wear for Composite with Short Palmyra Fiber

Level	A	B	C	D
1	-10.314	-12.112	-12.712	-18.095
2	-13.061	-12.671	-13.476	-15.924
3	-11.823	-13.432	-12.305	-10.800
4	-14.196	-11.178	-10.900	-4.576
Delta	3.882	2.254	2.577	13.518
Rank	2	4	3	1

Table 4. Comparison of Experimental Results with ANN Predicted Values

Specific wear rate (10^{-4} mm^3/N-m)			
Test Run	Experimental	ANN Predicted	Error %
1	6.360	6.359136	0.013
2	5.469	5.468302	0.012
3	3.625	3.601238	0.655
4	0.917	0.979166	6.837
5	3.856	4.343180	12.634
6	2.332	2.328292	0.159
7	7.818	7.773308	0.571
8	5.823	5.818631	0.075
9	1.444	1.443930	0.004
10	2.828	2.805736	0.787
11	6.430	6.425846	0.064
12	8.818	8.119834	7.917
13	7.469	7.382000	1.520
14	9.484	9.433750	0.529
15	2.666	2.654097	0.446
16	3.656	3.660072	0.111

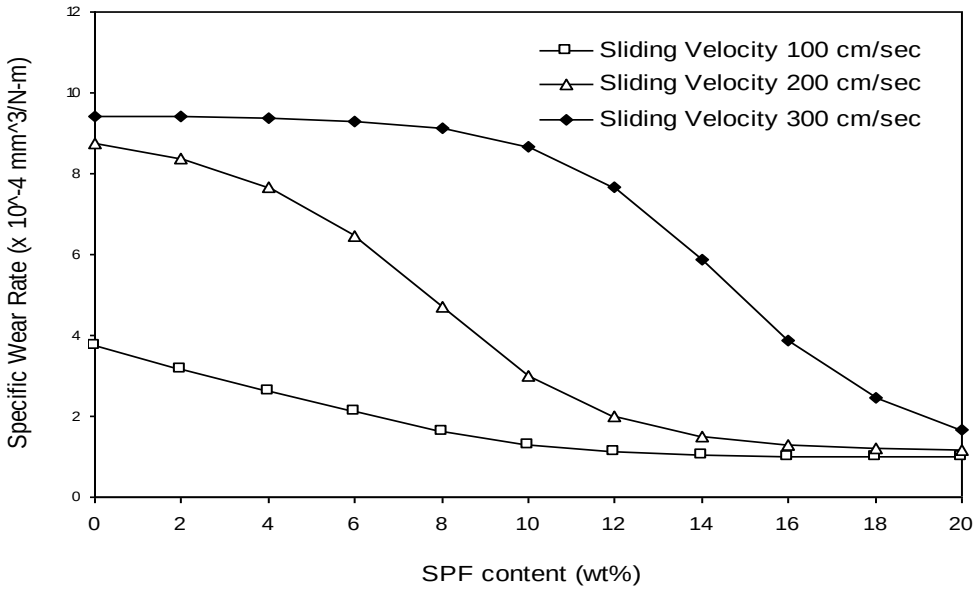

Figure 1. ANN prediction of variation in specific wear rate with SPF content for SPF-epoxy composite

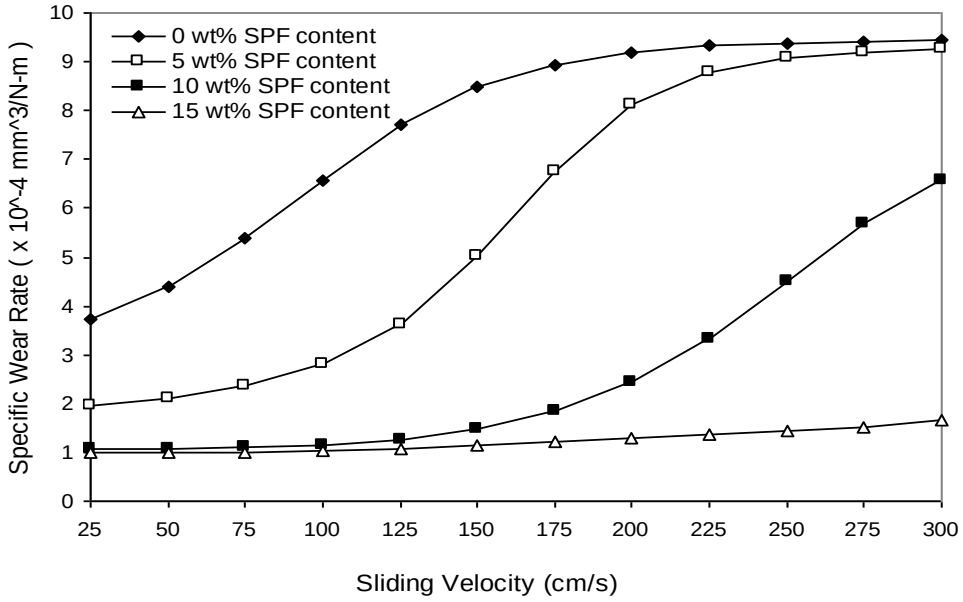

Figure 2. ANN prediction of variation in specific wear rate with sliding velocity for SPF-Epoxy composites.

2. Conclusions

The present experimental effort shows that successful fabrication of short palmyra fiber reinforced epoxy composites is possible and such composites can be employed in dry sliding wear situations. It is seen that by increasing the fiber loading, the wear resistance of neat epoxy can be significantly improved. A parametric appraisal of the wear process revealed that the fiber content and the sliding velocity are the most significant factors that affect the wear performance of the composites in an interacting environment. This work also illustrates the gainful use of artificial neural networks for predicting the specific wear rate of the composites with increase in fiber content and sliding velocity beyond the experimental domain.

3. References

[1] Chand N and Dwivedi UK 2007 *Polymer Composites* **28** 437-441.

[2] Yousif B F and Tayeb N S M 2009 *International Journal of Precision Technology* **1** 213-222.

[3] Tong J, Arnell R D and Ren L Q 1998 *Wear* **221** 37–46.

[4] Chin C W and Yousif B F 2009 *Wear* **267** 1550–1557.

[5] Tayeb N S M 2008 *Wear* **265** 223–235.

[6] Nirmal U, Yousif B F, Rilling D and Brevern P V 2010 *Wear* **268** 1354–1370.

[7] Siva I, Jappes J T W and Suresha B 2012 *Polymer Composites* **33** 723-732.

[8] Chand N and Dwivedi U K 2008 *Polymer Composites* **29** 280-284.

[9] Padhi P K and Satapathy A 2013 *Tribology Transactions* **56** 789-796.

[10] Kadi H E 2006 *Composite Structures* **73** 1–23.